THE DOWN-REGULATION OF KU70, DNA-PK$_{CS}$, AND PARP-1 IN MAMMALIAN CELL LINES

STEPHANIE WICKERSHAM
B. Sc. Neuroscience, University of Lethbridge, 2010

A Thesis
Submitted to the School of Graduate Studies
of the University of Lethbridge
in Partial Fulfillment of the
Requirements for the Degree

M. Sc. BIOLOGICAL SCIENCES

Department of Biological Sciences
University of Lethbridge
LETHBRIDGE, ALBERTA, CANADA

Dedicated to my loving parents – Kevin and Anita,
my siblings -- TJ, Tasha, and Tyler,
and Aaron –
for loving me always and being
there with me every step of the way.

Love you all!

Abstract

DNA double strand breaks (DSBs) are primarily repaired in eukaryotic cells by two different mechanisms – non-homologous end joining (NHEJ) or homologous recombination (HR). In mammalian somatic cells the balance between the two highly favours NHEJ. Gene targeting is a technique that exploits HR repair to alter a defined gene locus. While it holds potential to be implemented as a treatment option for several diseases, the outlook for using it in a clinical setting has been obstructed by a low gene targeting efficiency. This has been coupled to the low frequency of HR in mammalian cells. With the intention of shifting the repair balance, antibodies against DSB repair proteins will be introduced into mammalian cells. It is predicted that by targeting key repair proteins with antibodies, a compensatory increase in the frequency of HR can be fostered, ultimately resulting in improved gene targeting.

Acknowledgements:

Great thanks to my supervisor Dr. Igor Kovalchuk for his steady support, patience, and direction – and more importantly for his dedication to fostering each of his student's individual interests, goals, and strengths. Over the past 5 years this has been deeply appreciated. Also thanks to Dr. Andrey Golubov for his helpful suggestions and guidance -- without it I would have been lost.

Thanks to my committee members – Dr. Larry Kawchuk, Dr. Olga Kovalchuk, and Dr. Rob Sutherland – for their input and time.

Finally thanks to everyone in Hepler Hall. The daily encouragement, the helpful discussions, and the useful ideas have all proved to be very instrumental and valuable throughout my graduate degree.

Table of Contents

List of Tables:

List of Figures:

List of Abbreviations:

3-MB	3-methoxybenzamide
53BP1	p53 binding protein
AAV	Adeno-associated virus
Ab	Antibody
APC	Allophycocyanin
B-NHEJ	Back-up nonhomologous end joining
BER	Base excision repair
BRCA2	Breast cancer type 2 susceptibility protein
C-NHEJ (or NHEJ)	Classical nonhomologous end joining
CDK	Cyclin-dependent kinase
CHO	Chinese hamster ovary
CMV	Cytomegalovirus
CPP	Cell-penetrating peptide
D-loop	Displacement loop
DMEM	Dulbecco's modified eagle medium
DNA-PK	DNA protein kinase
DNA-PK_{CS}	DNA protein kinase catalytic subunit
DPBS	Dulbecco's phosphate buffered saline
DSB	Double strand break
dsDNA	Double-stranded DNA
EDTA	Ethylenediaminetetraacetic acid

ES cells	Embyonic stem cells
FACS	Fluorescence-activated cell sorting
FBS	Fetal bovine serum
FITC	Fluorescein isothiocyanate
FRET	Förster (or fluorescence) resonance energy transfer
G_0 phase	Gap 0 phase
G_1 phase	Gap 1 phase
G_2 phase	Gap 2 phase
GFP	Green fluorescent protein
HEK293	Human embryonic kidney 293
HR	Homologous recombination
hr	Hour
IR	Ionizing radiation
KIP	Kinase interacting protein
LigIII	DNA ligase III
LigIV	DNA ligase IV
MCF7	Michigan cancer foundation - 7
MRN	Mre11-Rad50-Nbs1
MRX	Mre11-Rad50-Xrs2
NHEJ (or C-NHEJ)	Nonhomologous end joining
PARP	Poly(ADP-ribosyl)ation polymerase
Parp1	Poly(ADP-ribosyl)ation polymerase 1
PE	Phycoerythrin

rAAV	Recombinant adeno-associated virus
RNAi	RNA interference
RPA	Replication protein A
S-phase	Sythesis phase
s.d.	Standard deviation
SCID	Severe combined immunodeficient
shRNA	Small hairpin RNA
siRNA	Small interfering RNA
SSB	Single-strand break
SSC	Side scatter
ssDNA	Single-stranded DNA
Swi2/Snf2	Switch2/sucrose nonfermentable2
XRCC	X-ray cross complementing
XLF	XRCC4-like factor
UniProtKB	UniProt Knowledgebase
UV	Ultraviolet

Chapter 1: Introduction

1.1 Introduction

DNA double strand break (DSB) repair is an essential cellular process (Hartlerode & Scully, 2009; Ohnishi et al., 2009; Sonoda et al., 2006). Every day cells are subjected to exogenous and endogenous factors causing DSBs including but not limited to ionizing radiation (IR) (Banath, 2003), chemical reagents (Hammond et al., 2003), V(D)J recombination (Klein et al., 1996), and senescence (Sedelnikova et al., 2004). If these breaks remain unrepaired they can be very damaging to the cell and culminate in translocations, DNA loss, mutations, and eventually even apoptosis (Jackson & Bartek, 2009; Ohnishi et al., 2009; Sonoda et al., 2006). There are two main competing pathways for repairing DNA DSBs in cells -- nonhomologous end joining (NHEJ) and homologous recombination (HR) (Helleday et al., 2007; Li & Heyer, 2008; Lieber, 2008). NHEJ involves the direct ligation of the DSB ends with little regard for homology, whereas in HR the broken strand is repaired using the homology of the strand's sister chromatid or homologous chromosome counterpart (Ohnishi et al., 2009; Tamura et al., 2002). It has been proposed that some degree of direct competition between these two repair pathways may exist (Sonoda et al., 2006).

In the past decade the manipulation of these DNA repair pathways has been investigated as a potential means to improve current gene targeting methods (de Boer et al., 2010; Fattah et al., 2008; Iiizumi et al., 2008; Pierce et al., 2001). Gene targeting is a type of

genetic engineering that utilizes the HR DNA repair pathway to replace a specific targeted gene loci within an organism's genome (Fattah et al., 2008). This approach has often been applied when generating knockouts through the deletion of an entire gene. By observing the resulting phenotype when a specific gene is absent its function, importance, and corresponding gene products can be elucidated. More recently, however, it has become applicable to the medical field through the development and investigation of gene therapy (Akhtar et al., 2011; Bainbridge et al. 2006; Fattah et al., 2008). Gene therapy essentially involves the rectification of disease-causing mutations by exchanging a mutated copy of a gene sequence for its healthy, wild-type equivalent (Fattah et al., 2008).

The field of gene therapy began to take shape when DNA was finally revealed as the driving force behind heredity, gene expression, and ultimately phenotype (Avery et al., 1944). The concept was defined in literature as early as 1947 in a study by Keeler (1947), however, it was not until later in the century that it began to be viewed as a viable treatment option for various genetic diseases (Osterman et al., 1970; Smithies et al., 1985; Tatum, 1966). Gene therapy, in theory, offers a way to permanently correct disease-inducing mutations. As well the inserted transgene if integrated via specific targeting will exist under normal physiological regulation and will not interrupt other genes. Today there are many debilitating diseases being considered as candidates for treatment in gene therapy studies including cystic fibrosis (Mueller & Flotte, 2008), cancer (Aboody et al., 2008; Dachs et al., 2005; Spitzweg, 2009), ocular diseases

(Bainbridge et al., 2006), cardiovascular diseases (Lavu et al., 2011; Vinge et al., 2008), and haemophilia (Murphy & High, 2008).

While the prospect of using HR-dependent gene targeting in a clinical setting for the correction of several disease-causing mutations within DNA holds much promise, the reality surrounding its actual implementation has been impeded by a few noted barriers including the low delivery and insertion efficiency of the corrected gene sequence into a cell's DNA through targeted integration (de Semir & Aran, 2006; Iiizumi et al., 2008). An observed low gene targeting efficiency was noted in several early studies. Smithies *et al.* (1985) revealed a targeted integration frequency of 1 in 10^3 when a plasmid that homologously targeted the beta-globin loci in a human cell line was used. Similarly, in a mammalian cell study by Thomas *et al.* (1986), the correction of a point-mutated gene could be corrected after copies of the corrected gene were injected into the nucleus but only at a low frequency of 1 in 10^3 cells. Later studies and publications have also highlighted the observed occurrence of minimal gene targeting frequencies (Thomas & Capecchi, 1987; Vasquez et al., 2001; Yanez & Porter, 1998). Though the low gene targeting integration frequency has shown to be a significant challenge preventing the clinical implementation of gene therapy, another difficulty is the existence of random vector integrations occurring at an even higher rate than targeted integrations (Iiizumi et al., 2008; Roth & Wilson, 1985, 1986; Vasquez et al., 2001). A study done in Chinese hamster ovary (CHO) cells found that not only was there a low level of targeted recombinants, but these events occurred once for every 4000 events of non-targeted integration (Adair et al., 1989). It is thought that NHEJ is likely responsible for most of

these random integrations (Iiizumi et al., 2008), however, research suggests more homology is involved than one would expect to see if classical NHEJ was involved (Merrihew et al., 1996). A suggested contributing factor for both challenges has been the high reliance on NHEJ for DNA repair in the somatic cells of higher organisms (Fattah et al., 2008). So while the machinery for HR, a process key to successful integration in gene targeting, is available, the limited presence of HR appears to be a challenge for those working to improve gene targeting techniques (Fattah et al., 2008).

In eukaryotic cells the presence of both NHEJ and HR DNA DSB repair mechanisms help maintain genomic stability. While both are important for genomic stability, the relative proportion of each varies among different eukaryotic cells. Single-celled eukaryotic organisms DSB repair is dominated by HR events, but in multicellular eukaryotic organisms it is dominated by NHEJ events (Liang et al., 1998; Lieber, Yu, & Raghavan, 2006). The genomes of multicellular eukaryotes are notably more intricate and repetitive causing inefficient homology searches and making the genome more vulnerable to instability as a result of large genomic rearrangements (Gorbunova & Levy, 1999; Lieber & Karanjawala, 2004; Puchta, 2005). In addition, NHEJ is also a much faster process and has been estimated to take approximately 30 minutes while HR is a considerably longer process taking around seven hours to complete (Mao et al., 2008a). Thus the predominant usage of NHEJ can contribute to a less interrupted replication cycle. Together these make NHEJ an attractive repair pathway in mammalian cells, however, it has also consequently produced barriers for gene therapy implementation.

HR is a repair pathway that utilizes the presence of a homologous template to restore a DSB. As a result of the template utilization it has been deemed a relatively error-free process. DNA DSBs are detected by γH2AX that recruit repair factors to the break site including those involved in HR (Pardo et al., 2009; Paull et al., 2000). For HR in vertebrates the Mre11-Rad50-Nbs1 (MRN) complex is recruited early to resection the break ends and produce 3' single-stranded DNA (ssDNA) overhangs (Misteli & Soutoglou, 2009). After the ends are processed, with the aid of Rad52 a ring-shaped oligomer and other members of the Rad family, the recombinase Rad51 is brought to the break site where it forms a right-handed helical polymer around the resected end to finish initiating the HR process. It is believed that the presynaptic nucleofilament randomly interacts with different regions of double-stranded (dsDNA) in its quest for homology. Once homology has been located, Rad51 and Rad52 facilitate the invasion of the homologous strand by the resected ssDNA end. Rad54, a member of the Swi2/Snf2 superfamily, also interacts with Rad51 during this process and aids with the subsequent formation of the D-loop and Holliday junction as well as removing and recycling the recombinases once they have completed their respective tasks. Once contact between the homologous template and 3' ssDNA overhang has been established DNA synthesis can copy the template strand and restore the information lost as a consequence of the break. Finally resolvases deconstruct the Holliday junction and return the strands to their original positions. Factors involved in the regulation of this process include replication protein A (RPA), a ssDNA binding protein that can either inhibit or stimulate the binding of Rad51 to ssDNA based on its relative abundance at the break site, and BRCA2, a

recombinase accessory factor that has been suggested to direct Rad52 to the nucleus and override RPA inhibition (Dudas & Chovanec, 2004; Filippo et al., 2008).

NHEJ on the other hand has little regard for homology and consequently has been labeled an error-prone process (Heidenreich et al., 2003). Some of the key proteins that have been implicated in NHEJ are Ku, DNA-dependent protein kinase catalytic subunit (DNA-PK_{CS}), Artemis, XRCC4, XLF, and DNA ligase IV (LigIV) (Iiizumi et al., 2008). The mechanism behind NHEJ is believed to be comprised of an initial recruitment of the heterodimer Ku protein that is composed of Ku70 and Ku80 to the ends of the DSB (Iiizumi et al., 2008). This stabilizes the broken strand and results in the association of the DNA-PKcs with the protein Artemis to form the active DNA-PK (DNA-dependent protein kinase) (Singleton et al., 1999). DNA-PK acts to process the ends and to prepare them for ligation (Iiizumi et al., 2008; Karran, 2000). In the subsequent ligation stage XRCC4, a cofactor for DNA ligase IV, is enlisted to the site of DNA damage by Ku and phosphorylated by DNA-PK (Grawunder et al., 1997; Rapp & Greulich, 2004). It pairs with the protein XLF and then associates with DNA ligase IV to complete the DSB repair (Ahnesorg et al., 2006; Iiizumi et al., 2008). We have chosen to focus on Ku70 and DNA-PK_{CS} because past research has shown its manipulation to be more effective in altering DSB repair than the manipulation of other NHEJ factors (Pierce et al., 2001). They also have been theorized to be involved in direct competition with HR factors for the ends of DSBs (Fattah et al., 2008).

With the knowledge that at least two separate mechanisms exist for DNA DSB repair in eukaryotic cells have come investigations into the mechanisms mediating entry into either HR or NHEJ. It is established that there is some cell cycle dependence mediating this choice (Hochegger et al., 2004). NHEJ is the dominant DSB repair pathway in mammalian cells and the dominance is even more pronounced in the resting, G_1, and early S phase. In the late S phase and G_2 phase the level of HR repair rises as the existence of two sister chromatids emerge. These conclusions have been supported by studies looking at the outcomes of IR-induced DSBs in HR and NHEJ deficient cell lines at different stages of the cell cycle. In chicken DT40 cells, those deficient in Ku70 showed increased IR-sensitivity in the G_1 to early S phase indicating that NHEJ plays an important role during this period of the cell cycle (Bezzubova et al., 1997; Takata et al., 1998). Conversely, DT40 cells deficient in Rad54 have increased sensitivity to IR during the late S and G_2 phases highlighting the importance of HR during these times. Supporting this is the observation that concentrations of cyclin-dependent kinases (CDKs) are low in S phase. CDKs have been shown to phosphorylate BRCA2, a HR protein, and prevent them from interacting with Rad51 (Pardo et al., 2009). In addition, cells deficient in both Ku70 and Rad54 showed a higher degree of IR-sensitivity in G_2 phase than is seen in either single mutant indicating some overlap may exist between the two repair mechanisms. Studies in both mice and humans have shown similar findings (Cheong et al., 1994; Fukushima et al., 2001; Takashima et al., 2009; Valerie & Povirk, 2003). Another mechanism closely tied to cell cycle regulation that appears to mediate the entry into either NHEJ or HR is DNA end resection (Aylon et al., 2004; Jazayeri et al., 2006; Pardo et al., 2009). Marginal resectioning is sufficient for NHEJ while more

extensive 5' DNA end resectioning initiates HR and impedes NHEJ (Pardo et al., 2009). Recently an *in vitro* system using a forked dsDNA substrate was utilised to investigate the interactions between purified human Ku, Mre11, Mre11-Rad50-Xrs2 (MRX) complex, and exonuclease 1 (Sun et al., 2012). The study revealed that Ku can block the resection of the forked dsDNA substrate. Once Ku is bound, MRX is not able to bind or displace Ku. Recently it has been shown that a Ku homolog which binds indefinitely to DNA ends can lead to decreases in resection of DNA ends and consequently - HR (Shao et al., 2012). Accordingly, it has been proposed that some degree of direct cooperation and competition between these two repair pathways may exist (Sonoda et al., 2006).

Cooperation and competition between HR and NHEJ are important and essential. The elimination of one or the other can have detrimental consequences for developing organisms (Orii et al., 2006), and as has already been suggested sometimes the prevalence of one or the other can bestow certain advantages to the organism. Components from both pathways can congregate at the same DSB sites (Rapp & Greulich, 2004; Richardson & Jasin, 2000). Co-localization, FRET imaging, & co-immunoprecipitation techniques in HaCaT cells with UV-A induced DSBs have provided evidence for the association and potentially even cooperation between proteins from both pathways at these sites (Rapp & Greulich, 2004). As well the concurrent loss of proteins from both repair pathways results in more severe phenotypes than the loss of a key player from one individual pathway (Couedel et al., 2004; Mills et al., 2004). Mice lacking both LigIV and Rad54 are more severely impaired in proliferation, unrepaired DSBs, and genomic instability (Mills et al., 2004). However, several studies have suggested that

while cooperation between the two may be present, competition plays a large part. In a study with the DT40 cell line, when cells were deficient in Ku70 the level of HR increased in response to restriction enzyme induced DSBs by I-*Sce*I (Fukushima et al., 2001). In addition, a DNA-PK_{CS} DSB repair deficiency could be relieved to some degree with the simultaneous reduction in Ku70 suggesting that Ku70 prevents other DSB repair pathways from functioning at the break site. Comparable results were seen in another study involving DT40 cells (Adachi et al., 2001). As well findings involving mouse embryonic cells support these results (Frank-Vaillant & Marcand, 2002; Pierce et al., 2001). Another study showed that HR can be inhibited by Ku when it is stabilized by Lif1 (Zhang et al., 2011). In support of competition existing between the two pathways is the observation that NHEJ factors like Ku70 are more abundant in the cell (Haber, 2000; Jackson & Bartek, 2009) and are recruited to the DSBs more rapidly than HR factors (Kim et al., 2005). Both implicate NHEJ as the key competitive DSB repairing process in mammalian cells.

Two predominant DNA DSB repair pathways exist – one of which is involved in mediating gene therapy. As a result of evidence that implicates some degree of competition between the two, one line of thought for improving gene targeting methods has been geared towards shifting the natural balance between the two major DNA repair mechanisms away from NHEJ and towards HR (de Boer et al., 2010; Fattah et al., 2008; Iiizumi et al., 2008; Pierce et al., 2001). Some approaches to accomplish this have been the up-regulation of genes related to HR, the down-regulation of genes related to NHEJ,

or even theoretically the simultaneous use of both (de Boer et al., 2010; Fattah et al., 2008; Iiizumi et al., 2008; Pierce et al., 2001).

Two of the key proteins implicated early in NHEJ are Ku70 and DNA-$PK_{CS.}$ The current study focuses on these two proteins because of their early role in NHEJ DSB repair. Moreover there have been several studies linking down-regulation of Ku70 and DNA-PK_{CS} in different eukaryotes to decreased NHEJ, increased HR, and in some cases an increased gene targeting frequency (Alshahni et al., 2011; Fattah et al., 2008; Pierce et al., 2001; Secretan et al., 2004; Zhang et al., 2011).

Several studies to date have targeted the reduction of Ku. A study in mammalian embryonic stem cells deficient in either Ku70, XRCC4, or DNA-PK_{CS} found that in all mutants, but especially those lacking Ku70, the frequency of HR increased (Pierce et al., 2001). However, the same study showed sister chromatid exchange and gene targeting frequency remained unaffected. In another study involving filamentous yeast the deletion of Ku70 and LigIV resulted in an increased gene targeting frequency at three separate loci to nearly 70%. Comparable findings have been seen in several other studies with yeast (Abdel-Banat et al., 2010; Alshahni et al., 2011; Arentshorst et al., 2012; Wang et al., 2011; Wesolowski-Louvel, 2011; Zhang et al., 2011). Another experiment utilized recombinant adeno-associated virus (rAAV) as a gene targeting vehicle to manufacture Ku70 deficient human somatic cells (Fattah et al., 2008). While $Ku70^{+/-}$ cells were successfully generated, all attempts to generate $Ku70^{-/-}$ cells were unsuccessful. Despite

unsuccessfully creating $Ku70^{-/-}$ cells, unexpectedly it was discovered that $Ku70^{+/-}$ cells yielded a 5 to 10 times higher gene targeting frequency than the wild type at multiple different loci. In addition the use of other techniques to deplete the level of Ku70 showed similar elevated gene targeting frequencies. In 2004, a study in mammalian cells with mutations in either Ku86 or DNA-PK_{CS} revealed NHEJ in Ku86-null cells was compromised, however, levels returned to normal when the cells were rescued with Ku86 (Secretan et al., 2004). Evidence of increased microhomology use was also seen at NHEJ sites along with an overall increased frequency of DNA insertions. Evidence indicates that at the same time the number of random integrations consequently decreases (Hamilton & Thacker, 1987; Jeggo & Smithravin, 1989; Vasquez et al., 2001). DNA-PK_{CS}-null mammalian cells revealed no changes in HR and NHEJ levels indicating there may be a DNA DSB repair mechanism that does not require DNA-PK_{CS}, but does depend on the presence of Ku (Secretan et al., 2004). Together these studies support the conclusion that Ku plays a crucial role in the NHEJ mechanism and implicates reductions in its presence with positive consequences for HR and gene targeting frequencies.

Along with some of the studies already described other research has also been done to investigate the effects of lowering DNA-PK_{CS} levels in cells. In CHO cells a DNA-PK_{CS} deficiency lead to an increase in HR that could be reversed with DNA-PK_{CS} complementation (Allen et al., 2002; Delacote et al., 2002; Shrivastav et al., 2009). DNA-PK_{CS} inhibition induced by DNA-PK_{CS} kinase inhibitors, conversely, have been shown to decrease HR levels and increase IR sensitivity due to overall decreased DSB repair (Allen et al., 2002). The deficient repair potentially may be a result of an inability to

remove DNA-PK$_{CS}$ from the DSB ends leaving them unavailable to repair proteins from other pathways (Allen et al., 2003). This is echoed by severe DSB repair impairments in rAAV-constructed DNA-PK$_{CS}$-deficient human somatic cells (Fattah et al., 2010). Because HR increases in the absence of DNA-PK$_{CS}$ but decreases in the presence of catalytically dysfunctional DNA-PK$_{CS}$, it suggests there is some direct competition for DSB ends between HR and NHEJ. Another study revealed gene therapy could successfully be used to correct a point mutated DNA-PK$_{CS}$ gene in thymoma T cells from severe combined immunodeficient (SCID) mice (Zayed et al., 2006).

The connection between DNA-PK$_{CS}$ and HR has also been investigated. Neal *et al.* (2011) showed that increasing amounts of DNA-PK$_{CS}$ expression plasmids increased HR suppression in DNA-PK$_{CS}$-deficient CHO cells containing a HR substrate. Furthermore, the study uncovered that phosphorylation of certain sites on DNA-PK$_{CS}$ could influence DSB repair choice by stimulating HR and deterring NHEJ (Neal et al., 2011). This study demonstrates changing DNA-PK$_{CS}$ levels can have repercussions for DSB repair pathway choice and corroborate the manipulation of DNA-PK$_{CS}$ as an approach to shift the balance between HR and NHEJ.

While the focus has been on the consequences of Ku and DNA-PK$_{CS}$ level manipulation, other NHEJ proteins can also influence the prevalence of the different DSB repair mechanisms and further provide validation for using such an approach to shift the balance between HR and NHEJ. LigIV -/- chicken DT40 and human Nalm-6 cell lines

displayed elevated gene targeting levels (Iiizumi et al., 2008). In DT40 cells this was accompanied by a reduction in random integrations. The same reduction in random integrations was also implicated in mouse LigIV-/- cells, but was not seen in Nalm-6 cells indicating some repair mechanism other than NHEJ may be responsible for them (Sado et al., 2001). In human cells a XRCC4-deficiency has been linked to severe DNA DSB impairments (Katsube et al., 2011), however, evidence in CHO cells suggests this impairment may be accompanied by a reduction in random integration events (Hamilton & Thacker, 1987; Jeggo & Smithravin, 1989; Vasquez et al., 2001). A mutation in XRCC4 has been shown to increase HR events (Delacote et al., 2002). In human somatic cells recombinant adeno-associated virus (rAAV) was used to manufacture Ku86, DNA-$PK_{CS,}$ XLF, and LigIV deficiencies (Fattah et al., 2010). Severe reductions in DNA DSB repair were detected in cells lacking DNA-$PK_{CS,}$ XLF, and LigIV. Interestingly in cells lacking Ku86 wild-type levels of NHEJ were observed, however, repair events were largely governed by microhomology. When the cells deficient in DNA-PK_{CS} and LigIV were paired with reduced levels of Ku70 the number of NHEJ frequency events increased and was also governed predominantly by microhomology. This evidence implicates the presence of another NHEJ pathway in the absence of the Ku-dependent NHEJ repair.

The notion that a back-up NHEJ (B-NHEJ) repair pathway exists has gained momentum over the last decade and appears to have implications for gene targeting efficiency (Bennardo et al., 2008; Iliakis, 2009; Mladenov & Iliakis, 2011; Perrault et al., 2004; Rass et al., 2012; Wang et al., 2003). B-NHEJ was originally proposed to explain DSB repair that could not be attributed to either classical NHEJ (C-NHEJ) or HR (Perrault et

al., 2004; Secretan et al., 2004; Sonoda et al., 1998; Wang, Zeng, Bui, DiBiase, et al., 2001; Wang, Zeng, Bui, Sonoda, et al., 2001). Even in the absence of NHEJ and HR, the majority of DNA DSBs are still repaired albeit at a slower rate (Wang, Zeng, Bui, DiBiase, et al., 2001; Wang, Zeng, Bui, Sonoda, et al., 2001). Unlike the C-NHEJ pathway that involves limited end processing and no homology utilization, the proposed back-up involves end resectioning and regular use of microhomologies (Rass et al., 2012). B-NHEJ is considered a decidedly mutagenic pathway because it is often associated with genomic deletions and may be responsible for the error prone nature previously attributed to classical NHEJ (C-NHEJ) (Rass et al., 2012). Also, unlike C-NHEJ it is active primarily in the G_2 phase (Wu et al., 2008). B-NHEJ also appears to work independently of the factors involved in C-NHEJ. Instead it has been linked to DNA Ligase III (LigIII), Poly [ADP-ribose] polymerase 1 (Parp-1), and histone H1 (Audebert et al., 2004; Iliakis, 2009; Mladenov & Iliakis, 2011; Wang et al., 2005). However, C-NHEJ proteins like Ku are believed to interact and influence B-NHEJ (Ariumi et al., 1999; Bennardo et al., 2008; Hochegger et al., 2006; Li et al., 2004; Saberi et al., 2007).

Parp-1 is part of the poly(ADP-ribosyl)ation polymerase (PARP) superfamily. Poly(ADP-ribosyl)ation involves the addition of ADP-ribose molecules as a post-translational modification that targets histones and various other nuclear proteins in response to breaks in DNA (Ame et al., 2004). As previously mentioned Parp-1 has been implicated in the proposed B-NHEJ pathway. It arrives at DNA breaks early and there is evidence of interactions between Parp-1 & NHEJ proteins (Ame et al., 2004; Sonoda et

al., 2006). In DT40 cells, immunoprecipitation of a non-DNA binding domain belonging to Parp-1 pulls down Ku70 and DNA-PK (Paddock et al., 2011). Furthermore Parp-$1^{-/-}$ results in diminished gene conversion but is restored with the depletion of Ku70 or LigIV indicating Parp-1 may influence NHEJ proteins (Paddock et al., 2011). The interaction is strengthened by electrophoretic mobility shift assays done using radioactively labelled DNA DSB substrate incubated with Ku and Parp-1 (Wang et al., 2006). Evidence indicated that Ku binds with 10-fold higher affinity than Parp-1, however, as the concentration of Parp-1 increases, increasing amounts of Ku are displaced from the DSB ends. Other studies also provide evidence of interaction between Parp-1 and NHEJ proteins (Ariumi et al., 1999; Galande & Kohwi-Shigematso, 1999; Li et al., 2004).

Parp-1 may also play role in HR, specifically by mediating the competition between Ku and the HR mechanism (Hochegger et al., 2006; Satoh & Lindahl, 1992; Satoh et al., 1993; Shall, 1995). In chicken DT40 cells, the absence of Parp-1 led to decreased HR levels while the concurrent absence of Parp-1 and Ku70 were implicated in HR increase and resistance to DNA damaging agents (Hochegger et al., 2006). Parp-1 chemical inhibition and depletion using shRNA has been linked to the improvement of AAV integration into the AAV genome a process linked to HR (Romanova et al., 2011). B-NHEJ may also be involved in random integrations previously attributed to C-NHEJ. Random integrations involve more homology than would be expected for C-NHEJ, a marker that often accompanies B-NHEJ (Merrihew et al., 1996). Inhibition of poly(ADP-ribosyl)ation resulted in decreased random integration and improved gene targeting frequency at the APRT locus in a CHO cell line (Waldman et al., 1996). The conclusions

drawn establish a role for Parp-1 in DNA DSB repair and potentially as a candidate for improving gene targeting.

The focus of the presented study was to observe the effects of down-regulating Ku70, DNA-PK_{CS}, and Parp-1 on the balance between NHEJ and HR DSB repair in mammalian somatic cells. Two fibroblast cell lines containing a GFP reporter cassette for either NHEJ or HR were utilized (Mao et al., 2008a; Mao et al., 2008b; Waldman et al., 1996). Upon induction of an artificial DSB, only the appropriate repair mechanism restored a functional GFP gene. Anti-Ku70, anti-DNA-PK_{CS}, and anti-Parp-1 antibodies were introduced into the cells lines and subsequent shifts in the DSB repair balance were quantified using flow cytometry. Because the natural frequency of HR, the mechanism responsible for gene targeting, is relatively low in somatic human cells it has been hypothesized that an increase in HR frequency would contribute to an increase in the gene targeting frequency and thus lead to improved gene targeting techniques (Fattah et al., 2008). The objective of this experiment was primarily to manipulate the balance of DNA repair within human cells so that it shifts away from NHEJ and towards HR in order to increase the gene targeting frequency.

By introducing anti-Ku70 antibodies and anti-DNA-PK_{CS} into mammalian cells, it is suspected there will be limitations placed on the amount of Ku70 and DNA-PK_{CS} that is available for the NHEJ mechanism. It is predicted that limiting the resources necessary for NHEJ will result in a decreased frequency of NHEJ and a subsequent compensatory

increased frequency of HR. The use of antibodies would make this shift temporary to circumvent the negative repercussions associated with permanent NHEJ deficits and cause only a limited upset in this balance to occur. It is also predicted that this temporary shift between the DNA repair mechanisms will translate into a temporary shift towards an increase in gene targeting frequencies given the relationship between gene targeting and HR.

The introduction of anti-Parp-1 antibodies will also be tested. Based on previous evidence, it is predicted the downregulation of Parp-1 using antibodies will result in a HR decrease, however, when paired with anti-Ku antibodies an increase in HR is predicted. As was the case with the use of antibodies to downregulate Ku and DNA-PK_{CS}, the temporary nature of this approach is attractive because it minimizes the long-term effects associated with the permanent depletion of this repair protein. Similarly to the use of anti-Ku and anti-DNA-PK_{CS}, the manipulation of HR levels in response to anti-Parp-1 antibodies in combination with anti-Ku70 antibodies may have positive repercussions for gene targeting in cells.

1.1 References

Abdel-Banat, B. M. A., Nonklang, S., Hoshida, H., & Akada, R. (2010). Random and targeted gene integrations through the control of non-homologous end joining in the yeast *Kluyveromyces marxianus*. *Yeast, 27*(1), 29-39. doi: 10.1002/yea.1729

Aboody, K. S., Najbauer, J., & Danks, M. K. (2008). Stem and progenitor cell-mediated tumor selective gene therapy. *Gene Therapy, 15*(10), 739-752. doi: 10.1038/gt.2008.41

Adachi, N., Ishino, T., Ishii, Y., Takeda, S., & Koyama, H. (2001). DNA ligase IV-deficient cells are more resistant to ionizing radiation in the absence of Ku70: Implications for DNA double-strand break repair. *Proceedings of the National Academy of Sciences of the United States of America, 98*(21), 12109-12113. doi: 10.1073/pnas.201271098

Adair, G. M., Nairn, R. S., Wilson, J. H., Seidman, M. M., Brotherman, K. A., Mackinnon, C., & Scheerer, J. B. (1989). Targeted homologous recombination at the endogenous adenine phosphoribosyltransferase locus in chinese-hamster cells. *Proceedings of the National Academy of Sciences of the United States of America, 86*(12), 4574-4578. doi: 10.1073/pnas.86.12.4574

Ahnesorg, P., Smith, P., & Jackson, S. P. (2006). XLF interacts with the XRCC4-DNA ligase IV complex to promote DNA nonhomologous end-joining. *Cell, 124*(2), 301-313. doi: 10.1016/j.cell.2005.12.031

Akhtar, N., *et al*. (2011). Gene therapy: A review article. *Journal of Medicinal Plants Research, 5*(10), 1812-1817.

Allen, C., Halbrook, J., & Nickoloff, J. A. (2003). Interactive competition between homologous recombination and non-homologous end joining. *Molecular Cancer Research, 1*(12), 913-920.

Allen, C., Kurimasa, A., Brenneman, M. A., Chen, D. J., & Nickoloff, J. A. (2002). DNA-dependent protein kinase suppresses double-strand break-induced and spontaneous homologous recombination. *Proceedings of the National Academy of Sciences of the United States of America, 99*(6), 3758-3763. doi: 10.1073/pnas.052545899

Alshahni, M. M., Makimura, K., Satoh, K., Nishiyama, Y., Kido, N., & Sawada, T. (2011). *Cryptococcus yokohamensis* sp nov., a basidiomycetous yeast isolated from trees and a Queensland koala kept in a Japanese zoological park. *International Journal of Systematic and Evolutionary Microbiology, 61*, 3068-3071. doi: 10.1099/ijs.0.027144-0

Ame, J. C., Spenlehauer, C., & de Murcia, G. (2004). The PARP superfamily. *Bioessays, 26*(8), 882-893. doi: 10.1002/bies.20085

Arentshorst, M., Ram, A. F. J., & Meyer, V. (2012). Using non-homologous end-joining-deficient strains for functional gene analyses in filamentous fungi. *Methods in molecular biology (Clifton, N.J.), 835*, 133-150.

Ariumi, Y., *et al*. (1999). Suppression of the poly(ADP-ribose) polymerase activity by DNA-dependent protein kinase in vitro. *Oncogene, 18*(32), 4616-4625. doi: 10.1038/sj.onc.1202823

Audebert, M., Salles, B., & Calsou, P. (2004). Involvement of poly(ADP-ribose) polymerase-1 and XRCC1/DNA ligase III in an alternative route for DNA double-strand breaks rejoining. *Journal of Biological Chemistry, 279*(53), 55117-55126. doi: 10.1074/jbc.M404524200

Avery, O. T., MacLeod, C. M., & McCarty, M. (1944). Studies on the chemical nature of the substance inducing transformation of pneumoccal types induction of transformation by a deoxyribonucleic acid fraction isolated from pneumococcus type III. *Journal of Experimental Medicine, 79*(2), 137-158. doi: 10.1084/jem.79.2.137

Aylon, Y., Liefshitz, B., & Kupiec, M. (2004). The CDK regulates repair of double-strand breaks by homologous recombination during the cell cycle. *Embo Journal, 23*(24), 4868-4875. doi: 10.1038/sj.emboj.7600469

Bainbridge, J. W. B., Tan, M. H., & Ali, R. R. (2006). Gene therapy progress and prospects: The eye. *Gene Therapy, 13*(16), 1191-1197. doi: 10.1038/sj.gt.3302812

Banath, J. P., Olive, P. L. (2003). Expression of phosphorylated histone H2AX as a surrogate of cell killing by drugs that create DNA double-strand breaks. *Cancer Research, 63*(15), 4347-4350.

Bennardo, N., Cheng, A., Huang, N., & Stark, J. M. (2008). Alternative-NHEJ is a mechanistically distinct pathway of mammalian chromosome break repair. *Plos Genetics, 4*(6). doi: e100011010.1371/journal.pgen.1000110

Bezzubova, O., Silbergleit, A., YamaguchiIwai, Y., Takeda, S., & Buerstedde, J. M. (1997). Reduced X-ray resistance and homologous recombination frequencies in a RAD54(-/-) mutant of the chicken DT40 cell line. *Cell, 89*(2), 185-193. doi: 10.1016/s0092-8674(00)80198-1

Cheong, N., Wang, X. M., Wang, Y., & Iliakis, G. (1994). Loss of S-phase-dependent radioresistance in IRS-1 cells exposed to X-rays. *Mutation Research, 314*(1), 77-85. doi: 10.1016/0921-8777(94)90063-9

Couedel, C., *et al*. (2004). Collaboration of homologous recombination and nonhomologous end-joining factors for the survival and integrity of mice and cells. *Genes & Development, 18*(11), 1293-1304. doi: 10.1101/gad.1209204

Dachs, G. U., Tupper, J., & Tozer, G. M. (2005). From bench to bedside for gene-directed enzyme prodrug therapy of cancer. *Anti-Cancer Drugs, 16*(4), 349-359. doi: 10.1097/00001813-200504000-00001

de Boer, P., Bastiaans, J., Touw, H., Kerkman, R., Bronkhof, J., van den Berg, M., & Offringa, R. (2010). Highly efficient gene targeting in Penicillium chrysogenum using the bi-partite approach in Delta lig4 or Delta ku70 mutants. *Fungal Genetics and Biology, 47*(10), 839-846. doi: 10.1016/j.fgb.2010.07.008

de Semir, D., & Aran, J. M. (2006). Targeted gene repair: The ups and downs of a promising gene therapy approach. *Current Gene Therapy, 6*(4), 481-504. doi: 10.2174/156652306777934847

Delacote, F., Han, M. G., Stamato, T. D., Jasin, M., & Lopez, B. S. (2002). An Xrcc4 defect or Wortmannin stimulates homologous recombination specifically induced by double-strand breaks in mammalian cells. *Nucleic Acids Research, 30*(15), 3454-3463. doi: 10.1093/nar/gkf452

Dudas, A., & Chovanec, M. (2004). DNA double-strand break repair by homologous recombination. *Mutation Research-Reviews in Mutation Research, 566*(2), 131-167. doi: 10.1016/j.mrrev.2003.07.001

Fattah, F., Lee, E. H., Weisensel, N., Wang, Y. B., Lichter, N., & Hendrickson, E. A. (2010). Ku regulates the non-homologous end joining pathway choice of DNA double-strand break repair in human somatic cells. *Plos Genetics, 6*(2). doi: e100085510.1371/journal.pgen.1000855

Fattah, F. J., Lichter, N. F., Fattah, K. R., Oh, S., & Hendrickson, E. A. (2008). Ku70, an essential gene, modulates the frequency of rAAV-mediated gene targeting in human somatic cells. *Proceedings of the National Academy of Sciences of the United States of America, 105*(25), 8703-8708. doi: 10.1073/pnas.0712060105

Filippo, J. S., Sung, P., & Klein, H. (2008). Mechanism of eukaryotic homologous recombination. *Annual Review of Biochemistry, 77*, 229-257.

Frank-Vaillant, M., & Marcand, S. (2002). Transient stability of DNA ends allows nonhomologous end joining to precede homologous recombination. *Molecular Cell, 10*(5), 1189-1199. doi: 10.1016/s1097-2765(02)00705-0

Fukushima, T., *et al*. (2001). Genetic analysis of the DNA-dependent protein kinase reveals an inhibitory role of Ku in late S-G(2) phase DNA double-strand break repair. *Journal of Biological Chemistry, 276*(48), 44413-44418. doi: 10.1074/jbc.M106295200

Galande, S., & Kohwi-Shigematso, T. (1999). Poly(ADP-ribose) polymerase and Ku autoantigen form a complex and synergistically bind to matrix attachment sequences. *Journal of Biological Chemistry, 274*(29), 20521-20528. doi: 10.1074/jbc.274.29.20521

Gorbunova, V., & Levy, A. A. (1999). How plants make ends meet: DNA double-strand break repair. *Trends in Plant Science, 4*(7), 263-269. doi: 10.1016/s1360-1385(99)01430-2

Grawunder, U., Wilm, M., Wu, X. T., Kulesza, P., Wilson, T. E., Mann, M., & Lieber, M. R. (1997). Activity of DNA ligase IV stimulated by complex formation with XRCC4 protein in mammalian cells. *Nature, 388*(6641), 492-495.

Haber, J. E. (2000). Partners and pathways - repairing a double-strand break. *Trends in Genetics, 16*(6), 259-264. doi: 10.1016/s0168-9525(00)02022-9

Hamilton, A. A., & Thacker, J. (1987). Gene recombination in X-ray-sensitive hamster-cells. *Molecular and Cellular Biology, 7*(4), 1409-1414.

Hammond, E. M., Dorie, M. J., & Giaccia, A. J. (2003). ATR/ATM targets are phosphorylated by ATR in response to hypoxia and ATM in response to reoxygenation. *Journal of Biological Chemistry, 278*(14), 12207-12213. doi: 10.1074/jbc.M212360200

Hartlerode, A. J., & Scully, R. (2009). Mechanisms of double-strand break repair in somatic mammalian cells. *Biochemical Journal, 423*, 157-168. doi: 10.1042/bj20090942

Heidenreich, E., Novotny, R., Kneidinger, B., Holzmann, V., & Wintersberger, U. (2003). Non-homologous end joining as an important mutagenic process in cell cycle-arrested cells. *Embo Journal, 22*(9), 2274-2283. doi: 10.1093/emboj/cdg203

Helleday, T., Lo, J., van Gent, D. C., & Engelward, B. P. (2007). DNA double-strand break repair: From mechanistic understanding to cancer treatment. *DNA Repair, 6*(7), 923-935. doi: 10.1016/j.dnarep.2007.02.006

Hochegger, H., *et al*. (2006). Parp-1 protects homologous recombination from interference by Ku and ligase IV in vertebrate cells. *Embo Journal, 25*(6), 1305-1314. doi: 10.1038/sj.emboj.7601015

Hochegger, H., Sonoda, E., & Takeda, S. (2004). Post-replication repair in DT40 cells: translesion polymerises versus recombinases. *Bioessays, 26*(2), 151-158. doi: 10.1002/bies.10403

Iiizumi, S., *et al*. (2008). Impact of non-homologous end-joining deficiency on random and targeted DNA integration: implications for gene targeting. *Nucleic Acids Research, 36*(19), 6333-6342. doi: 10.1093/nar/gkn649

Iliakis, G. (2009). Backup pathways of NHEJ in cells of higher eukaryotes: Cell cycle dependence. *Radiotherapy and Oncology, 92*(3), 310-315. doi: 10.1016/j.radonc.2009.06.024

Jackson, S. P., & Bartek, J. (2009). The DNA-damage response in human biology and disease. *Nature, 461*(7267), 1071-1078. doi: 10.1038/nature08467

Jazayeri, A., Falck, J., Lukas, C., Bartek, J., Smith, G. C. M., Lukas, J., & Jackson, S. P. (2006). ATM- and cell cycle-dependent regulation of ATR in response to DNA double-strand breaks. *Nature Cell Biology, 8*(1), 37-U13. doi: 10.1038/ncb1337

Jeggo, P. A., & Smithravin, J. (1989). Decreased stable transfection frequencies of 6 X-ray-sensitive CHO strains, all members of the XRS complementation group. *Mutation Research, 218*(2), 75-86. doi: 10.1016/0921-8777(89)90013-x

Karran, P. (2000). DNA double strand break repair in mammalian cells. *Current Opinion in Genetics & Development, 10*(2), 144-150. doi: 10.1016/s0959-437x(00)00069-1

Katsube, T., Mori, M., Tsuji, H., Shiomi, T., Shiomi, N., & Onoda, M. (2011). Differences in sensitivity to DNA-damaging agents between XRCC4- and artemis-deficient human cells. *Journal of Radiation Research, 52*(4), 415-424. doi: 10.1269/jrr.10168

Keeler, C. E. (1947). Gene therapy. *Journal of Heredity, 38*(10), 294-298.

Kim, J. S., Krasieva, T. B., Kurumizaka, H., Chen, D. J., Taylor, A. M. R., & Yokomori, K. (2005). Independent and sequential recruitment of NHEJ and HR factors to DNA damage sites in mammalian cells. *Journal of Cell Biology, 170*(3), 341-347. doi: 10.1083/jcb.200411083

Klein, S., Zenvirth, D., Dror, V., Barton, A. B., Kaback, D. B., & Simchen, G. (1996). Patterns of meiotic double-strand breakage on native and artificial yeast chromosomes. *Chromosoma, 105*(5), 276-284. doi: 10.1007/bf02524645

Lavu, M., Gundewar, S., & Lefer, D. J. (2011). Gene therapy for ischemic heart disease. *Journal of Molecular and Cellular Cardiology, 50*(5), 742-750. doi: 10.1016/j.yjmcc.2010.06.007

Li, B. M., Navarro, S., Kasahara, N., & Comai, L. (2004). Identification and biochemical characterization of a Werner's syndrome protein complex with Ku70/80 and poly(ADP-ribose) polymerase-1. *Journal of Biological Chemistry, 279*(14), 13659-13667. doi: 10.1074/jbc.M311606200

Li, X., & Heyer, W. D. (2008). Homologous recombination in DNA repair and DNA damage tolerance. *Cell Research, 18*(1), 99-113. doi: 10.1038/cr.2008.1

Liang, F., Han, M. G., Romanienko, P. J., & Jasin, M. (1998). Homology-directed repair is a major double-strand break repair pathway in mammalian cells. *Proceedings of the National Academy of Sciences of the United States of America, 95*(9), 5172-5177. doi: 10.1073/pnas.95.9.5172

Lieber, M. R. (2008). The mechanism of human nonhomologous DNA end joining. *Journal of Biological Chemistry, 283*(1), 1-5. doi: 10.1074/jbc.R700039200

Lieber, M. R., & Karanjawala, Z. E. (2004). Ageing, repetitive genomes and DNA damage. *Nature Reviews Molecular Cell Biology, 5*(1), 69-75. doi: 10.1038/nrm1281

Lieber, M. R., Yu, K., & Raghavan, S. C. (2006). Roles of nonhomologous DNA end joining, V(D)J recombination, and class switch recombination in chromosomal translocations. *DNA Repair, 5*(9-10), 1234-1245. doi: 10.1016/j.dnarep.2006.05.013

Mao, Z., Bozzella, M., Seluanov, A., & Gorbunova, V. (2008a). Comparison of nonhomologous end joining and homologous recombination in human cells. *DNA Repair, 7*(10), 1765-1771. doi: 10.1016/j.dnarep.2008.06.018

Mao, Z., Bozzella, M., Seluanov, A., & Gorbunova, V. (2008b). DNA repair by nonhomologous end joining and homologous recombination during cell cycle in human cells. *Cell Cycle, 7*(18), 2902-2906. doi: 10.4161/cc.7.18.6679

Merrihew, R. V., Marburger, K., Pennington, S. L., Roth, D. B., & Wilson, J. H. (1996). High-frequency illegitimate integration of transfected DNA at preintegrated target sites in a mammalian genome. *Molecular and Cellular Biology, 16*(1), 10-18.

Mills, K. D., Ferguson, D. O., Essers, J., Eckersdorff, M., Kanaar, R., & Alt, F. W. (2004). Rad54 and DNA Ligase IV cooperate to maintain mammalian chromatid stability. *Genes & Development, 18*(11), 1283-1292. doi: 10.1101/gad.1204304

Misteli, T., & Soutoglou, E. (2009). The emerging role of nuclear architecture in DNA repair and genome maintenance. *Nature Reviews Molecular Cell Biology, 10*(4), 243-254. doi: 10.1038/nrm2651

Mladenov, E., & Iliakis, G. (2011). Induction and repair of DNA double strand breaks: The increasing spectrum of non-homologous end joining pathways. *Mutation Research-Fundamental and Molecular Mechanisms of Mutagenesis, 711*(1-2), 61-72. doi: 10.1016/j.mrfmmm.2011.02.005

Mueller, C., & Flotte, T. R. (2008). Gene therapy for cystic fibrosis. *Clinical Reviews in Allergy & Immunology, 35*(3), 164-178. doi: 10.1007/s12016-008-8080-3

Murphy, S. L., & High, K. A. (2008). Gene therapy for haemophilia. *British Journal of Haematology, 140*(5), 479-487. doi: 10.1111/j.1365-2141.2007.06942.x

Neal, J. A., Dang, V., Douglas, P., Wold, M. S., Lees-Miller, S. P., & Meek, K. (2011). Inhibition of homologous recombination by DNA-dependent protein kinase requires kinase activity, is titratable, and is modulated by autophosphorylation. *Molecular and Cellular Biology, 31*(8), 1719-1733. doi: 10.1128/mcb.01298-10

Ohnishi, T., Mori, E., & Takahashi, A. (2009). DNA double-strand breaks: Their production, recognition, and repair in eukaryotes. *Mutation Research-Fundamental and Molecular Mechanisms of Mutagenesis, 669*(1-2), 8-12. doi: 10.1016/j.mrfmmm.2009.06.010

Orii, K. E., Lee, Y., Kondo, N., & McKinnon, P. J. (2006). Selective utilization of nonhomologous end-joining and homologous recombination DNA repair pathways during nervous system development. *Proceedings of the National Academy of Sciences of the United States of America, 103*(26), 10017-10022. doi: 10.1073/pnas.0602436103

Osterman, J. V., Waddell, A., & Aposhian, H. V. (1970). DNA and gene therapy - Uncoating of polyoma pseudovirus in mouse embryo cells. *Proceedings of the National Academy of Sciences of the United States of America, 67*(1), 37-&. doi: 10.1073/pnas.67.1.37

Paddock, M. N., Bauman, A. T., Higdon, R., Kolker, E., Takeda, S., & Scharenberg, A. M. (2011). Competition between PARP-1 and Ku70 control the decision between high-fidelity and mutagenic DNA repair. *DNA Repair, 10*(3), 338-343. doi: 10.1016/j.dnarep.2010.12.005

Pardo, B., Gomez-Gonzalez, B., & Aguilera, A. (2009). DNA repair in mammalian cells. *Cellular and Molecular Life Sciences, 66*(6), 1039-1056. doi: 10.1007/s00018-009-8740-3

Paull, T. T., Rogakou, E. P., Yamazaki, V., Kirchgessner, C. U., Gellert, M., & Bonner, W. M. (2000). A critical role for histone H2AX in recruitment of repair factors to nuclear foci after DNA damage. *Current Biology, 10*(15), 886-895. doi: 10.1016/s0960-9822(00)00610-2

Perrault, R., Wang, H. C., Wang, M. L., Rosidi, B., & Iliakis, G. (2004). Backup pathways of NHEJ are suppressed by DNA-PK. *Journal of Cellular Biochemistry, 92*(4), 781-794. doi: 10.1002/jcb.20104

Pierce, A. J., Hu, P., Han, M. G., Ellis, N., & Jasin, M. (2001). Ku DNA end-binding protein modulates homologous repair of double-strand breaks in mammalian cells. *Genes & Development, 15*(24), 3237-3242. doi: 10.1101/gad.946401

Puchta, H. (2005). The repair of double-strand breaks in plants: mechanisms and consequences for genome evolution. *Journal of Experimental Botany, 56*(409), 1-14. doi: 10.1093/jxb/eri025

Rapp, A., & Greulich, K. O. (2004). After double-strand break induction by UV-A, homologous recombination and nonhomologous end joining cooperate at the same DSB if both systems are available. *Journal of Cell Science, 117*(21), 4935-4945. doi: 10.1242/jcs.01355

Rass, E., Grabarz, A., Bertrand, P., & Lopez, B. S. (2012). Double strand break repair, one mechanism can hide another: Alternative non-homologous end joining. *Cancer Radiotherapie, 16*(1), 1-10. doi: 10.1016/j.canrad.2011.05.004

Richardson, C., & Jasin, M. (2000). Coupled homologous and nonhomologous repair of a double-strand break preserves genomic integrity in mammalian cells. *Molecular and Cellular Biology, 20*(23), 9068-9075. doi: 10.1128/mcb.20.23.9068-9075.2000

Romanova, L. G., Zacharias, J., Cannon, M. L., & Philpott, N. J. (2011). Effect of poly(ADP-ribose) polymerase 1 on integration of the adeno-associated viral vector genome. *Journal of Gene Medicine, 13*(6), 342-352. doi: 10.1002/jgm.1577

Roth, D. B., & Wilson, J. H. (1985). Relative rates of homologous and nonhomologous recombination in transfected DNA. *Proceedings of the National Academy of Sciences of the United States of America, 82*(10), 3355-3359. doi: 10.1073/pnas.82.10.3355

Roth, D. B., & Wilson, J. H. (1986). Nonhomologous recombination in mammalian-cells - Role for short sequence homologies in the joining reaction. *Molecular and Cellular Biology, 6*(12), 4295-4304.

Saberi, A., *et al*. (2007). RAD18 and poly(ADP-ribose) polymerase independently suppress the access of nonhomologous end joining to double-strand breaks and facilitate homologous recombination-mediated repair. *Molecular and Cellular Biology, 27*(7), 2562-2571. doi: 10.1128/mcb.01243-06

Sado, K., Ayusawa, D., Enomoto, A., Suganuma, T., Oshimura, M., Sato, K., & Koyama, H. (2001). Identification of a mutated DNA ligase IV gene in the X-ray-hypersensitive mutant SX10 of mouse FM3A cells. *Journal of Biological Chemistry, 276*(13), 9742-9748. doi: 10.1074/jbc.M010530200

Satoh, M. S., & Lindahl, T. (1992). Role of poly(ADP-ribose) formation in DNA repair. *Nature, 356*(6367), 356-358. doi: 10.1038/356356a0

Satoh, M. S., Poirier, G. G., & Lindahl, T. (1993). NAD+-dependent repair of damaged DNA by human cell-extracts. *Journal of Biological Chemistry, 268*(8), 5480-5487.

Secretan, M. B., Scuric, Z., Oshima, J., Bishop, A. J. R., Howlett, N. G., Yau, D., & Schiestl, R. H. (2004). Effect of Ku86 and DNA-PKcs deficiency on non-homologous end-joining and homologous recombination using a transient transfection assay. *Mutation Research-Fundamental and Molecular Mechanisms of Mutagenesis, 554*(1-2), 351-364. doi: 10.1016/j.mrf,,,.2004.05.016

Sedelnikova, O. A., Horikawa, I., Zimonjic, D. B., Popescu, N. C., Bonner, W. M., & Barrett, J. C. (2004). Senescing human cells and ageing mice accumulate DNA lesions with unrepairable double-strand breaks. *Nature Cell Biology, 6*(2), 168-170. doi: 10.1038/ncb1095

Shall, S. (1995). ADP-ribosylation reactions. *Biochimie, 77*(5), 313-318. doi: 10.1016/0300-9084(96)88140-5

Shao, Z., *et al*. (2012). Persistently bound Ku at DNA ends attenuates DNA end resection and homologous recombination. *DNA Repair, 11*(3), 310-316. doi: 10.1016/j.dnarep.2011.12.007

Shrivastav, M., Miller, C. A., De Haro, L. P., Durant, S. T., Chen, B. P. C., Chen, D. J., & Nickoloff, J. A. (2009). DNA-PKcs and ATM co-regulate DNA double-strand break repair. *DNA Repair, 8*(8), 920-929. doi: 10.1016/j.dnarep.2009.05.006

Singleton, B. K., Torres-Arzayus, M. I., Rottinghaus, S. T., Taccioli, G. E., & Jeggo, P. A. (1999). The C terminus of Ku80 activates the DNA-dependent protein kinase catalytic subunit. *Molecular and Cellular Biology, 19*(5), 3267-3277.

Smithies, O., Gregg, R. G., Boggs, S. S., Koralewski, M. A., & Kucherlapati, R. S. (1985). Insertion of DNA-sequences into the human chromosomal beta-globin locus by homologous recombination. *Nature, 317*(6034), 230-234. doi: 10.1038/317230a0

Sonoda, E., Hochegger, H., Saberi, A., Taniguchi, Y., & Takeda, S. (2006). Differential usage of non-homologous end-joining and homologous recombination in double strand break repair. *DNA Repair, 5*(9-10), 1021-1029. doi: 10.1016/j.dnarep.2006.05.022

Sonoda, E., *et al*. (1998). Rad51-deficient vertebrate cells accumulate chromosomal breaks prior to cell death. *EMBO Journal, 17*(2), 598-608. doi: 10.1093/emboj/17.2.598

Spitzweg, C. (2009). Gene therapy in thyroid cancer. *Hormone and Metabolic Research, 41*(6), 500-509. doi: 10.1055/s-0029-1220744

Sun, J., Lee, K. J., Davis, A. J., & Chen, D. J. (2012). Human Ku70/80 protein blocks exonuclease 1-mediated DNA resection in the presence of human Mre11 or Mre11/Rad50 protein complex. *Journal of Biological Chemistry, 287*(7), 4936-4945. doi: 10.1074/jbc.M111.306167

Takashima, Y., Sakuraba, M., Koizumi, T., Sakamoto, H., Hayashi, M., & Honma, M. (2009). Dependence of DNA double strand break repair pathways on cell cycle phase in human lymphoblastoid cells. *Environmental and Molecular Mutagenesis, 50*(9), 815-822. doi: 10.1002/em.20481

Takata, M., *et al*. (1998). Homologous recombination and non-homologous end-joining pathways of DNA double-strand break repair have overlapping roles in the maintenance of chromosomal integrity in vertebrate cells. *Embo Journal, 17*(18), 5497-5508. doi: 10.1093/emboj/17.18.5497

Tamura, K., Adachi, Y., Chiba, K., Oguchi, K., & Takahashi, H. (2002). Identification of Ku70 and Ku80 homologues in *Arabidopsis thaliana*: Evidence for a role in the repair of DNA double-strand breaks. *Plant Journal, 29*(6), 771-781. doi: 10.1046/j.1365-313X.2002.01258.x

Tatum, E. L. (1966). Molecular biology, nucleic acids, and the future of medicine. *Perspectives in Biology and Medicine, 10*(1), 19-32.

Thomas, K. R., & Capecchi, M. R. (1987). Site-directed mutagenesis by gene targeting in mouse embryo-derived stem-cells. *Cell, 51*(3), 503-512. doi: 10.1016/0092-8674(87)90646-5

Thomas, K. R., Folger, K. R., & Capecchi, M. R. (1986). High-frequency targeting of genes to specific sites in the mammalian genome. *Cell, 44*(3), 419-428. doi: 10.1016/0092-8674(86)90463-0

Valerie, K., & Povirk, L. F. (2003). Regulation and mechanisms of mammalian double-strand break repair. *Oncogene, 22*(37), 5792-5812. doi: 10.1038/sj.onc.1206679

Vasquez, K. M., Marburger, K., Intody, Z., & Wilson, J. H. (2001). Manipulating the mammalian genome by homologous recombination. *Proceedings of the National Academy of Sciences of the United States of America, 98*(15), 8403-8410. doi: 10.1073/pnas.111009698

Vinge, L. E., Raake, P. W., & Koch, W. J. (2008). Gene therapy in heart failure. *Circulation Research, 102*(12), 1458-1470. doi: 10.1161/circresaha.108.173195

Waldman, B. C., Oquinn, J. R., & Waldman, A. S. (1996). Enrichment for gene targeting in mammalian cells by inhibition of poly(ADP-ribosylation). *Biochimica et Biophysica Acta-Gene Structure and Expression, 1308*(3), 241-250. doi: 10.1016/0167-4781(96)00111-x

Wang, H. C., Perrault, A. R., Takeda, Y., Qin, W., Wang, H. Y., & Iliakis, G. (2003). Biochemical evidence for Ku-independent backup pathways of NHEJ. *Nucleic Acids Research, 31*(18), 5377-5388. doi: 10.1093/nar/gkg728

Wang, H. C., Rosidi, B., Perrault, R., Wang, M. L., Zhang, L. H., Windhofer, F., & Iliakis, G. (2005). DNA ligase III as a candidate component of backup pathways of nonhomologous end joining. *Cancer Research, 65*(10), 4020-4030. doi: 10.1158/0008-5472.can-04-3055

Wang, H. C., *et al*. (2001). Nonhomologous end-joining of ionizing radiation-induced DNA double-stranded breaks in human tumor cells deficient in BRCA1 or BRCA2. *Cancer Research, 61*(1), 270-277.

Wang, H. C., Zeng, Z. C., Bui, T. A., Sonoda, E., Takata, M., Takeda, S., & Iliakis, G. (2001). Efficient rejoining of radiation-induced DNA double-strand breaks in vertebrate cells deficient in genes of the RAD52 epistasis group. *Oncogene, 20*(18), 2212-2224. doi: 10.1038/sj.onc.1204350

Wang, M. L., Wu, W. Z., Wu, W. Q., Rosidi, B., Zhang, L. H., Wang, H. C., & Iliakis, G. (2006). PARP-1 and Ku compete for repair of DNA double strand breaks by distinct NHEJ pathways. *Nucleic Acids Research, 34*(21), 6170-6182. doi: 10.1093/nar/gkl840

Wang, N. Y., Yang, S. L., Lin, C. H., & Chung, K. R. (2011). Gene inactivation in the citrus pathogenic fungus *Alternaria alternata* defect at the Ku70 locus associated with non-homologous end joining. *World Journal of Microbiology & Biotechnology, 27*(8), 1817-1826. doi: 10.1007/s11274-010-0640-z

Wesolowski-Louvel, M. (2011). An efficient method to optimize *Kluyveromyces lactis* gene targeting. *Fems Yeast Research, 11*(6), 509-513. doi: 10.1111/j.1567-1364.2011.00741.x

Wu, W., Wang, M., Mussfeldt, T., & Iliakis, G. (2008). Enhanced use of backup pathways of NHEJ in G(2) in Chinese hamster mutant cells with defects in the classical pathway of NHEJ. *Radiation Research, 170*(4), 512-520. doi: 10.1667/rr1456.1

Yanez, R. J., & Porter, A. C. G. (1998). Therapeutic gene targeting. *Gene Therapy, 5*(2), 149-159. doi: 10.1038/sj.gt.3300601

Zayed, H., McIvor, R. S., Wiest, D. L., & Blazar, B. R. (2006). In vitro functional correction of the mutation responsible for murine severe combined immune deficiency by small fragment homologous replacement. *Human Gene Therapy, 17*(2), 158-166. doi: 10.1089/hum.2006.17.158

Zhang, J. X., *et al*. (2011). Ku80 gene is related to non-homologous end-joining and genome stability in *Aspergillus niger*. *Current Microbiology, 62*(4), 1342-1346. doi: 10.1007/s00284-010-9853-5

Chapter 2: Materials and Methods

2.1 General Protocols

Cell Culture – HEK293

Human wildtype HEK293 cells were grown in Dulbecco's Modified Eagle Medium (DMEM) High Glucose (Life Technologies) supplemented with 10% fetal bovine serum (FBS; Thermo Scientific) and 100 U/ml penicillin-streptomycin (Sigma). Cells were grown in a humidified incubator maintained at 6% CO_2 with a temperature of 37°C.

Cell Lines/Constructs Used – HI5c and I9a

Immortalised human foreskin fibroblast cell lines, HCA2-hTERT, containing either a reporter cassette for HR or NHEJ, H15c and I9a respectively, were obtained from Dr. Gorbunova's Lab (University of Rochester). Cells were grown in Eagle's Minimum Essential Medium (ATCC) containing Earles Balanced Salt Solution supplemented with 15% fetal bovine serum (FBS; Thermo Scientific) and 100 U/ml penicillin-streptomycin (Sigma). Growth conditions were kept constant at 6% CO_2 and 37°C.

These reporter cassettes were designed to detect DSB repair events allowing for the quantification of shifts in the frequency of both HR and NHEJ upon the introduction of antibodies against DSB repair proteins. The HR reporter construct integrated into the genome of HCA2-hTERT cells contains two mutated copies of the GFP gene under the

control of a CMV promoter (Mao, et al., 2008a, 2008b)(Figure 2.1). One copy is disrupted by a stuffer sequence that contains a 22 nucleotide deletion in addition to the insertion of two I-*Sce*I recognition sites in inverted orientation to one another. The second copy is truncated and lacks the ATG transcriptional start codon. Only DSBs repaired by HR will result in the restoration of a functional GFP gene. The NHEJ reporter cassette consists of a GFP gene containing an intron from the rat Pem1 gene which has been interrupted by an adenoviral exon that is flanked by I-*Sce*I recognition sites in direct orientation to one another (Mao et al., 2008a, 2008b)(Figure 2.2). Following induction of DSBs by I-*Sce*I, repair by NHEJ will result in GFP expression. To induce DSBs within these cell lines an I-*Sce*I coding vector was used.

Splitting Cells

Cells were grown to target confluency in 10 cm cell culture plates (Sarstedt), the media was removed and the cells were washed with 4 ml of 1x Dulbecco's Phosphate Buffered Saline (DPBS) (Lonza BioWhittaker). Cells were treated with 1 ml of 1x Trysin EDTA (cellgro) and then incubated at 37°C for 2-5 minutes. The appropriate media for the cell line was used to wash the bottom of the plate and evenly suspend the cells. The cells were then transferred to new culture plates or well plates.

Transfections

Cells were grown and then divided into well plates 24 hours prior to transfection. When using Lipofectamine 2000 (Life Technologies), transfection was done at a confluency of about 90%. All treatment samples were transfected using 10 µl of Lipofectamine 2000 (Life Technologies). Chariot (Active Motif) transfections were done when cells were about 40-50% confluent and 6 µl of Chariot (Active Motif) was used per transfection sample. When using Lipofectamine LTX with PLUS Reagent (Life Technologies) or TranSIT LT1 (Mirus), transfection was done at a confluency of about 90%. Unless specified, treatment samples were transfected using 1 µl of PLUS Reagent (Life Technologies) and 5 µl of Lipofectamine LTX (Life Technologies). If using TranSIT LT1 (Mirus), treatment samples were transfected into cells using 0.3 µl of transfection reagent per 100 µl of DNA. Cells were otherwise transfected as per the transfection reagents respective instructions. Cells were incubated at 6% CO_2 and 37°C. Triplicates were used for each experimental and control treatment.

Harvesting Cells – 6-Well Plates (9.6 cm^2/well)

Twenty-four hours after transfection, cells were harvested. The media was removed and the cells were washed with 1 ml of 1x DPBS. Cells were treated with 200 µl of 1x Trysin EDTA (cellgro) and then incubated at 37°C for 2-5 minutes. The trypsinized cells were washed with 3 ml of appropriate media to evenly suspend the cells. The resuspended cells were centrifuged at 4ºC, 3000 rpm for 5 minutes. The media was removed and the cells were resuspended in 10 ml of 1x DPBS then centrifuged again at 4ºC, 3000 rpm for 5

minutes. The DPBS was removed, the cells were resuspended in 2 ml of 1x DPBS, and then kept on ice.

Harvesting Cells – 24-Well Plates (2 cm^2/well)

Twenty-four hours after transfection, cells were harvested. The media was removed and the cells were washed with 0.5 ml of 1x DPBS. Cells were treated with 50 µl of 1x Trysin EDTA (cellgro) and then incubated at 37°C for 2-5 minutes. The trypsinized cells were washed with 1 ml of appropriate media to evenly suspend the cells. The resuspended cells were centrifuged at 4ºC, 1400 rpm for 5 minutes. The media was removed and the cells were resuspended in 1 ml of 1x DPBS then centrifuged again at 4ºC, 1400 rpm for 5 minutes. The DPBS was removed, the cells were resuspended in 0.5-1 ml of 1x DPBS, and then kept on ice.

FACS Analysis

Cells were kept on ice prior to flow cytometer analysis. FACS analysis was done with a BD FACSCanto II flow cytometer. Gating was established using cells only, control plasmid only, gWIZ-GFP (Genlantis) only, and transfection control only treatments when available (Figure 2.3). In cases where there was no gWIZ-GFP only or transfection control plasmid only treatment, gating was done to diagonally split the scatterplot in half around the cells only or control plasmid treatments (Figure 2.3). A FITC versus PE fluorescence or FITC versus APC fluorescence scatterplot was used to analyse the cells.

Viability was determined by gating around the prominent population of expected size on a SSC versus FSC scatterplot. Viability was only calculated in experiments that analysed all events rather than just the viable events. Experiments where only the viable events were analysed are indicated as such. A minimum of 10000 events were analysed for each treatment sample. The software utilised for FACS analysis was BD FACSDiva Software v6.1.3.

General Data Analysis

To counteract the normal differences in transfection efficiencies between treatment samples, normalisation was done using the levels of transfection control plasmid expression. A consistent amount of control plasmid was transfected into each experimental treatment. After data collection, the percentages of both GFP and DsRed or APC positive events for each sample were converted to decimal fractions. The calculated fraction of GFP positive events was then divided by the fraction of DsRed or APC positive events. This value was termed the relative amount of GFP positive events. Normalisation was only done in treatments where a consistent amount of the transfection control was present.

Statistical Analysis

For each treatment group consisting of more than one treatment sample, the mean and standard deviation were calculated (Microsoft Excel for Mac 2011). One-tailed unpaired *t*-tests were used to determine the statistical significance of the experimental data when no change was expected between treatments (Microsoft Excel for Mac 2011). Two-tailed

unpaired *t*-tests were used to determine the statistical significance of the experimental data when either an increase or decrease in the data was expected (Microsoft Excel 2011).

2.2 Delivery of gWIZ-GFP and Antibodies Against GFP into HEK293 Cells

The purpose of introducing both gWIZ-GFP (Genlantis) and antibodies against GFP was to demonstrate through flow cytometry that antibodies could be delivered simultaneously with plasmids into cells. pDsRed-Express2-N1 (Clontech) was used as a transfection control. Mouse monoclonal IgG_{2a} GFP (B-2) antibodies were used (Santa Cruz Biotechnology).

Testing the transfection efficiency of gWIZ-GFP (Genlantis) and pDsRed-Express2-N1 (Clontech) in HEK293.

Four different treatments were done: cells only, 300 ng of gWIZ-GFP (Genlantis), 300 ng of pDsRed-Express2-N1 (Clontech), and 300 ng of control plasmid (pZP500). Cells were split into 6-well plates and transfected using Lipofectamine 2000 (Life Technologies). Following a 24 hour post-transfection incubation period, all treatment samples were harvested and immediately analysed on a BD FACSCanto II flow cytometer.

Comparing the utilisation of Lipofectamine 2000 (Life Technologies) and Chariot (Active Motif) as transfection reagents in HEK293.

Experiment 1:

Lipofectamine 2000 (Life Technologies) was used to transfect 300 ng of control plasmid (pZP500), 300 ng of each gWIZ-GFP (Genlantis) and pDsRed-Express2-N1 (Clontech), or 300 ng of each gWIZ-GFP (Genlantis) and pDsRed-Express2-N1 (Clontech) in addition to 2 μg, 4 μg, or 6 μg of anti-GFP antibodies into HEK293 cells (Table 2.1). Three other treatments were done – one using both Lipofectamine 2000 (Life Technologies) and Chariot (Active Motif) and the other two using only Chariot (Active Motif) (Table 2.1). In the treatment that used both transfection reagents, Lipofectamine 2000 (Life Technologies) was used to introduce 300 ng of each gWIZ-GFP (Genlantis) and pDsRed-Express2-N1 (Clontech) into the cells and 21 hours later Chariot (Active Motif) was used to introduce 3 μg of anti-GFP antibodies into the cells (Table 2.1). This treatment was transfected with Lipofectamine 2000 (Life Technologies) when cells were 70% confluent instead of 90% because Chariot (Active Motif) is more successful when applied to cells at a lower confluency. In the Chariot (Active Motif) only treatment, 300 ng of each gWIZ-GFP (Genlantis) and pDsRed-Express2-N1 (Clontech) in addition to 3 μg of anti-GFP antibodies was used. Cells were split into 6-well plates. Twenty-four hours later the Lipofectamine 2000 (Life Technologies) treatment samples were transfected and then an additional 21 hours later the Chariot (Active Motif) treatment samples were transfected. Cells were harvested 24 hours after transfection of the Lipofectamine-treated treatment samples and 3 hours after transfection of the Chariot

(Active Motif)-treated treatment samples. All treatment samples were harvested and immediately analysed on a BD FACSCanto II flow cytometer.

Experiment 2:

In a second experiment, the following treatments were done in HEK293 using Lipofectamine 2000 (Life Technologies) and Chariot (Active Motif) as transfection reagents: cells only, 300 ng of control plasmid (pZP500), 300 ng of each gWIZ-GFP (Genlantis) and pDsRed-Express2-N1 (Clontech), and 300 ng of each gWIZ-GFP (Genlantis) and pDsRed-Express2-N1 (Clontech) in addition to 1µg of anti-GFP antibodies (Table 2.2). Two additional treatments for Chariot (Active Motif) contained 300 ng of each gWIZ-GFP (Genlantis) and pDsRed-Express2-N1 (Clontech) as well as either 2 µg or 4 µg of anti-GFP antibodies (Table 2.2). Cells were split into 6-well plates. Twenty-four hours later the Lipofectamine-transfected treatment samples were transfected and then an additional 21.5 hours later the Chariot (Active Motif) treatments were transfected. The media was changed for the Chariot (Active Motif)-treated treatment samples 0.5 hours after their transfection and then incubated for an additional 2 hours. Cells were harvested 24 hours after transfection of the Lipofectamine-treated treatment samples and 2.5 hours after transfection of the Chariot (Active Motif)-treated treatment samples. All treatment samples were harvested and immediately analysed on a BD FACSCanto II flow cytometer.

Determining the success of anti-GFP antibody delivery via Lipofectamine 2000 (Life Technologies) through observations of GFP fluorescence changes.

Experiment 1:

HEK293 cells were transfected in 6-well plates with the following different experimental control treatments: cells only, 300 ng of control plasmid (pZP500), 300ng of pDsRed-Express2-N1 (Clontech), and 300ng of both gWIZ-GFP (Genlantis) and pDsRed-Express2-N1 (Clontech) (Table 2.3). Experimental treatments were comprised of 300ng of gWIZ-GFP (Genlantis) and pDsRed-Express2-N1 (Clontech) in addition to either 1 µg, 2 µg, or 5 µg of anti-GFP antibodies (Table 2.3). Cells were split into 6-well plates and then transfected with the respective treatments using Lipofectamine 2000 (Life Technologies). All treatment samples were harvested after 24 hours and immediately analysed on a BD FACSCanto II flow cytometer.

Experiment 2:

The experiment was done similar to Experiment 1, however a few revisions were made (Table 2.4). Cells were split into 24-well plates instead of 6-well plates. Two additional experimental control treatments were done. One contained 300 ng of gWIZ-GFP (Genlantis) only and the other had 5 µg of anti-GFP antibody, 300 ng of gWIZ-GFP (Genlantis) and pDsRed-Express2-N1 (Clontech), and no transfection reagent (Table 2.4). The cells only control was removed. All treatment samples were harvested in 700 µl of 1x DPBS containing 2% FBS. The centrifugation conditions during harvest were room

temperature, 1400 rpm for 5 minutes. A minimum of 20000 viable cells were analysed per treatment sample on the BD FACSCantoII flow cytometer.

Experiment 3:

The experiment was done similar to Experiment 2 (Table 2.4). The only two changes were the utilisation of 6-well plates instead of 24-well plates and a minimum of 20000 events consisting of both viable and nonviable events were analysed per treatment sample.

2.3 Delivery of I-*Sce*I Expression Vector and Antibodies Against DSB DNA Repair Factors into HI5c and I9a Cells

An I-*Sce*I expression vector and antibodies against DSB DNA repair factors were transfected into HI5c and I9a to demonstrate through changes in GFP fluorescence how antibodies affect levels of HR and NHEJ in mammalian cells. The I-*Sce*I expression vector was generously provided by the Gorbunova Lab (University of Rochester). Sequencing had previously been done to verify the expression vector. Mouse monoclonal IgG_{2b} to Ku70 [N3H10] and mouse monoclonal IgG_1 to DNA-PK_{CS} [18-2] antibodies from abcam were used. Additionally, mouse monoclonal IgG_{2a} to PARP-1 (F-2) antibodies (Santa Cruz Biotechnology) were used.

The transfection success of Lipofectamine 2000 (Life Technologies), Lipofectamine LTX with PLUS Reagent (Life Technologies), and TranSIT LT1 (Mirus) in HI5c and I9a.

Experiment 1:

In HI5c cells the following control treatments were transfected into cells using Lipofectamine 2000 (Life Technologies): cells only, 300 ng of pDsRed-Express2-N1 (Clontech), and 300 ng of gWIZ-GFP (Genlantis). In experimental treatments, 300 ng of pDsRed-Express2-N1 (Clontech) was co-transfected with 300 ng, 600 ng, or 1200 ng of I-*Sce*I expression vector. Transfections were conducted in 6-well plates. After the post-transfection incubation, cells were harvested and immediately analyzed by flow cytometry. There were two replicates done per treatment.

Experiment 2:

HI5c and I9a cells were each split into 6-well plates and transfected using Lipofectamine 2000 (Life Technologies). A cells only treatment was used as a control in each cell line. Experimental treatments consisted of either 300 ng, 600 ng, or 1200 ng of pDsRed-Express2-N1 (Clontech) or 300 ng, 600 ng, or 1200 ng of gWIZ-GFP (Genlantis). After the post-transfection incubation, cells were harvested and immediately analyzed by flow cytometry. There were two replicates done per treatment.

Experiment 3:

HI5c and I9a cells were split into 24-well plates and 24 hours later transfected with either Lipofectamine LTX with PLUS Reagent (Life Technologies) or TranSIT LT1 (Mirus). TranSIT LT1 (Mirus) transfections were done using 3 µl of the transfection reagents. Both transfection reagents were used to deliver the following treatments into both cell lines: cells only, 500 ng of pDsRed-Express2-N1 (Clontech), and 500 ng of both pDsRed-Express2-N1 (Clontech) and I-*Sce*I expression vector. Twenty-four hours after transfection, cells were harvested and immediately analyzed by a BD FACSCanto II flow cytometer. The centrifugation conditions during harvest were 2000 rpm at 4ºC for 5 minutes.

Determining the optimal incubation time between transfection and harvest in HI5c and I9a.

Cells were grown and split into 24-well plates. The experimental control treatments used included: 600 ng of control plasmid (pZP500), 600 ng of pDSRed-Express2-N1 (Clontech), and 600 ng of gWIZ-GFP (Genlantis) (Table 2.5). Two experimental treatments were done. The first contained 50 µl of pDsRed-Express2-N1 (Clontech) and 550 µl of I-*Sce*I expression vector (Table 2.5). The second contained 100 µl of pDSRed-Express2-N1 (Clontech) and 1100 µl of I-*Sce*I expression vector (Table 2.5). Each experimental control treatment and experimental treatment was harvested at three different time points – 24 hours post-transfection, 48 hours post-transfection, and 72 hours post-transfection. Treatment samples were transfected using TranSIT LT1 (Mirus).

All treatment samples were harvested in 500 µl of 1x DPBS containing 2% FBS. A minimum of 20000 cells were analysed per treatment sample on the BD FACSCantoII flow cytometer.

Comparing the transfection success of two potential control plasmids -- pDsRed-Express2-N1 (Clontech) and pCMV-Neo-Bam APC (Addgene) – in HI5c and I9a.

HI5c and I9a cells were grown and split into 24-well plates. Five different control treatments were used: cells only, 600 ng of pDsRed-Express2-N1 (Clontech), 600 ng of pCMV-Neo-Bam APC (Addgene), 600 ng of I-*Sce*I expression vector, or 600 ng of gWIZ-GFP (Genlantis) (Table 2.6). Experimental treatments utilized either pDsRed-Express2-N1 (Clontech) or pCMV-Neo-Bam APC (Addgene) as a control plasmid when transfecting I-*Sce*I expression vector into I9a and HI5c cells in ratios of either 300 ng of control plasmid to 300 ng of I-*Sce*I expression vector, 500 ng of control plasmid to 500 ng of I-*Sce*I expression vector, or 400 ng of control plasmid to 600 ng of I-*Sce*I expression vector (Table 2.6). Treatment samples were transfected using Lipofectamine LTX with PLUS reagent. In treatments containing 600 ng of DNA, 3 µl of transfection reagent and 1 µl of PLUS reagent were used. In treatments containing 1000 ng of DNA, 5 µl of transfection reagent and 1 µl of PLUS reagent were used. After a 30 hour post-transfection incubation, cells were harvested in 1 ml of 1x DPBS containing 2% FBS and then analyzed by a BD FACSCanto II flow cytometer. A minimum of 10000 viable events were analysed for each treatment sample.

Checking the I-SceI expression vector in HI5c and I9a.

Experiment 1:

HI5c and I9a cells were transfected with three different controls and four different experimental treatments using Lipofectamine LTX with PLUS reagent (Life Technologies). Cells only, 600 ng of gWIZ-GFP (Genlantis) only, and 600 ng of I-*Sce*I expression vector only were the three controls used. Experimental treatments consisted of either 600 ng of I-*Sce*I expression vector or 1000 ng of I-*Sce*I expression vector using either 3 µl or 5 µl of transfection reagent. Treatments were done as single replicates and can be seen in Table 2.7. Cells were harvested 24 hours later in 1 ml of 1x DPBS. The centrifugation conditions during harvest were 4ºC, 2000 rpm for 5 minutes. All treatment samples underwent FACS analysis.

Experiment 2:

The control treatments used for this experiment were: 600 ng of pZP500 only, 600 ng of pDsRed-Express2-N1 (Clontech) only, and 600 ng of gWIZ-GFP (Genlantis) only (Table 2.8). There were four control treatments each containing 500 ng of one of four different I-*Sce*I expression vector stocks and 100 ng of pDsRed-Express2-N1 (Clontech) as a transfection control (Table 2.8). Cells were transfected using 3 µl of Lipofectamine LTX (Life Technologies) with 1 µl of PLUS reagent (Life Technologies) in all treatments.

Treatments were done as single replicates. Cells were harvested 30 hours later in 500 µl of 1x DPBS containing 2% FBS and analysed by flow cytometer.

Determining the effect of anti-Ku, anti-DNA-PK$_{CS}$, anti-PARP-1 antibodies on HR and NHEJ levels in HI5c and I9a cells.

Experiment 1:

Cells were grown and split into 24-well plates 24 hours prior to transfection. Transfections were done using Lipofectamine LTX with Plus Reagent (Life Technologies). Control treatments for the experiment included: cells only, 400 ng of pDsRed-Express2-N1 (Clontech), 600 ng of I-*Sce*I expression vector, and one using both 400 ng of pDsRed-Express2-N1 (Clontech) and 600 ng of I-*Sce*I expression vector (Table 2.9). In experimental treatments where antibodies were delivered simultaneously with the plasmids, 400 ng of pDsRed-Express2-N1 (Clontech) and 600 ng of *I-SceI* expression vector were used (Table 2.9). Two amounts of each antibody were used, 2.5 µg and 5.0 µg (Table 2.9). The antibodies tested were mouse monoclonal antibodies to Ku70 and mouse monoclonal antibodies to DNA-PK$_{CS}$. Cells were harvested in 1 ml of 1x DPBS and analysed on the flow cytometer. The centrifugation conditions during harvest were 4ºC, 2000 rpm for 5 minutes.

Experiment 2:

Cells were grown and split one day prior to transfection into 24-well plates. Transfections were done using Lipofectamine LTX with Plus Reagent (Life Technologies). 600 ng of a control plasmid (pZP500), gWIZ-GFP (Genlantis), and pDsRed-Express2-N1 (Clontech) were each used as controls (Table 2.10). Another control containing both 700 ng of I-*Sce*I expression vector and 100 ng of pDsRed-Express2-N1 (Clontech) was also used (Table 2.10). In experimental treatments where antibodies were delivered simultaneously with the plasmids, 700 ng of I-*Sce*I expression vector and 100 ng of pDsRed-Express2-N1 (Clontech) were used (Table 2.10). Each of the following antibodies were tested: mouse monoclonal anti-6X His tag antibody (abcam), mouse monoclonal antibodies to Ku70, mouse monoclonal antibodies to DNA-PK_{CS}, and mouse monoclonal antibodies to PARP-1 (Table 2.10). The concentrations of antibodies applied were 2.5 µg and 5.0 µg (Table 2.10). One additional treatment group included the use of both Ku70 and DNA-PK_{CS} antibodies, at two concentrations of 1.25 µg each and 2.5 µg each (Table 2.10). In treatments containing 600 ng of DNA, 3 µl of transfection reagent and 1 µl of PLUS reagent were used. In treatments containing 800 ng of DNA, 3.5 µl of transfection reagent and 1 µl of PLUS reagent were used. Cells were harvested 30 hrs after transfection in 700 µl of 2% FBS 1x DPBS and analysed on the flow cytometer. A BD FACSCanto II flow cytometer was used for FACS analysis. For each sample at least 20000 cells were analysed.

Table 2.1: Treatments for comparing Lipofectamine 2000 (Life Technologies) and Chariot (Active Motif) as transfection reagents in HEK293. The treatments also worked to observe how transfecting anti-GFP antibodies in conjunction with gWIZ-GFP (Genlantis) affect GFP fluorescence.

No.	Treatment	Delivery Method	gWIZ-GFP (ng)	pDsRed-Express2-N1 (ng)	pZP500 (ng)	Anti-GFP (µg)
1	pZP500	Lipofectamine 2000	---------	---------	300	------
2	gWIZ-GFP, pDsRed-Express2-N1	Lipofectamine 2000	300	300	---------	------
3	gWIZ-GFP, pDsRed-Express2-N1, Ab	Lipofectamine 2000	300	300	---------	2
4	gWIZ-GFP, pDsRed-Express2-N1, Ab	Lipofectamine 2000	300	300	---------	4
5	gWIZ-GFP, pDsRed-Express2-N1, Ab	Lipofectamine 2000	300	300	---------	6
6	gWIZ-GFP, pDsRed-Express2-N1, Ab	Lipofectamine 2000/Chariot	300	300	---------	3
7	gWIZ-GFP, pDsRed-Express2-N1, Ab	Chariot	300	300	---------	3

Table 2.2: Treatments for comparing Lipofectamine 2000 (Life Technologies) and Chariot (Active Motif) as transfection reagents in HEK293.

No.	Treatment	Delivery Method	gWIZ-GFP (ng)	pDsRed-Express2-N1 (ng)	pZP500 (ng)	Anti-GFP (µg)
1	Cells Only	Lipofectamine 2000	----------	----------	----------	--------
2	Cells Only	Chariot	----------	----------	----------	--------
3	gWIZ-GFP, pDsRed-Express2-N1	Lipofectamine 2000	300	300	----------	--------
4	gWIZ-GFP, pDsRed-Express2-N1	Chariot	300	300	----------	--------
5	pZP500	Lipofectamine 2000	----------	----------	300	--------
6	pZP500	Chariot	----------	----------	300	--------
7	gWIZ-GFP, pDsRed-Express2-N1, Ab	Lipofectamine 2000	300	300	----------	1
8	gWIZ-GFP, pDsRed-Express2-N1, Ab	Chariot	300	300	----------	1
9	gWIZ-GFP, pDsRed-Express2-N1, Ab	Chariot	300	300	----------	2
10	gWIZ-GFP, pDsRed-Express2-N1, Ab	Chariot	300	300	----------	4

Table 2.3: Treatments in Experiment 1 for determining the success of anti-GFP antibody delivery via Lipofectamine 2000 (Life Technologies) through observations of GFP fluorescence changes.

No.	Treatment	pZP500 (ng)	pDsRed-Express2-N1 (ng)	gWIZ-GFP (ng)	Anti-GFP (µg)
1	Cells Only	----------	----------	----------	----------
2	pZP500	300	----------	----------	----------
3	pDsRed-Express2-N1	----------	300	----------	----------
4	pDsRed-Express2-N1, gWIZ-GFP	----------	300	300	----------
5	Anti-GFP Antibody – 1 µg	----------	300	300	1
6	Anti-GFP Antibody – 2 µg	----------	300	300	2
7	Anti-GFP Antibody – 5 µg	----------	300	300	5

Table 2.4: Treatments in Experiment 2 and 3 for determining the success of anti-GFP antibody delivery via Lipofectamine 2000 (Life Technologies) through observations of GFP fluorescence changes.

No.	Treatment	Delivery Method	pZP500 (ng)	pDsRed-Express2-N1 (ng)	gWIZ-GFP (ng)	Anti-GFP (µg)
1	pZP500	Lipofectamine 2000	300	----------	----------	----------
2	pDsRed-Express2-N1	Lipofectamine 2000	----------	300	----------	----------
3	gWIZ-GFP	Lipofectamine 2000	----------	----------	300	----------
4	pDsRed-Express2-N1, gWIZ-GFP	Lipofectamine 2000	----------	300	300	----------
5	GFP Antibody – 1 µg	Lipofectamine 2000	----------	300	300	1
6	GFP Antibody – 2 µg	Lipofectamine 2000	----------	300	300	2
7	GFP Antibody – 5 µg	Lipofectamine 2000	----------	300	300	5
8	GFP Antibody – 5 µg NO TR	None	----------	----------	----------	5

Table 2.5: Treatments for determining the optimal incubation time between transfection and harvest in HI5c and I9a. All treatments were transfected with TranSIT LT1 (Mirus) and then harvested at a 24 hour, 48 hour, or 72 hour post-transfection time point.

No.	Treatment	pZP500 or pDsRed-Express2-N1(ng)	pI-*Sce*I or gWIZ-GFP(ng)	TR (µl)	Time btwn Transfection & Harvest (hrs)
1	pZP500	600	----------	1.8	24/48/72
2	pDsRed-Express2-N1	600	----------	1.8	24/48/72
3	gWIZ-GFP	----------	600	1.8	24/48/72
4	DsRed:*I-SceI* LOW	50	550	1.8	24/48/72
5	DsRed:*I-SceI* HIGH	100	1100	3.6	24/48/72

Table 2.6: Treatments for comparing the transfection success of two potential control plasmids -- pDsRed-Express2-N1 (Clontech) and pCMV-Neo-Bam APC (Addgene) – in HI5c and I9a. All treatments were transfected with Lipofectamine LTX with PLUS Reagent (Invitrogen).

No.	Treatment	pCMV-Neo-Bam APC or pDsRed-Express2-N1(ng)	pI-*Sce*I or gWIZ-GFP(ng)
1	Cells Only	----------	----------
2	pDsRed-Express2-N1	600	----------
3	pCMV-Neo-Bam APC	600	----------
4	I-*Sce*I expression vector	----------	600
5	gWIZ-GFP	----------	600
6	pCMV-Neo-Bam APC + I-*Sce*I expression vector 300:300	300	300
7	pCMV-Neo-Bam APC + I-*Sce*I expression vector 500:500	500	500
8	pCMV-Neo-Bam APC + I-*Sce*I expression vector 400:600	400	600
9	pCMV-Neo-Bam APC + I-*Sce*I expression vector 300:300	300	300
10	pCMV-Neo-Bam APC + I-*Sce*I expression vector 500:500	500	500
11	pCMV-Neo-Bam APC + I-*Sce*I expression vector 400:600	400	600

Table 2.7: Treatments in Experiment 1 to check the I-*Sce*I expression vector in HI5c and I9a. All treatments were transfected with Lipofectamine LTX with PLUS Reagent (Invitrogen).

No.	Treatment	gWIZ-GFP (ng)	pI-*Sce*I (ng)	TR (µl)
1	Cells Only	----------	----------	3
2	gWIZ-GFP	600	----------	3
3	I-*Sce*I expression vector - 600ng	----------	600	3
4	I-*Sce*I expression vector - 1000ng	----------	1000	3
5	I-*Sce*I expression vector - 600ng	----------	600	5
6	I-*Sce*I expression vector - 1000ng	----------	1000	5

Table 2.8: Treatments in Experiment 2 to check the I-*Sce*I expression vector in HI5c. All treatments were transfected with Lipofectamine LTX with PLUS Reagent (Invitrogen).

No.	Treatment	pZP500 (ng)	pDsRed-Express2-N1 (ng)	gWIZ-GFP or pI-*Sce*I (ng)
1	pZP500	600	----------	----------
2	pDsRed-Express2-N1	----------	600	----------
3	gWIZ-GFP	----------	----------	600
4	I-*Sce*I expression vector A	----------	100	500
5	I-*Sce*I expression vector B	----------	100	500
6	I-*Sce*I expression vector C	----------	100	500
7	I-*Sce*I expression vector D	----------	100	500

Table 2.9: Treatments in Experiment 1 for examining the effect of anti-Ku and anti-DNA-PK$_{CS}$ antibodies on HR and NHEJ levels in HI5c and I9a cells. The transfection reagent used for all treatments was Lipofectamine LTX with PLUS Reagent (Invitrogen).

No.	Treatment	pDsRed-Express2-N1 (ng)	pI-*Sce*I (ng)	Anti-GFP (µg)
1	Cells Only	----------	--------	------
2	pDsRed-Express2-N1	400	--------	------
3	I-*Sce*I expression vector	----------	600	------
4	pDsRed-Express2-N1 + I-*Sce*I expression vector	400	600	------
5	pDsRed-Express2-N1 + I-*Sce*I expression vector + DNA-PK 0.5 µg	400	600	0.5
6	pDsRed-Express2-N1 + I-*Sce*I expression vector + DNA-PK 1 µg	400	600	1
7	pDsRed-Express2-N1 + I-*Sce*I expression vector + Ku70 0.5 µg	400	600	0.5
8	pDsRed-Express2-N1 + I-*Sce*I expression vector + Ku70 1 µg	400	600	1

Table 2.10: Treatments in Experiment 2 for examining the effect of anti-Ku, anti-DNA-PK$_{CS}$, anti-PARP-1 antibodies on HR and NHEJ levels in HI5c and I9a cells.

All treatments were transfected with Lipofectamine LTX with PLUS Reagent (Invitrogen).

No.	Treatment	pDsRed-Express2-N1 (ng)	pI-SceI or gWIZ-GFP (ng)	Anti-GFP (µg)
1	pZP500	600	----------	------
2	pDsRed_Express2-N1	600	----------	------
3	gWIZ-GFP	----------	600	------
4	pDsRed-Express2-N1 + I-*Sce*I expression vector	100	700	------
5	pDsRed-Express2-N1 + I-*Sce*I expression vector + Ctr Ab 2.5 µg	100	700	0.5
6	pDsRed-Express2-N1 + I-*Sce*I expression vector + Ctr Ab 5 µg	100	700	1
7	pDsRed-Express2-N1 + I-*Sce*I expression vector + Ku70 2.5 µg	100	700	0.5
8	pDsRed-Express2-N1 + I-*Sce*I expression vector + Ku70 1 µg	100	700	1
9	pDsRed-Express2-N1 + I-*Sce*I expression vector + DNA-PK 0.5 µg	100	700	0.5
10	pDsRed-Express2-N1 + I-*Sce*I expression vector + DNA-PK 1 µg	100	700	1
11	pDsRed-Express2-N1 + I-*Sce*I expression vector + Parp1 0.5 µg	100	700	0.5
12	pDsRed-Express2-N1 + I-*Sce*I expression vector + Parp1 1 µg	100	700	1

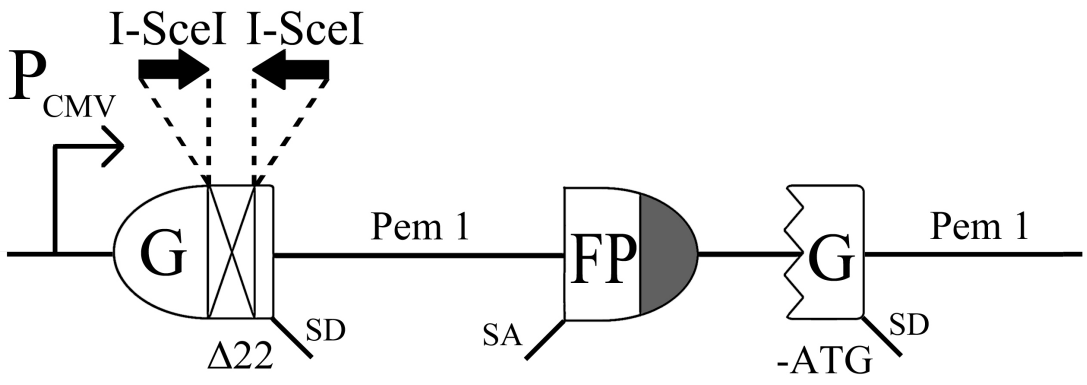

Figure 2.1: HR Reporter Cassette. The HR reporter construct contains two mutated copies of the GFP gene under the control of a CMV promoter (P_{CMV}). One copy is disrupted by a stuffer sequence (+) and contains a 22 nucleotide deletion (Δ22) in addition to the insertion of two I-*Sce*I recognition sites in inverted orientation to one another. The second copy is truncated and lacks the ATG transcriptional start codon (-ATG). SA – splice acceptor, SD – splice donor, dark grey shaded semi-circle.

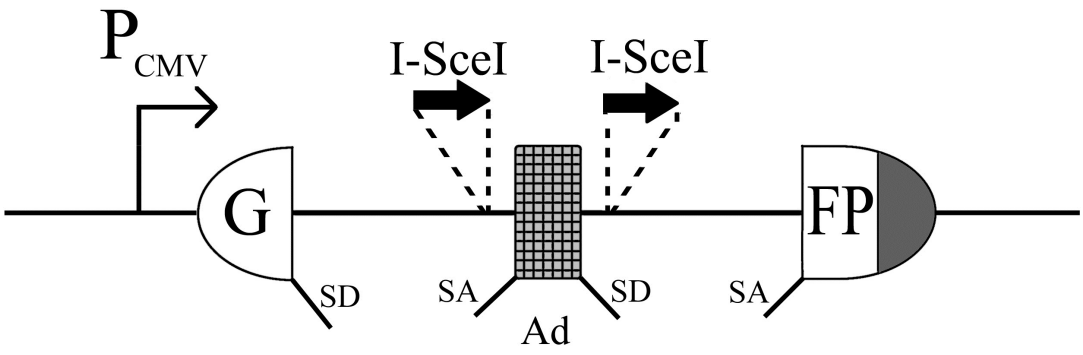

Figure 2.2: NHEJ Reporter Cassette. The NHEJ reporter cassette consists of a GFP gene containing an intron from the rat Pem1 gene which has been interrupted by an adenoviral exon (Ad, light grey crosshatched box) that is flanked by I-*Sce*I recognition sites in direct orientation to one another. SA – splice acceptor, SD – splice donor, dark grey shaded semi-circle, P_{CMV} – CMV promoter.

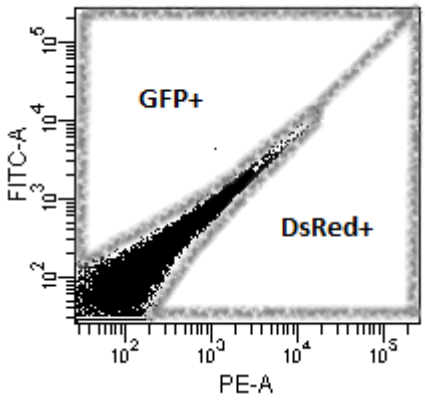

Figure 2.3: Sample FACS Analysis Gating. Grey lines are representative of FACS analysis gating boundaries. Events within the GFP+ gated area were considered to be GFP positive events. Events within the DsRed+ gated area were considered to be DsRed positive events.

2.4 References

Mao, Z., Bozzella, M., Seluanov, A., & Gorbunova, V. (2008a). Comparison of nonhomologous end joining and homologous recombination in human cells. *DNA Repair, 7*(10), 1765-1771. doi: 10.1016/j.dnarep.2008.06.018

Mao, Z., Bozzella, M., Seluanov, A., & Gorbunova, V. (2008b). DNA repair by nonhomologous end joining and homologous recombination during cell cycle in human cells. *Cell Cycle, 7*(18), 2902-2906. doi: 10.4161/cc.7.18.6679

Chapter 3: Results

3.1 Delivery of gWIZ-GFP (Genlantis) and Antibodies Against GFP into HEK293 Cells

Optimal Conditions for the Transfection of gWIZ-GFP (Genlantis) and pDsRed-Express2-N1 (Clontech).

Unpublished work done previously in the lab tested the optimal amount of DNA, ratio of gWIZ-GFP (Genlantis) to pDsRed-Express2-N1 (Clontech), time between transfection and harvest, and cell line to be used were determined. Optimizations had been done in two cell lines, MCF7 and HEK293, and harvested at two post-transfection incubation time points, 24 hours and 48 hours (Table 3.1). Three different amounts of total DNA – 300 ng, 600 ng, and 1200 ng – were tested. Each total DNA amount was used in five different ratios of gWIZ-GFP (Genlantis) to pDsRed-Express2-N1 (Clontech) -- 1:0, 1:1, 2:1, 1:2, and 0:1. It was determined the overall highest level of positive fluorescent events was in the treatment with HEK293, a 24 hour post-transfection incubation period, and 600 ng of total DNA in a ratio of 300 ng gWIZ-GFP (Genlantis) to 300 ng pDsRed-Express2-N1 (Clontech). As a result, all experiments were done using these conditions.

Two experiments were initially done using the optimized conditions to determine how the concurrent introduction of 0.5 µg, 0.75 µg, or 1 µg of anti-GFP antibodies with the

gWIZ-GFP (Genlantis) plasmid affects GFP fluorescence. The cells were fixed in ethanol and then stored for five weeks prior to FACS analysis. In all these treatments there was little to no fluorescence observed including the gWIZ-GFP (Genlantis) only control. Ethanol creates large enough perforations in cells for GFP to leak out making it an inappropriate method of cell harvest preparation for this project (Palm et al., 1999). Thus, in all ensuing experiments, cells were harvested and prepared for FACS analysis without using ethanol fixation.

The transfection success of 300 ng of gWIZ-GFP (Genlantis) and 300 ng of pDsRed-Express2-N1 (Clontech) was also tested individually. There was no fluorescence signal detected in cells only and pZP500 only treatments (Figure 3.1). In the gWIZ-GFP (Genlantis) only treatment there were several GFP positive fluorescing events detected while in the pDsRed-Express2-N1 (Clontech) only treatment there were several DsRed positive events (Figure 3.1).

An unexpected observation was the difference in the percentages of viable events between the treatments (Figure 3.2). Harvesting samples was initiated at the same time for all treatments, however, because not all the treatment samples could be placed in the centrifuge at once, cells from Treatments 3 (pDsRed-Express2-N1 (Clontech) only) and 4 (pZP500 only) were left on the ice for about 45 minutes longer and analysed about 90 minutes later than those from Treatments 1 (cells only) and 2 (gWIZ-GFP (Genlantis) only). The viability percentages from Treatments 3 and 4 were similar and significantly

(*t*-test, $P<0.01$ in all cases, n = 3) lower than the viability percentages seen in Treatments 1 and 2. There was no significant difference in viability between Treatments 1 and 2 or between Treatments 3 and 4 (Table 3.2). The lengthy time lapse between harvest initiation and FACS analysis may have an effect on sample viability. To prevent this factor from influencing future results, cells were harvested in smaller batches with one batch being harvested and processed in entirety before harvest initiation of the next.

The experiments showed gWIZ-GFP (Genlantis) and pDsRed-Express2-N1 (Clontech) could be successfully transfected into HEK293 cells and the fluorescence of expressed GFP and DsRed could be successfully detected using flow cytometry. The experiments also influenced how future experiments in this project were designed and how cells were harvested and processed for FACS analysis.

Comparing the utilisation of Lipofectamine 2000 (Life Technologies) and Chariot (Active Motif) as transfection reagents in HEK293 for the co-delivery of gWIZ-GFP (Genlantis), pDsRed-Express2-N1 (Clontech), and anti-GPF antibody.

Two different delivery mechanisms were used to introduce gWIZ-GFP (Genlantis), pDsRed-Express2-N1 (Clontech), and anti-GPF antibodies into HEK293 cells (Table 3.3). Lipofectamine 2000 is a routine transfection reagent used in our lab while Chariot

was chosen because it is a commercially available cell-penetrating peptide (CPP) capable of delivering antibodies into cells.

In treatments containing gWIZ-GFP (Genlantis) and pDsRed-Express2-N1 (Clontech), GFP and DsRed positive events were respectively seen in HEK293 cells when Lipofectamine 2000 was utilized as the transfection reagent (Figure 3.3a). When 2 μg or 6 μg of anti-GFP antibodies were introduced along with both plasmids into HEK293 cells, there was an elevated but not significant change in GFP positive events. However, when 4 μg of the antibody was used there was a slight but significant (*t*-test, $P<0.05$) increase in GFP fluorescent events. No significant differences in data among the antibody treatments were identified. When the relative number of GFP events was normalised using the fraction of DsRed positive events in each sample, there were no significant differences in the relative amount of GFP events between the control and antibody treatments (Figure 3.4a). The level of GFP positive events after normalisation does however appear to spike in the presence of 2 μg of antibody. Then as the antibody amount increases, they drop back down to the levels of GFP positive events seen in the control.

The standard deviation for the viability and GFP positive events in the 2 μg (Treatment 3) and 4 μg (Treatment 5) antibody treatments was noticeably large compared to the other treatments (Figures 3.3, 3.4 and 3.5). After looking at the data it was apparent that one sample per treatment was responsible. The removal of this data point and subsequent

analysis reveals there was still no significant change in fluorescence patterns when 2 µg of antibody was introduced and there was still a significant (*t*-test, $P<0.05$) increase in the percentage of GFP positive events when 4 µg of antibody was introduced (Figure 3.3b). It is interesting to note, however, that with the removal of the two data points there was now a slight but significant (*t*-test, $P<0.05$) increase in the percentage of GFP positive events in the 6 µg antibody treatment when compared to the no antibody control. There were no significant changes in the GFP fluorescence percentages among the antibody treatments both before and after the outliers were removed. After normalisation, there was no significant differences in the level of GFP positive events between the control and the treatment containing 6 µg of anti-GFP antibodies, but there was a significant (*t*-test, $P<0.05$ in both cases) increase in the GFP positive events when both 2 µg and 4 µg of antibody was present (Figure 3.4b). Similar to when the outliers were present, there was a spike in GFP positive events with 2 µg of antibody which then dropped down to control levels as the amount increased. Among the antibody treatments, a significant (*t*-test, $P<0.05$) difference was only seen between the 2 µg and 6 µg treatments.

The percentage of DsRed positive events displayed the same pattern both before and after the removal of the outlier data points (Figures 3.3 and 3.5). The percentage drops significantly (*t*-test, $P<0.001$ both before and after outlier removal) in the presence of 2 µg of anti-GFP antibody; then increases with increasing amounts of antibody. The increases between antibody treatments were not significant. Additionally, the percentages of DsRed events in the 4 µg and 6 µg treatments did not differ significantly from the no antibody control.

In the treatment transfected only with Chariot the same observations were not seen. In all cases, based on fluorescence, there was no indication that either gWIZ-GFP (Genlantis) or pDsRed-Express2-N1 (Clontech) was transfected into and expressed in HEK293 cells (Figure 3.3 and 3.4). These findings were supported by a second experiment. It compared Lipofectamine 2000 and Chariot as transfection reagents for the following treatments in HEK293: cells only, 300 ng of control plasmid (pZP500), 300 ng of each gWIZ-GFP (Genlantis) and pDsRed-Express2-N1 (Clontech), and 300 ng of each gWIZ-GFP (Genlantis) and pDsRed-Express2-N1 (Clontech) in addition to 1 μg of anti-GFP antibodies (Supplementary Table 3.1). Two additional treatments for Chariot (Active Motif) contained 300 ng of each gWIZ-GFP (Genlantis) and pDsRed-Express2-N1 (Clontech) as well as either 2 μg or 4 μg of anti-GFP antibodies. GFP and DsRed positive events were only detected in treatments transfected with Lipofectamine 2000 (Supplementary Figure 3.1 and 3.2).

A final treatment in this experiment used Lipofectamine 2000 to transfect plasmids into cells 24 hours prior to harvest and then used Chariot to deliver antibodies three hours prior to harvest. This was done to utilize the different transfection reagents in their specific delivery role. This allowed for both protocols to be followed while also providing enough time for the plasmids to be expressed. Unlike Chariot only treatments, in this treatment there were GFP and DsRed positive events present (Figure 3.3 and 3.5). Based on fluorescence because there was little difference in GFP positive events when

compared to the control, there was also no indication the antibodies were successfully delivered both before and after normalisation (Figure 3.4). There was also diminutive change in DsRed positive events compared to the no antibody control (Figure 3.3 and 3.5). Based on the two experiments done, Lipofectamine 2000 was the reagent chosen to use for all future experiments in HEK293.

Determining the success of anti-GFP antibody delivery via Lipofectamine 2000 through observations of GFP fluorescence changes.

Three experiments were done to test how anti-GFP antibodies affect the percentage of GFP positive events in HEK293 cells transfected with Lipofectamine 2000 in the presence of gWIZ-GFP (Genlantis) and anti-GFP antibodies (Table 3.4 and 3.5). For each experiment, three different amounts of antibodies were tested: 1 µg, 2 µg, and 5 µg.

In all three experiments the same two general trends were present – the presence of anti-GFP antibodies was associated with elevated GFP positive events and as the amount of antibodies increased the number of DsRed positive events decreased (Figure 3.6). The increase in GFP positive events was significant (*t*-test, $P<0.05$ in all cases) in all experiments when 1 µg of anti-GFP antibodies were present (Table 3.6). When 2 µg of antibodies were present the increase was significant (*t*-test, $P<0.01$ in both cases) in two of the experiments, and when 5 µg was present the increase was only significant (*t*-test,

P<0.01) in one experiment. The decrease in DsRed positive events was significant (*t*-test, *P*<0.05 for Experiment 1 and *P*<0.05 for Experiment 2) in two experiments when 5 µg of antibodies was present and also significant (*t*-test, *P*<0.05 for Experiment 1 and *P*<0.001 for Experiment 2) in two experiments when 2 µg of antibodies was present. There were no instances when the presence of 1 µg of anti-GFP antibodies was associated with a significant decrease in DsRed positive events.

There was also a common trend among all three experiments after normalisation. With increasing amounts of anti-GFP antibodies there was an increase in relative amounts of GFP positive events (Figure 3.7). The increase in GFP positive events was only significant (*t*-test, *P*<0.01) in the first experiment between the no antibody control and the treatment with 5 µg of antibodies (Table 3.6). The third experiment saw significant (*t*-test, *P*<0.05 for 2 µg and *P*<0.001 for 5 µg) increases in the relative amounts of GFP positive events when both 2 µg and 5 µg of antibodies were present. Consequently there was also a significant (*t*-test, *P*<0.05) difference between those two treatments. In the second experiment, a significant (*t*-test, *P*<0.001 for 1 µg and *P*<0.01 for both 2 µg and 5 µg) increase was seen for 1 µg, 2 µg, and 5 µg of antibodies when compared to the no antibody control. The increase in GFP positive events when compared to the control was accompanied by significant (*t*-test, *P*<0.01 between 1 µg and 2 µg and *P*<0.05 between Treatments 2 µg and 5 µg) increases as the amount of antibodies increased between treatments. There were no significant differences between the viability of the antibody treatments and the 0 µg antibody control in all cases (Supplementary Figure 3.3).

3.2 Delivery of I-*Sce*I Expression Vector and Antibodies Against DSB DNA Repair Factors into HI5c and I9a Cells

The transfection success of Lipofectamine 2000, Lipofectamine LTX with PLUS Reagent, and TranSIT LT1 in HI5c and I9a.

Using three different experiments, three transfection reagents were used to try to successfully transfect the HR and NHEJ reporter cassette containing cell lines, respectively HI5c and I9a, with the I-*Sce*I expression vector.

The first experiment used the transfection reagent Lipofectamine 2000 to simultaneously introduce 300 ng of pDsRed-Express2-N1 (Clontech) with 300 ng, 600 ng, or 1200 ng of I-*Sce*I expression vector into the HI5c cell line. Low levels of GFP positive events were detected in the gWIZ-GFP (Genlantis) only treatment and negligible amounts were detected in treatments containing the I-*Sce*I expression vector both before and after normalisation when compared to the controls (Figure 3.8 and 3.9, Supplementary Figure 3.4). Because there were GFP positive events present in the pDsRed-Express2-N1 (Clontech) control, this treatment was used as the baseline to compare to the treatments containing either gWIZ-GFP (Genlantis) or I-*Sce*I expression vector (Figure 3.8). DsRed expression was detected in all treatments where pDsRed-Express2-N1 (Clontech) was present, however, there was also some expression detected in the gWIZ-GFP (Genlantis) control (Figure 3.8). Interestingly, as the amount of I-*Sce*I expression vector increased so did the percentage of DsRed positive events when compared to the pDsRed-Express2-N1

(Clontech) control even though they all contained 300 ng of the DsRed encoding plasmid. The increase was significant (*t*-test, $P<0.05$ for 300 ng of I-*Sce*I expression vector and $P<0.01$ for 600 ng and 1200 ng of I-*Sce*I expression vector) when each experimental treatment containing I-*Sce*I expression vector was compared to the pDsRed-Express2-N1 (Clontech) control and also significant (*t*-test, $P<0.05$ in all cases) when the treatments with increasing I-*Sce*I expression vector were compared to each other.

In a later trial experiment Lipofectamine 2000 was utilized to introduce either 300 ng, 600 ng, or 1200 ng of pDsRed-Express2-N1 (Clontech) or 300 ng, 600 ng, or 1200 ng of gWIZ-GFP (Genlantis) into HI5c and I9a. This experiment also showed very low percentages of GFP and DsRed positive cells when Lipofectamine 2000 was used as a transfection reagent (Supplementary Figure 3.5 and 3.6). Also noticeable, overall the transfection rate appeared to be lower in I9a when transfected with the same treatments as HI5c.

The final experiment compared the success of Lipofectamine LTX with PLUS Reagent and TranSIT LT1 as transfection reagents for the HI5c and I9a cell lines. Both transfection reagents were used to deliver the following treatments into each cell line: cells only, 500 ng of pDsRed-Express2-N1 (Clontech), and 500 ng of both pDsRed-Express2-N1 (Clontech) and I-*Sce*I expression vector. Similar to the first experiment, negligible amounts of GFP positive events were detected in treatments containing the I-*Sce*I expression vector both before and after normalisation when compared to the controls

(Figure 3.10, Supplementary Figure 3.7). DsRed positive events were prevalent in HI5c and I9a when either transfection reagent was used (Figure 3.10). DsRed events were significantly (*t*-test, $P<0.01$ in HI5c and $P<0.05$ in I9a) higher when Lipofectamine LTX with PLUS reagent was used for pDsRed-Express2-N1 (Clontech) only controls and similar to TranSIT LT1 transfected cells when the treatment also included the I-*Sce*I expression vector. The consistency of transfection overall was better within a treatment when TranSIT LT1 was used. Like the second experiment, the overall transfection rate was lower in the I9a cell line when transfected with the same treatments as the HI5c cell line.

Despite the low transfection rates observed with all transfection reagents tested, because the lowest were seen with Lipofectamine 2000 transfection rates it was not used in further experiments. Lipofectamine LTX with PLUS reagent and TranSIT LT1 were used for all future transfections.

Determining the optimal incubation time between transfection and harvest in HI5c and I9a.

Three post-transfection harvest time points – 24 hours, 48 hours, and 72 hours -- were investigated based on the work done in Mao *et al.* (2008). The experiment utilized a low, 50 ng of pDsRed-Express2-N1 (Clontech) and 550 ng of I-*Sce*I expression vector, and

high, 100 ng of pDsRed-Express2-N1 (Clontech) and 1100 ng of I-*Sce*I expression vector, amount of plasmid in the experimental treatments.

In all cases the controls were as expected. There was no fluorescence detected in the pZP500 control, there was only GFP positive events observed in the gWIZ-GFP (Genlantis) control, and there were only DsRed positive events in the pDsRed-Express2-N1 (Clontech) control (Figure 3.11, Table 3.7, Supplementary Figure 3.8). Similar to other experiments, despite using 600 ng of plasmid for all controls the percentage of GFP positive events was higher than the percentage of DsRed positive events.

In the HI5c cell line, the percentage of GFP positive events in the gWIZ-GFP (Genlantis) control decreased as the length of the harvest time point increased (Figure 3.11, Table 3.7, Supplementary Figure 3.8). This was significant (*t*-test, $P<0.05$ in both cases) between the 72 hour time point and the others but not between the 24 hour and 48 hour time points. The percentage of DsRed positive events was highest at 48 hours but only significantly (*t*-test, $P<0.05$ in the pDsRed-Express2-N1 (Clontech) control, $P<0.01$ in the high experimental treatment, and $P<0.001$ in the low experimental treatment) when compared to the 72 hour time point (Figure 3.11, Table 3.7, Supplementary Figure 3.8). The levels were similar between the 24 and 72 hour time points in the experimental treatments. Overall the percentage of positive fluorescent events was low ranging from 0.13% to 1.17%.

In I9a the percentage of GFP positive events in the GFP control was the lowest at the 48 hour post-transfection time point, however, there was no significant difference between any of the time points (Figure 3.12, Table 3.8, Supplementary Figure 3.9). The percentage of DsRed positive events was the highest at the 72 hours but only significantly (*t*-test, $P<0.05$ in both cases) higher when compared to the 24 hour time point experimental treatments (Figure 3.12, Table 3.8, Supplementary Figure 3.9). Similar to HI5c the overall percentage of positive fluorescent events was low ranging from 0.15% to 1.37%.

As in previous experiments, there were negligible amounts of GFP positive events observed in all treatments containing the I-*Sce*I expression vector both before and after normalisation (Figure 3.11, 3.12, and 3.13, Table 3.7 and 3.8).

With consideration for viability, there was no clear optimal time point. There was variation among treatments within time points, as well as variation between time points (Figure 3.14). In the HI5c cell line, a minimum of 20000 events were analysed from each sample with the exception of two at the 24 hour time point -- one in the low experimental treatment (15033 events were analysed) and another from the high experimental treatment (10882 events were analysed). Within the I9a treatments there were several samples that did not reach the minimum of 20000 events (Supplementary Figure 3.10). In addition, there were only two samples instead of three in Treatments 1 and 4 at the I9a 24 hour time point.

Because the values for all positive fluorescent events were so low it was difficult to draw any definitive conclusion. Ultimately the best time point was determined based only on the gWIZ-GFP (Genlantis) control. This was largely because it had higher percentages of detected events when compared to any of the treatments containing pDsRed-Express2-N1 (Clontech). In addition, like gWIZ-GFP (Genlantis) the I-*Sce*I expression vector expresses GFP. As a result, depending on flow cytometer availability all future experiments used either a 24 or 30 hour post-transfection time point.

Comparing the transfection success of two potential control plasmids -- pDsRed-Express2-N1 (Clontech) and pCMV-Neo-Bam APC (Addgene) – in HI5c and I9a.

Two different plasmids were tested as transfection controls using 3 different ratios of control plasmid to I-*Sce*I expression vector: 300:300, 500:500, and 400:600 (Table 3.9). The ratios were chosen based on preliminary work done with pDsRed-Express2-N1 (Clontech), pCMV-Neo-Bam APC (Addgene), and the I-*Sce*I expression vector (data not shown).

In their respective treatments, the percentage of DsRed positive events was higher than the percentage of APC positive events (Figure 3.16). APC positive events were low in all pCMV-Neo-Bam APC (Addgene)-containing treatments and only slightly higher than the

cells only control. In addition, there were APC positive events in pDsRed-Express2-N1 (Clontech) treatments and, to a lesser extent, DsRed positive events in pCMV-Neo-Bam APC (Addgene) treatments. This is because DsRed and APC emission spectrums overlap. As a result there is some degree of backflow into the others detection channel. Based on the results of this experiment, pDsRed-Express2-N1 (Clontech) was retained as the transfection control.

GFP positive events were detected in the gWIZ-GFP (Genlantis) control, however, there was negligible GFP fluorescence detected in any of the treatments containing the I-*Sce*I expression vector (Figure 3.17).

Checking the I-SceI expression vector in HI5c and I9a.

In support of earlier work, two final experiments were done to check the functionality of the I-*Sce*I expression vector.

In the first, experimental treatments consisted of either 600 ng or 1000 ng of I-*Sce*I expression vector and either 3 µl or 5 µl of the transfection reagent Lipofectamine LTX with PLUS reagent (Table 3.10). In both cell lines there was GFP fluorescence in the gWIZ-GFP (Genlantis) control and no fluorescence in the cells only control (Figure 3.18). However despite the distinct fluorescence detected in the gWIZ-GFP (Genlantis)

control, there were very low levels (less than 0.5%) of GFP positive events in I9a and none in HI5c when only the I-*Sce*I expression vector was present. The viability percentages in each treatment were variable and in general low (HI5c: 30-90%; I9a: 20-50%) (Supplementary Figure 3.11). Only one-third of samples analysed met the 10000 events minimum (Supplementary Figure 3.12).

In the final experiment, all four stocks of I-*Sce*I expression vector were tested in HI5c. Again GFP fluorescence was seen in samples transfected with gWIZ-GFP (Genlantis) (Figure 3.19). Also DsRed fluorescence was seen in both the control and experimental treatments transfected with DsRed. As seen previously, GFP fluorescence was not seen in samples transfected with any of the I-*Sce*I expression vector stocks. Viability was also relatively low ranging from about 50-70% (Supplementary Figure 3.13).

Determining the effect of anti-Ku, anti-DNA-PK$_{CS}$, anti-PARP-1 antibodies on HR and NHEJ levels in HI5c and I9a cells.

Despite the lack of success with the I-*Sce*I expression vector, an experiment was done using the vector and two different amounts of antibodies against Ku70 and DNA-PK$_{CS}$ (Table 3.11). In the HI5c cell line, although there was a trend of decreasing GFP positive events with increasing amounts of anti-Ku70 and anti-DNA-PK$_{CS}$ antibodies (Figure 3.20), the decrease was only significant (*t*-test, $P<0.01$ and $P<0.05$ respectively) between

the 2.5 µg and 5 µg anti-Ku70 treatments and between the 2.5 µg anti-DNA-PK_{CS} and anti-Ku70 treatments. After normalisation none of the antibody treatments differed significantly from one another (Figure 3.21). There was also no significant difference between the no antibody control and the antibody treatments both before and after normalisation (Figure 3.20 and 3.21). In the I9a cell line there was negligible to no GFP positive events in all eight treatments both before and after normalisation (Figure 3.20 and 3.21).

There were DsRed positive events in the pDsRed-Express2-N1 (Clontech) control as well as in the experimental treatments where it acted as a transfection control (Figure 3.20). The percentages of viable events were in general lower for I9a treatments (50-65%) in comparison to those in HI5c (70-85%) (Supplementary Figure 3.14). Also while all the HI5c samples consistently had 10000 FACS analysed events, there were five samples among the I9a treatments that did not reach the 10000 minimum – two in the Treatment 2 (6696 and 6882 events), one in Treatment 4 (5487 events), one in Treatment 7 (5735 events), and one in Treatment 8 (5518 events).

The concerns with this experiment were the low number of positive fluorescent events, the larger margins of error in some treatments, the lower percentages of viability, and unexpected results in some of the controls. In the HI5c pDsRed-Express2-N1 (Clontech) control there should be no GFP expression because there was no plasmid present that encodes GFP (Figure 3.20).

In a second experiment, three additional antibody treatments – antibodies against His-Tag, Parp1, or a combination against Ku70 and DNA-PK_{CS} -- were tested using either 2.5 µg or 5 ug (Table 3.12). GFP fluorescence was only seen in samples transfected with gWIZ-GFP (Genlantis) (data not shown). Despite the presence of DsRed expression from the transfection control in experimental treatments, there was no GFP expression detected from the I-*Sce*I expression vector hampering any ability to test the effects of the antibodies on DSB repair (data not shown). Because of the results seen, all three samples were analysed by flow cytometer for only I9a Treatments 1-7. In the remaining I9a and HI5c treatments only one sample from each triplicate was analysed.

Table 3.1: Treatments for optimizing DNA amounts, the ratio of gWIZ-GFP (Genlantis) to pDsRed-Express2-N1 (Clontech), and the post-transfection incubation time in HEK293 and MCF7. Each treatment contained a single replicate. TR, Transfection Reagent.

No.	Treatment	Total (ng)	DNA Ratio (ng)	Incubation Time	TR (ul)
1	Cells Only 24 hrs	-------	---------	24hr	4
2	gWIZ-GFP 300 24 hrs	300	---------	24hr	4
3	gWIZ-GFP 600 24 hrs	600	---------	24hr	4
4	gWIZ-GFP 1200 24 hrs	1200	---------	24hr	4
5	pDsRed-Express2-N1 300 24 hrs	300	---------	24hr	4
6	pDsRed-Express2-N1 600 24 hrs	600	---------	24hr	4
7	pDsRed-Express2-N1 1200 24 hrs	1200	---------	24hr	4
8	gWIZ-GFP: pDsRed-Express2-N1 150:150 24 hrs	300	150:150	24hr	4
9	gWIZ-GFP: pDsRed-Express2-N1 200:100 24 hrs	300	200:100	24hr	4
10	gWIZ-GFP: pDsRed-Express2-N1 100:200 24 hrs	300	100:200	24hr	4
11	gWIZ-GFP: pDsRed-Express2-N1 300:300 24 hrs	600	300:300	24hr	4
12	gWIZ-GFP: pDsRed-Express2-N1 400:200 24 hrs	600	400:200	24hr	4
13	gWIZ-GFP: pDsRed-Express2-N1 200:400 24 hrs	600	200:400	24hr	4
14	gWIZ-GFP: pDsRed-Express2-N1 600:600 24 hrs	1200	600:600	24hr	4
15	gWIZ-GFP: pDsRed-Express2-N1 800:400 24 hrs	1200	800:400	24hr	4
16	gWIZ-GFP: pDsRed-Express2-N1 400:800 24 hrs	1200	400:800	24hr	4
17	Cells Only 48 hrs	-------	---------	48hr	4
18	gWIZ-GFP 300 48 hrs	300	---------	48hr	4
19	gWIZ-GFP 600 48 hrs	600	---------	48hr	4
20	gWIZ-GFP 1200 48 hrs	1200	---------	48hr	4
21	pDsRed-Express2-N1 300 48 hrs	300	---------	48hr	4
22	pDsRed-Express2-N1 600 48 hrs	600	---------	48hr	4
23	pDsRed-Express2-N1 1200 48 hrs	1200	---------	48hr	4
24	gWIZ-GFP: pDsRed-Express2-N1 150:150 48 hrs	300	150:150	48hr	4
25	gWIZ-GFP: pDsRed-Express2-N1 200:100 48 hrs	300	200:100	48hr	4
26	gWIZ-GFP: pDsRed-Express2-N1 100:200 48 hrs	300	100:200	48hr	4
27	gWIZ-GFP: pDsRed-Express2-N1 300:300 48 hrs	600	300:300	48hr	4
28	gWIZ-GFP: pDsRed-Express2-N1 400:200 48 hrs	600	400:200	48hr	4
29	gWIZ-GFP: pDsRed-Express2-N1 200:400 48 hrs	600	200:400	48hr	4
30	gWIZ-GFP: pDsRed-Express2-N1 600:600 48 hrs	1200	600:600	48hr	4
31	gWIZ-GFP: pDsRed-Express2-N1 800:400 48 hrs	1200	800:400	48hr	4
32	gWIZ-GFP: pDsRed-Express2-N1 400:800 48 hrs	1200	400:800	48hr	4

Table 3.2: Comparison of the changes in viability between treatments when HEK293 cells were transfected with 300 ng of gWIZ-GFP (Genlantis) (Treatment 2), pDsRed-Express2-N1 (Clontech) (Treatment 3), or pZP500 (Treatment 4) using Lipofectamine 2000 (Life Technologies). Treatment 1 was a cells only control. Cells were harvested 24 hours after transfection. The time between initiation of harvest and FACS analysis was longer for Treatments 3 and 4. Each treatment contained three replicates. A minimum of 10000 events were analysed per sample. When the second treatment listed showed a significant decrease in viability compared to the first treatment, a downward arrow was used to indicate the change. An upward arrow indicated a significant increase. Two asterisks represent $P<0.01$. No significant change between treatments is signified by n.s.

Treatments Compared	Significant Increase or Decrease Present
1 vs. 3	⇩/**
1 vs. 4	⇩/**
2 vs. 3	⇩/**
2 vs. 4	⇩/**
1 vs. 2	n.s.
3 vs. 4	n.s.

Table 3.3: Treatments for comparing Lipofectamine 2000 (Life Technologies) and Chariot (Active Motif) as transfection reagents in HEK293. The treatments also worked to observe how transfecting anti-GFP antibodies (Santa Cruz Biotechnology) in conjunction with gWIZ-GFP (Genlantis) impacts GFP fluorescence. Cells were harvested 24 hours after transfection. Each treatment contained three replicates. A minimum of 10000 events were analysed per sample on a BD FACSCanto II flow cytometer.

No.	Treatment	Delivery Method	gWIZ-GFP (ng)	pDsRed-Express2-N1 (ng)	pZP500 (ng)	Anti-GFP (µg)
1	pZP500 Only	Lipofectamine 2000	---------	---------	300	------
2	gWIZ-GFP, pDsRed-Express2-N1	Lipofectamine 2000	300	300	---------	------
3	gWIZ-GFP, pDsRed-Express2-N1, Ab	Lipofectamine 2000	300	300	---------	2
4	gWIZ-GFP, pDsRed-Express2-N1, Ab	Lipofectamine 2000	300	300	---------	4
5	gWIZ-GFP, pDsRed-Express2-N1, Ab	Lipofectamine 2000	300	300	---------	6
6	gWIZ-GFP, pDsRed-Express2-N1, Ab	Lipofectamine 2000/Chariot	300	300	---------	3
7	gWIZ-GFP, pDsRed-Express2-N1, Ab	Chariot	300	300	---------	3

Table 3.4: Treatments in Experiment 1 for determining the success of anti-GFP antibody delivery via Lipofectamine 2000 (Life Technologies) through observations of GFP fluorescence changes. Cells were harvested 24 hours after transfection. Each treatment contained three replicates. A minimum of 10000 events were analysed per sample on a BD FACSCanto II flow cytometer.

No.	Treatment	pZP500 (ng)	pDsRed-Express2-N1 (ng)	gWIZ-GFP (ng)	Anti-GFP (µg)
1	Cells Only	----------	----------	----------	----------
2	pZP500	300	----------	----------	----------
3	pDsRed-Express2-N1	----------	300	----------	----------
4	pDsRed-Express2-N1, gWIZ-GFP	----------	300	300	----------
5	Anti-GFP Antibody – 1 µg	----------	300	300	1
6	Anti-GFP Antibody – 2 µg	----------	300	300	2
7	Anti-GFP Antibody – 5 µg	----------	300	300	5

Table 3.5: Treatments in Experiment 2 and 3 for determining the success of anti-GFP antibody delivery via Lipofectamine 2000 (Life Technologies) through observations of GFP fluorescence changes. Cells were harvested 24 hours after transfection. Each treatment contained three replicates. A minimum of 20000 events were analysed per sample on a BD FACSCanto II flow cytometer.

No.	Treatment	Delivery Method	pZP500 (ng)	pDsRed-Express2-N1 (ng)	gWIZ-GFP (ng)	Anti-GFP (µg)
1	pZP500	Lipofectamine 2000	300	----------	----------	----------
2	pDsRed-Express2-N1	Lipofectamine 2000	----------	300	----------	----------
3	gWIZ-GFP	Lipofectamine 2000	----------	----------	300	----------
4	pDsRed-Express2-N1, gWIZ-GFP	Lipofectamine 2000	----------	300	300	----------
5	GFP Antibody – 1 µg	Lipofectamine 2000	----------	300	300	1
6	GFP Antibody – 2 µg	Lipofectamine 2000	----------	300	300	2
7	GFP Antibody – 5 µg	Lipofectamine 2000	----------	300	300	5
8	GFP Antibody – 5 µg NO TR	None	----------	----------	----------	5

Table 3.6: Comparing the changes in positive events between experiments when HEK293 cells are transfected with 300 ng of both gWIZ-GFP (Genlantis) and pDsRed-Express2-N1 (Clontech) in addition to either 0 µg, 1 µg, 2 µg, or 5 µg of anti-GFP antibodies using Lipofectamine 2000 (Life Technologies). Treatment 4 contained no antibodies; Treatments 5-7 contained 1 µg, 2 µg, and 5 µg of antibodies respectively. Treatments 4-7 contained 300 ng of each gWIZ-GFP and pDsRed-Express2-N1. Each treatment contained three replicates. Cells were harvested 24 hours after transfection. For Experiment 1 a minimum of 10000 events were analysed per sample on a BD FACSCanto II flow cytometer, for Experiment 2 a minimum of 20000 viable events were analysed per sample, and for Experiment 3 a minimum of 20000 events were analysed per sample. When the second treatment listed showed a significant change in fluorescent events compared to the first treatment, a downward arrow (decrease) or upward arrow (increase) was used to indicate the directional change. A $P<0.05$ is represented by an asterisk. Two asterisks represent $P<0.01$ and three asterisks represent $P<0.001$. No significant change between treatments is signified by n.s.

	Experiment 1			**Experiment 2**			**Experiment 3**		
Treatments Compared	GFP	DsRed	GFP/ DsRed	GFP	DsRed	GFP/ DsRed	GFP	DsRed	GFP/ DsRed
4 (0 µg) vs. 5 (1 µg)	⇧/*	n.s.	n.s.	⇧/*	n.s.	⇧/***	⇧/*	n.s.	n.s.
4 (0 µg) vs. 6 (2µg)	⇧/**	⇩/*	n.s.	n.s.	⇩/**	⇧/**	⇧/**	n.s.	⇧/*
4 (0 µg) vs. 7 (5 µg)	⇧/**	⇩/*	⇧/**	n.s.	⇩/***	⇧/**	n.s.	n.s.	⇧/***
5 (1 µg) vs. 6 (2 µg)	n.s.	n.s.	n.s.	⇩/**	⇩/**	⇧/*	n.s.	n.s.	n.s.
5 (1 µg) vs. 7 (5 µg)	n.s.	n.s.	n.s.	⇩/***	⇩/***	⇧/**	n.s.	n.s.	n.s.
6 (2 µg) vs. 7 (5 µg)	n.s.	n.s.	n.s.	n.s.	⇩/*	⇧/**	n.s.	⇩/*	⇧/*

Table 3.7: Comparing the percentage of positive fluorescing events in HI5c cells at three different post-transfection harvest time points: 24, 48, or 72 hours. Cells were transfected with: 600 ng of pZP500 (Treatment 1); 600 ng of pDsRed-Express2-N1 (Clontech) (Treatment 2); 600 ng of gWIZ-GFP (Genlantis) (Treatment 3); and two different amounts of the I-*Sce*I expression vector and pDsRed-Express2-N1 (Clontech) using TranSIT LT1 (Mirus). Treatment 4 contained 550 ng of I-*Sce*I expression vector and 50 ng of pDsRed-Express2-N1 (Clontech) while Treatment 5 contained 1100 ng and 100 ng respectively. Each treatment contained three replicates. A minimum of 20000 events were analysed per sample on a BD FACSCanto II flow cytometer. When the second treatment listed showed a significant decrease in viability or fluorescent events compared to the first treatment, a downward arrow was used to indicate the change. An upward arrow indicated a significant increase. A $P<0.05$ is represented by an asterisk. Two asterisks represent $P<0.01$ and three asterisks represent $P<0.001$. No significant change between treatments is signified by n.s.

Treatment	Time Points Compared	Viability	GFP	DsRed	GFP/DsRed
1	24 hr vs. 48 hr	n.s.	n.s.	n.s.	n.s.
	24 hr vs. 72 hr	⇧*	n.s.	n.s.	n.s.
	48 hr vs. 72 hr	⇧**	n.s.	n.s.	n.s.
2	24 hr vs. 48 hr	n.s.	n.s.	n.s.	n.s.
	24 hr vs. 72 hr	n.s.	n.s.	⇩*	N/A
	48 hr vs. 72 hr	⇧***	n.s.	⇩*	N/A
3	24 hr vs. 48 hr	⇩**	n.s.	n.s.	N/A
	24 hr vs. 72 hr	n.s.	⇩*	n.s.	N/A
	48 hr vs. 72 hr	⇧**	⇩*	n.s.	N/A
4	24 hr vs. 48 hr	⇩**	n.s.	n.s.	n.s.
	24 hr vs. 72 hr	n.s.	n.s.	n.s.	n.s.
	48 hr vs. 72 hr	⇧**	n.s.	⇩***	n.s.
5	24 hr vs. 48 hr	⇩***	n.s.	n.s.	n.s.
	24 hr vs. 72 hr	n.s.	n.s.	n.s.	n.s.
	48 hr vs. 72 hr	⇧***	n.s.	⇩**	n.s.

Table 3.8: Comparing the percentage of positive fluorescing events in I9a cells at three different post-transfection harvest time points: 24, 48, or 72 hours. Cells were transfected with: 600 ng of pZP500 (Treatment 1); 600 ng of pDsRed-Express2-N1 (Clontech) (Treatment 2); 600 ng of gWIZ-GFP (Genlantis) (Treatment 3); and two different amounts of the I-*Sce*I expression vector and pDsRed-Express2-N1 (Clontech) using TranSIT LT1 (Mirus). Treatment 4 contained 550 ng of I-*Sce*I expression vector and 50 ng of pDsRed-Express2-N1 (Clontech) while Treatment 5 contained 1100 ng and 100 ng respectively. Each treatment contained three replicates. A minimum of 20000 events were analysed per sample on a BD FACSCanto II flow cytometer. When the second treatment listed showed a significant decrease in viability or fluorescent events compared to the first treatment, a downward arrow was used to indicate the change. An upward arrow indicated a significant increase. A $P<0.05$ is represented by an asterisk. Two asterisks represent $P<0.01$ and three asterisks represent $P<0.001$. A negative sign shows there was no significant change between treatments.

Treatment	Time Points Compared	Viability	GFP	DsRed	GFP/DsRed
1	24 hr vs. 48 hr	n.s.	n.s.	n.s.	N/A
	24 hr vs. 72 hr	n.s.	n.s.	n.s.	N/A
	48 hr vs. 72 hr	n.s.	n.s.	n.s.	N/A
2	24 hr vs. 48 hr	⇩*	n.s.	⇩*	N/A
	24 hr vs. 72 hr	⇧***	n.s.	n.s.	N/A
	48 hr vs. 72 hr	⇩*	n.s.	⇧*	N/A
3	24 hr vs. 48 hr	n.s.	n.s.	n.s.	N/A
	24 hr vs. 72 hr	⇩***	n.s.	n.s.	N/A
	48 hr vs. 72 hr	n.s.	n.s.	n.s.	N/A
4	24 hr vs. 48 hr	n.s.	n.s.	n.s.	n.s.
	24 hr vs. 72 hr	⇩***	n.s.	⇧*	n.s.
	48 hr vs. 72 hr	⇩***	n.s.	n.s.	n.s.
5	24 hr vs. 48 hr	⇧*	n.s.	⇧**	n.s.
	24 hr vs. 72 hr	n.s.	n.s.	⇧*	n.s.
	48 hr vs. 72 hr	⇩**	n.s.	n.s.	n.s.

Table 3.9: Treatments for comparing the transfection success of two potential control plasmids -- pDsRed-Express2-N1 (Clontech) and pCMV-Neo-Bam APC (Addgene) – in HI5c and I9a. All treatments were transfected with Lipofectamine LTX with PLUS Reagent (Invitrogen). Cells were harvested 30 hours after transfection. Each treatment contained three replicates and a minimum of 10000 viable events were analysed per sample on a BD FACSCanto II flow cytometer.

No.	Treatment	pCMV-Neo-Bam APC or pDsRed-Express2-N1(ng)	pI-*Sce*I or gWIZ-GFP (ng)
1	Cells Only	----------	----------
2	pDsRed-Express2-N1	600	----------
3	pCMV-Neo-Bam APC	600	----------
4	I-*Sce*I expression vector	----------	600
5	gWIZ-GFP	----------	600
6	pCMV-Neo-Bam APC + I-*Sce*I expression vector 300:300	300	300
7	pCMV-Neo-Bam APC + I-*Sce*I expression vector 500:500	500	500
8	pCMV-Neo-Bam APC + I-*Sce*I expression vector 400:600	400	600
9	pDsRed-Express2-N1 + I-*Sce*I expression vector 300:300	300	300
10	pDsRed-Express2-N1 + I-*Sce*I expression vector 500:500	500	500
11	pDsRed-Express2-N1 + I-*Sce*I expression vector 400:600	400	600

Table 3.10: Treatments in Experiment 1 checking the I-*Sce*I expression vector in HI5c and I9a. All treatments were transfected with Lipofectamine LTX with PLUS Reagent (Invitrogen). Cells were harvested 24 hours after transfection. Each treatment contained one replicate. A minimum of 10000 events were analysed per sample on a BD FACSCanto II flow cytometer. TR, Transfection Reagent.

No.	Treatment	gWIZ-GFP (ng)	p*I-SceI* (ng)	TR (µl)
1	Cells Only	----------	----------	3
2	gWIZ-GFP	600	----------	3
3	I-*Sce*I expression vector – 600 ng	----------	600	3
4	I-*Sce*I expression vector – 1000 ng	----------	1000	3
5	I-*Sce*I expression vector – 600 ng	----------	600	5
6	I-*Sce*I expression vector – 1000 ng	----------	1000	5

Table 3.11: Treatments in Experiment 1 for determining the effect of anti-Ku and anti-DNA-PK$_{CS}$ antibodies on HR and NHEJ levels in HI5c and I9a cells. All treatments were transfected with Lipofectamine LTX with PLUS Reagent (Invitrogen). Cells were harvested 24 hours after transfection. Each treatment contained three replicates. A minimum of 10000 events were analysed per sample on a BD FACSCanto II flow cytometer.

No.	Treatment	pDsRed-Express2-N1 (ng)	pI-*Sce*I (ng)	Anti-GFP (µg)
1	Cells Only	----------	----------	----------
2	pDsRed-Express2-N1	400	----------	----------
3	I-*Sce*I expression vector	----------	600	----------
4	pDsRed-Express2-N1 + I-*Sce*I expression vector	400	600	----------
5	pDsRed-Express2-N1 + I-*Sce*I expression vector + DNA-PK 0.5 µg	400	600	0.5
6	pDsRed-Express2-N1 + I-*Sce*I expression vector + DNA-PK 1 µg	400	600	1
7	pDsRed-Express2-N1 + I-*Sce*I expression vector + Ku70 0.5 µg	400	600	0.5
8	pDsRed-Express2-N1 + I-*Sce*I expression vector + Ku70 1 µg	400	600	1

Table 3.12: Treatments in Experiment 2 for determining the effect of anti-Ku, anti-DNA-PK$_{CS}$, anti-PARP-1 antibodies on HR and NHEJ levels in HI5c and I9a cells. All treatments were transfected with Lipofectamine LTX with PLUS Reagent (Invitrogen). Cells were harvested 30 hours after transfection. Each treatment contained three replicates. A minimum of 20000 events were analysed per sample on a BD FACSCanto II flow cytometer.

No.	Treatment	pDsRed-Express2-N1 (ng)	pI-*Sce*I or gWIZ-GFP (ng)	Anti-GFP (µg)
1	pZP500	600	----------	----------
2	pDsRed-Express2-N1	600	----------	----------
3	gWIZ-GFP	----------	600	----------
4	pDsRed-Express2-N1 + I-*Sce*I expression vector	100	700	----------
5	pDsRed-Express2-N1 + I-*Sce*I expression vector + Ctr Ab 0.5 µg	100	700	0.5
6	pDsRed-Express2-N1 + I-*Sce*I expression vector + Ctr Ab 1 µg	100	700	1
7	pDsRed-Express2-N1 + I-*Sce*I expression vector + Ku70 0.5 µg	100	700	0.5
8	pDsRed-Express2-N1 + I-*Sce*I expression vector + Ku70 1 µg	100	700	1
9	pDsRed-Express2-N1 + I-*Sce*I expression vector + DNA-PK 0.5 µg	100	700	0.5
10	pDsRed-Express2-N1 + I-*Sce*I expression vector + DNA-PK 1 µg	100	700	1
11	pDsRed-Express2-N1 + I-*Sce*I expression vector + Parp1 0.5 µg	100	700	0.5
12	pDsRed-Express2-N1 + I-*Sce*I expression vector + Parp1 1 µg	100	700	1

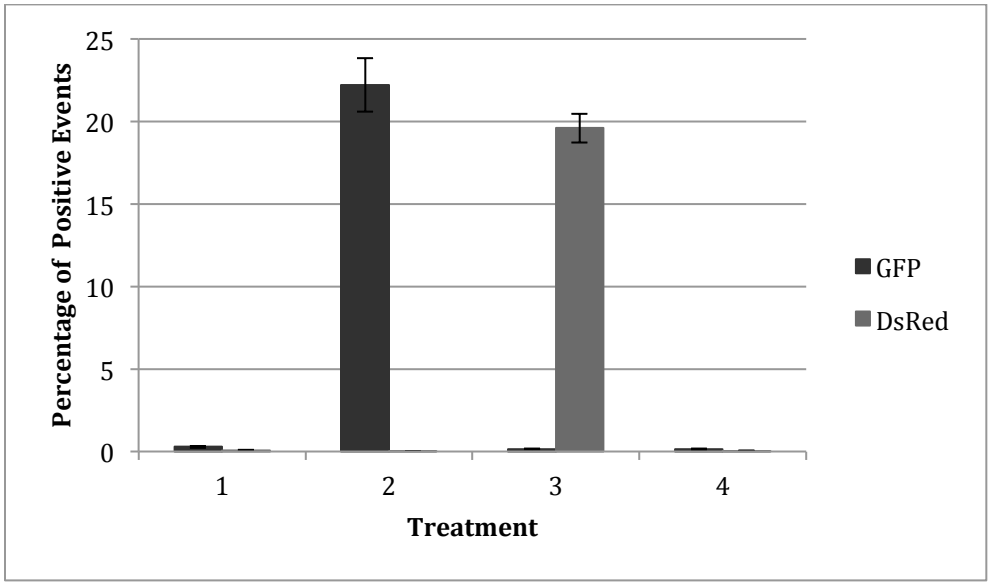

Figure 3.1: The percentage of positive fluorescing events in HEK293 cells transfected with 300 ng of gWIZ-GFP (Genlantis) (Treatment 2), pDsRed-Express2-N1 (Clontech) (Treatment 3), or pZP500 (Treatment 4) using Lipofectamine 2000 (Life Technologies). Treatment 1 was a cells only control. Cells were harvested 24 hours after transfection. Fluorescence was measured using a BD FACSCanto II flow cytometer. Each treatment contained three replicates and a minimum of 10000 events were analysed per sample. The data are shown as an average percentage of positive events per treatment sample with s.d.

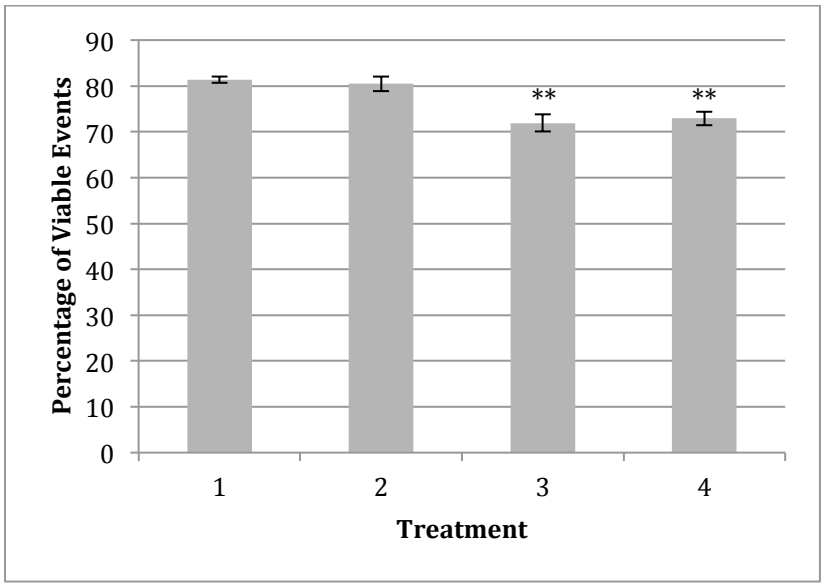

Figure 3.2: The percentage of viable events in HEK293 cells transfected with 300 ng of gWIZ-GFP (Genlantis) (Treatment 2), pDsRed-Express2-N1 (Clontech) (Treatment 3), or pZP500 (Treatment 4) using Lipofectamine 2000 (Life Technologies). Treatment 1 was a cells only control. Cells were harvested 24 hours after transfection. Each treatment contained three replicates. A minimum of 10000 events were analysed per sample on a BD FACSCanto II flow cytometer. The data are shown as an average number of viable events per treatment with s.d. A significant change in viability from Treatment 1 where $P<0.01$ is represented by an two asterisks.

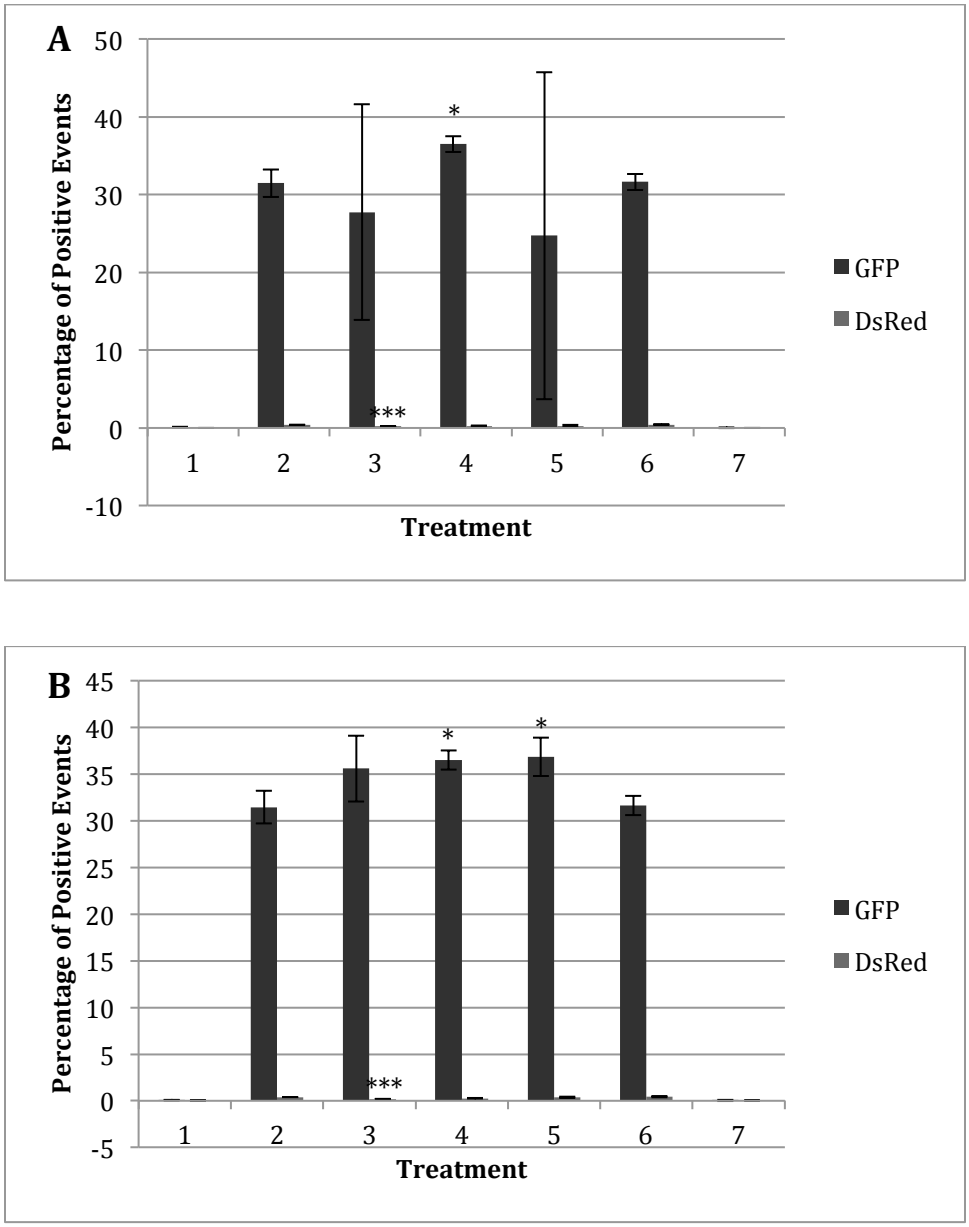

Figure 3.3: The percentage of positive fluorescing events in HEK293 cells transfected with 300 ng of both gWIZ-GFP (Genlantis) and pDsRed-Express2-N1 (Clontech) in addition to 2 µg, 3 µg, 4 µg, or 6 µg of anti-GFP antibodies (Santa Cruz Biotechnology) using either Lipofectamine 2000 (Life Technologies) or Chariot (Active Motif). Treatment 1 is a pZP500 only control; Treatment 2 contained no antibodies; Treatments 3-5 contained 2 µg, 4 µg, and 6 µg of antibodies respectively;

Treatments 6 and 7 both contained 3 µg. Treatments 2-7 also contained 300 ng of each gWIZ-GFP and pDsRed-Express2-N1. Treatments 1-5 were transfected with Lipofectamine 2000 (Life Technologies), Treatment 6 was transfected with Lipofectamine 2000 (Life Technologies) and Chariot (Active Motif), and Treatment 7 was transfected with only Chariot (Active Motif). Fluorescence was measured using a BD FACSCanto II flow cytometer. Cells were harvested 24 hours after transfection. Each treatment contained three replicates. A minimum of 10000 events were analysed per sample. The data are shown as an average percentage of positive events per treatment with s.d. A significant change in the percentage of positive fluorescing events in Treatments 3-6 (antibodies present) when compared to Treatment 2 (no antibody control) where $P<0.05$ is represented by an asterisk and three asterisks represent $P<0.001$.

A: Percentage of GFP and DsRed positive events per total number of events with the outlier data points present in Treatment 3 and 5.

B: Percentage of GFP and DsRed positive events per total number of events with the outlier data points absent in Treatment 3 and 5.

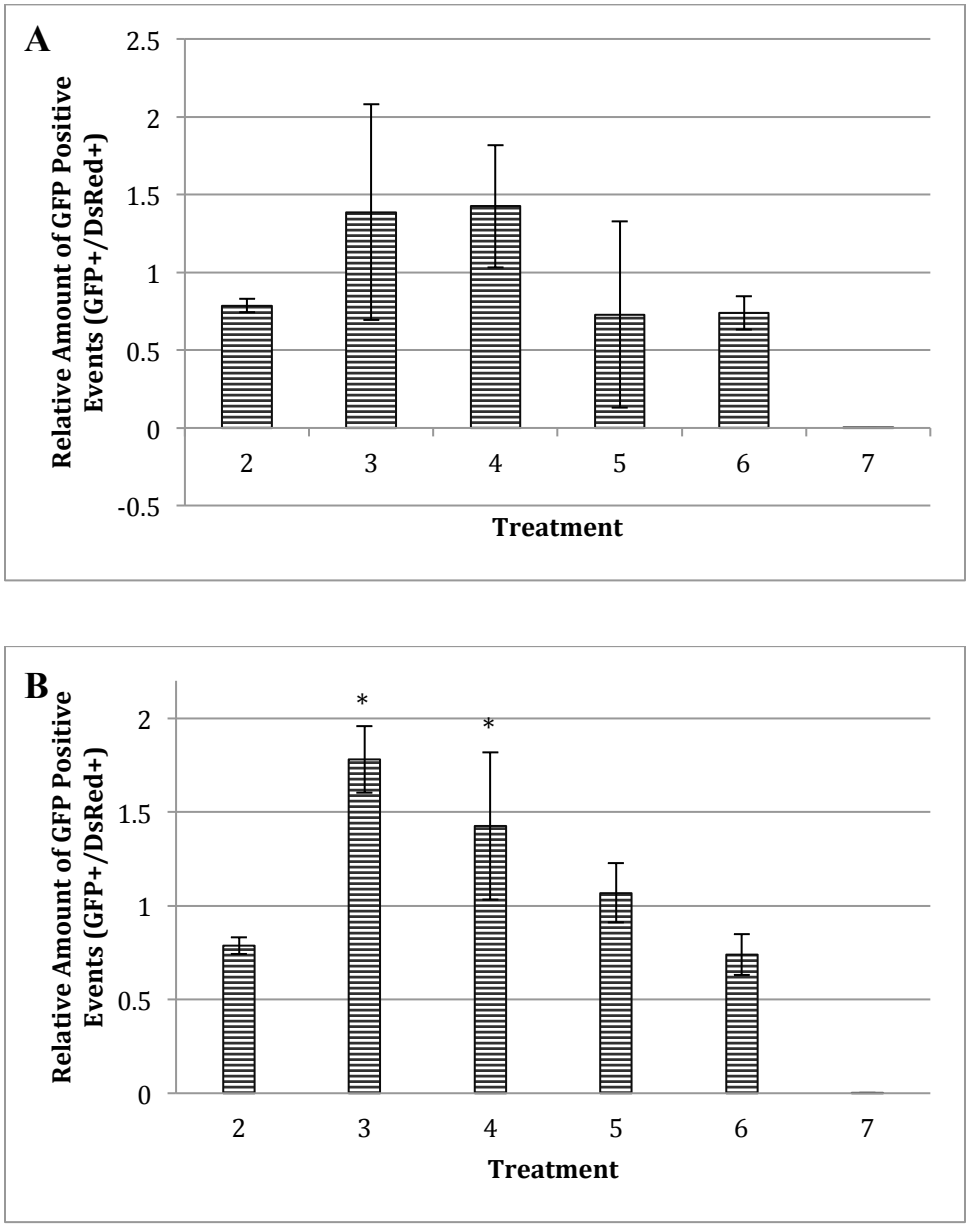

Figure 3.4: The relative amount of GFP positive events after normalisation in HEK293 cells transfected with 300 ng of both gWIZ-GFP (Genlantis) and pDsRed-Express2-N1 (Clontech) in addition to 2 µg, 3 µg, 4 µg, or 6 µg of anti-GFP antibodies (Santa Cruz Biotechnology) using either Lipofectamine 2000 (Life Technologies) or Chariot (Active Motif). Treatment 1 is a pZP500 only control; Treatment 2 contained no antibodies; Treatments 3-5 contained 2 µg, 4 µg, and 6 µg of

antibodies respectively; Treatments 6 and 7 both contained 3 μg. Treatments 2-7 also contained 300 ng of each gWIZ-GFP and pDsRed-Express2-N1. Treatments 1-5 were transfected with Lipofectamine 2000 (Life Technologies), Treatment 6 was transfected with Lipofectamine 2000 (Life Technologies) and Chariot (Active Motif), and Treatment 7 was transfected with Chariot (Active Motif). Fluorescence was measured using a BD FACSCanto II flow cytometer. Cells were harvested 24 hours after transfection. Each treatment contained three replicates and a minimum of 10000 events were analysed per sample. The data are shown as an average relative amount of GFP positive events per treatment with s.d. A significant change in the relative amount of GFP positive events in Treatments 3-6 (antibodies present) when compared to Treatment 2 (no antibody control) where $P<0.05$ is represented by an asterisk.

A: Percentage of GFP and DsRed positive events per total number of events with the outlier data points present in Treatment 3 and 5.

B: Percentage of GFP and DsRed positive events per total number of events with the outlier data points absent in Treatment 3 and 5.

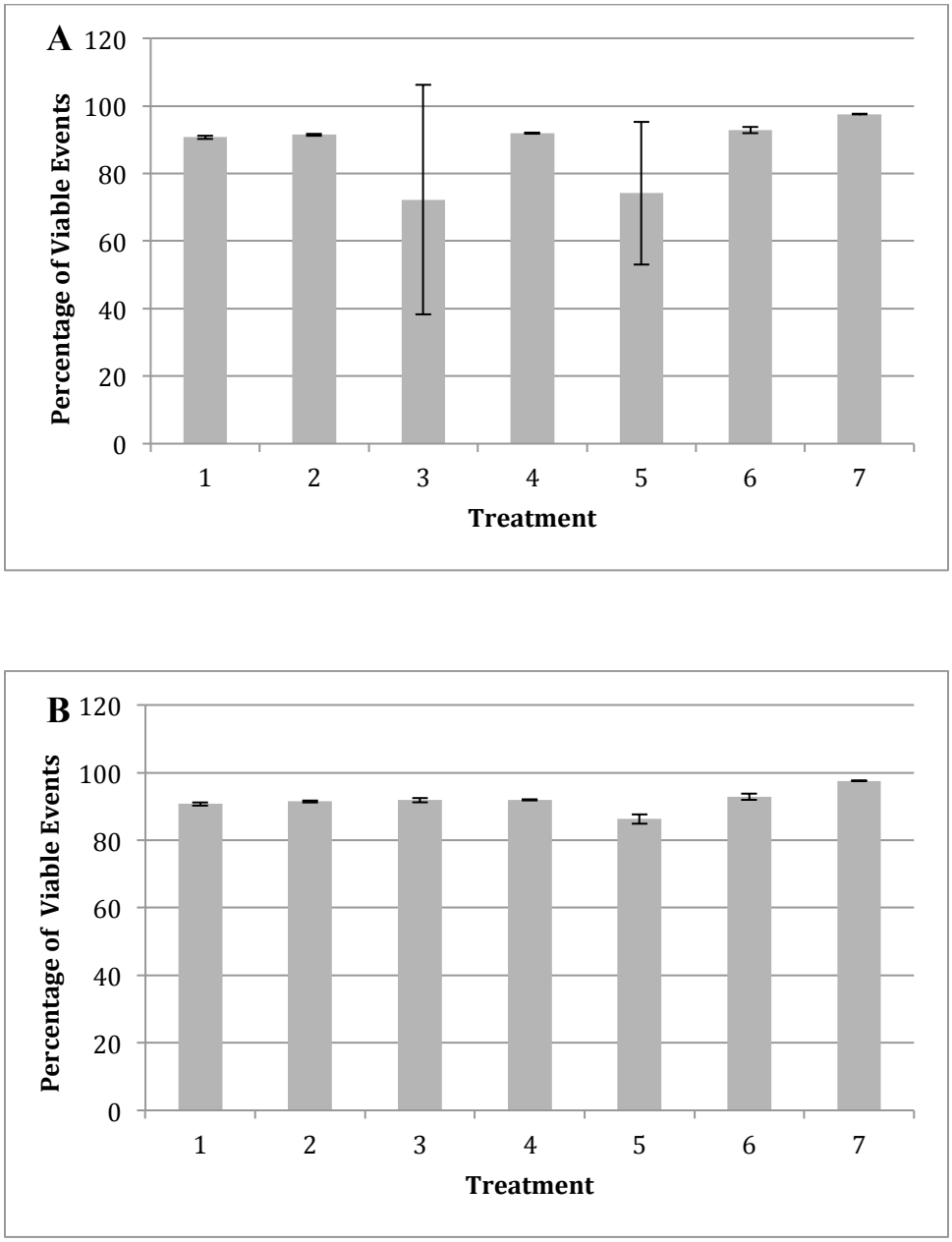

Figure 3.5: The percentage of viable events in HEK293 cells transfected with 300 ng of both gWIZ-GFP (Genlantis) and pDsRed-Express2-N1 (Clontech) in addition to 2 µg, 3 µg, 4 µg, or 6 µg of anti-GFP antibodies (Santa Cruz Biotechnology) using either Lipofectamine 2000 (Life Technologies) or Chariot (Active Motif). Treatment 1 is a pZP500 only control; Treatment 2 contained no antibodies; Treatments 3-5 contained 2 µg, 4 µg, and 6 µg of antibodies respectively; Treatments 6 and 7 both

contained 3 µg. Treatments 2-7 also contained 300 ng of each gWIZ-GFP and pDsRed-Express2-N1. Treatments 1-5 were transfected with Lipofectamine 2000 (Life Technologies), Treatment 6 was transfected with Lipofectamine 2000 (Life Technologies) and Chariot (Active Motif), and Treatment 7 was transfected with Chariot (Active Motif). Cells were harvested 24 hours after transfection. Each treatment contained three replicates. A minimum of 10000 events were analysed per sample. The data are shown as an average percentage of viable events per treatment with s.d.

A: Percentage of GFP and DsRed positive events per total number of events with the outlier data points present in Treatment 3 and 5.

B: Percentage of GFP and DsRed positive events per total number of events with the outlier data points absent in Treatment 3 and 5.

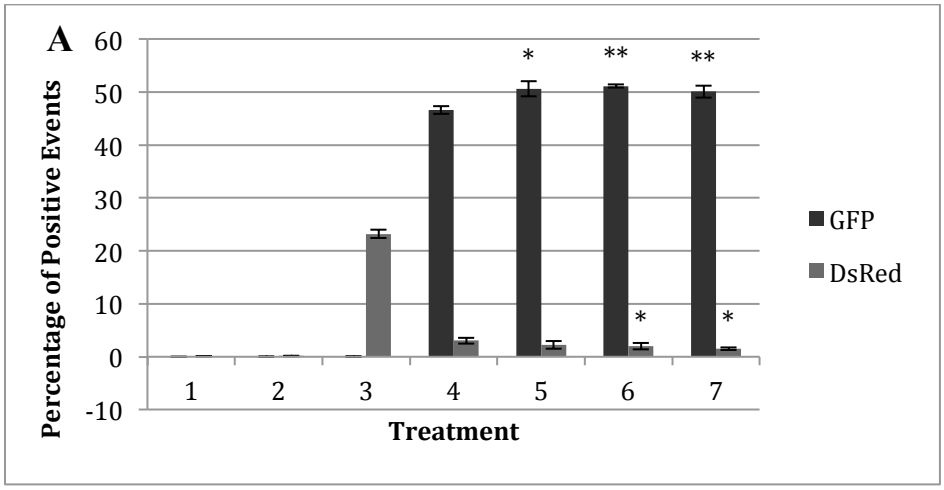
A
Percentage of Positive Events
60
50
40
30
20
10
0
-10
1
2
3
4
5
6
7
Treatment
*
**
**
*
*
GFP
DsRed

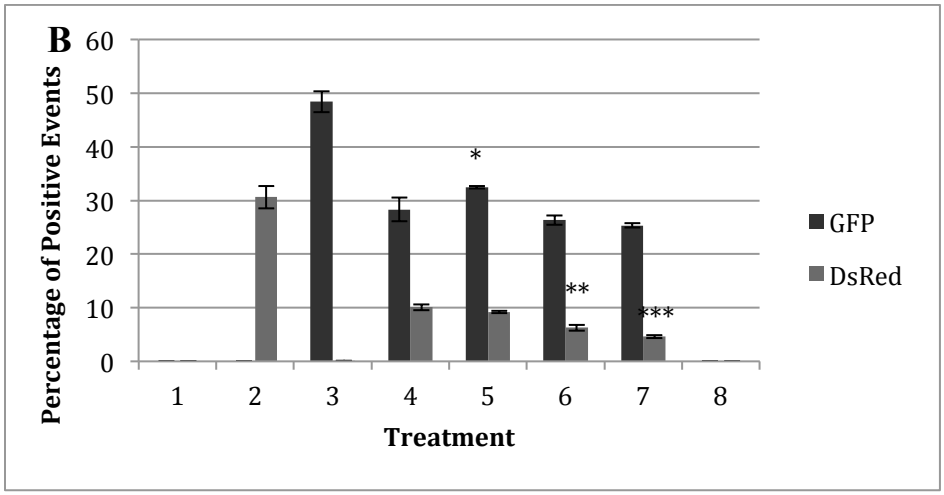
B
Percentage of Positive Events
60
50
40
30
20
10
0
1
2
3
4
5
6
7
8
Treatment
*
**
***
GFP
DsRed

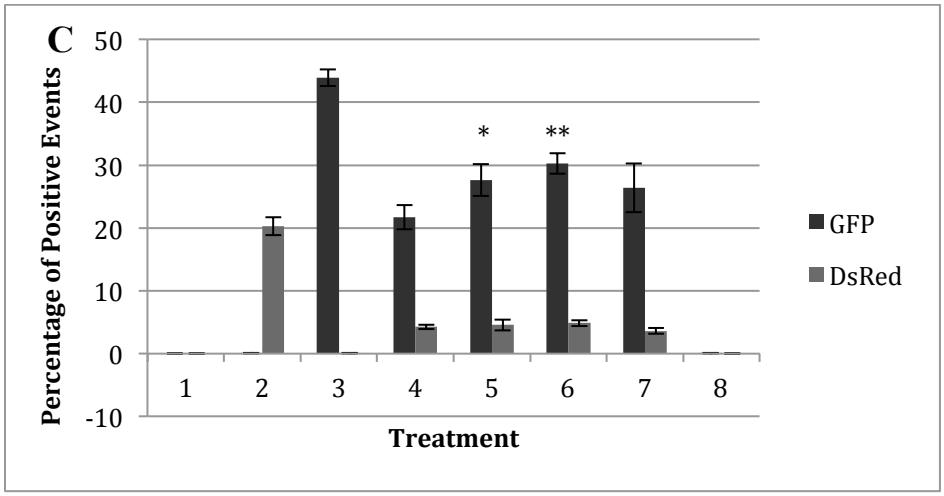
C
Percentage of Positive Events
50
40
30
20
10
0
-10
1
2
3
4
5
6
7
8
Treatment
*
**
GFP
DsRed

Figure 3.6: The percentage of positive fluorescing events in HEK293 cells transfected with 300 ng of both gWIZ-GFP (Genlantis) and pDsRed-Express2-N1 (Clontech) in addition to either 1 µg, 2 µg, or 5 µg of anti-GFP antibodies using Lipofectamine 2000 (Life Technologies). Fluorescence was measured using a BD FACSCanto II flow cytometer. Cells were harvested 24 hours after transfection. Each treatment contained three replicates. The data are shown as an average percentage of positive events per treatment with s.d. A significant change in the percentage of positive events in Treatments 5-7 (antibodies present) when compared to Treatment 4 (no antibody control) where $P<0.05$ is represented by an asterisk; two asterisks represents $P<0.01$ and three asterisks represent $P<0.001$.

A: Experiment 1 -- A minimum of 10000 total events were analysed per sample. Treatment 1 is a cells only control; Treatment 2 is a pZP500 only control; Treatment 3 is a pDsRed-Express2-N1 only control; Treatment 4 contained no antibodies; Treatments 5-7 contained 1 µg, 2 µg, and 5 µg of antibodies respectively. Treatments 4-7 contained 300 ng of each gWIZ-GFP and pDsRed-Express2-N1.

B: Experiment 2 -- A minimum of 20000 viable events were analysed per sample. Treatment 1 is a pZP500 only control; Treatment 2 is a pDS-Red-Express2-N1 only control; Treatment 3 is a gWIZ-GFP only control; Treatment 4 contained no antibodies; Treatments 5-7 contained 1 µg, 2 µg, and 5 µg of antibodies respectively. Treatments 4-7 contained 300 ng of each gWIZ-GFP and pDsRed-Express2-N1. Treatment 8 was a no transfection reagent control with 5 µg of antibodies.

C: Experiment 3 -- A minimum of 20000 total events were analysed per sample. See Experiment 2 for treatment descriptions.

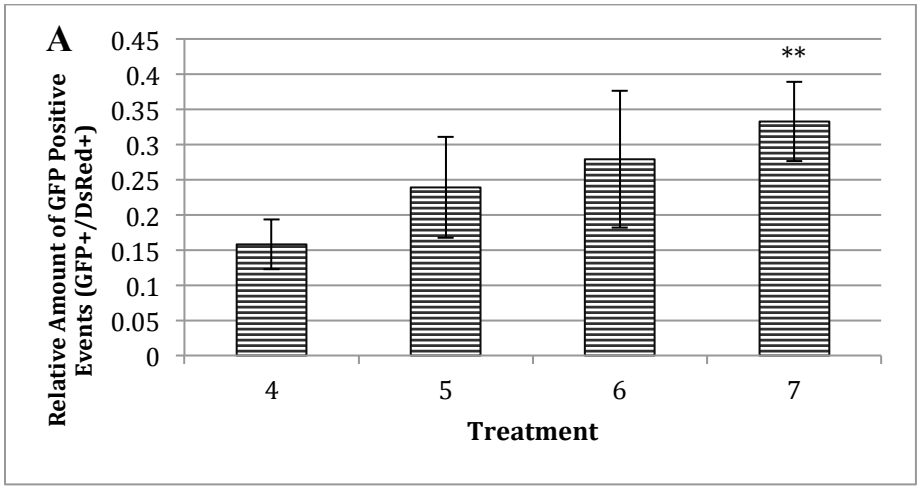
A
Relative Amount of GFP Positive Events (GFP+/DsRed+)
0.45
0.4
0.35
0.3
0.25
0.2
0.15
0.1
0.05
0
**
4
5
6
7
Treatment

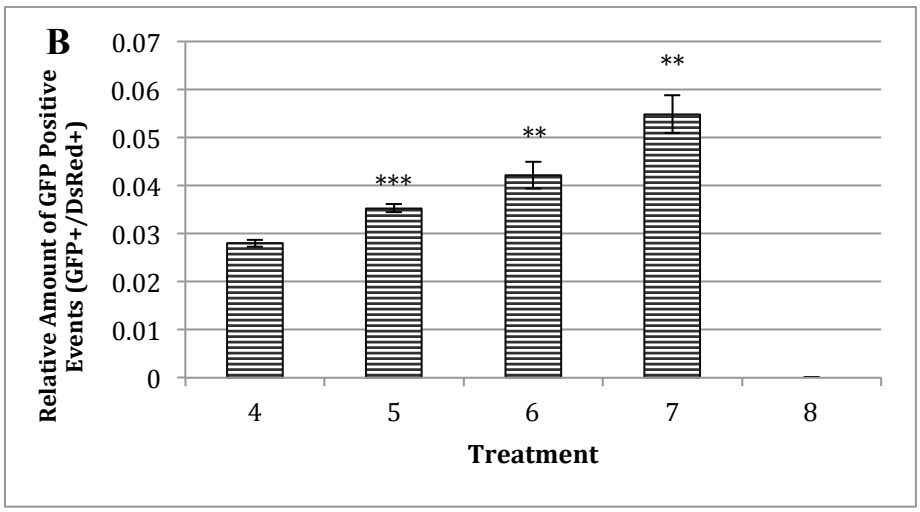
B
Relative Amount of GFP Positive Events (GFP+/DsRed+)
0.07
0.06
0.05
0.04
0.03
0.02
0.01
0
***
**
**
4
5
6
7
8
Treatment

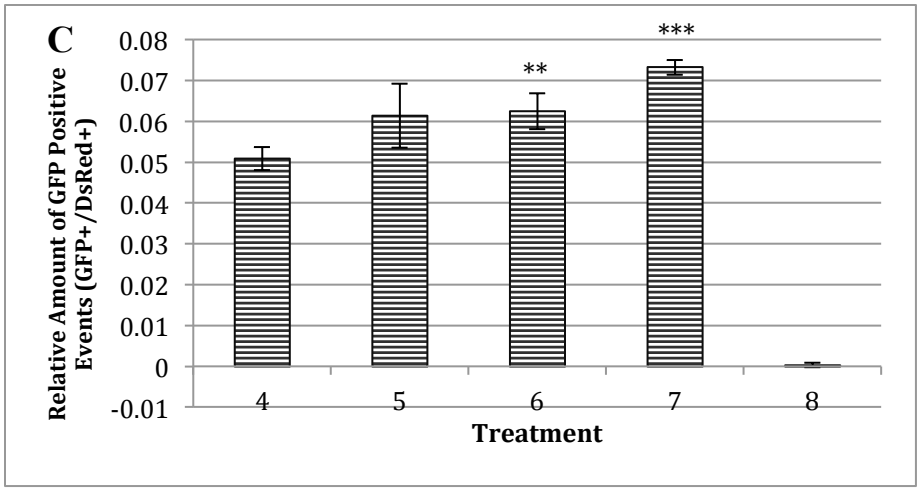
C
Relative Amount of GFP Positive Events (GFP+/DsRed+)
0.08
0.07
0.06
0.05
0.04
0.03
0.02
0.01
0
-0.01
**
***
4
5
6
7
8
Treatment

Figure 3.7: The relative amount of GFP positive events after normalisation in HEK293 cells transfected with 300 ng of both gWIZ-GFP (Genlantis) and pDsRed-Express2-N1 (Clontech) in addition to either 1 µg, 2 µg, or 5 µg of anti-GFP antibodies using Lipofectamine 2000 (Life Technologies). Fluorescence was measured using a BD FACSCanto II flow cytometer. Cells were harvested 24 hours after transfection. Each treatment contained three replicates. The data are shown as an average relative amount of GFP positive events per treatment with s.d. A significant change in the relative amount of GFP positive events in Treatments 5-7 (antibodies present) when compared to Treatment 4 (no antibody control) where $P<0.05$ is represented by an asterisk; two asterisks represents $P<0.01$ and three asterisks represent $P<0.001$.

A: Experiment 1 -- A minimum of 10000 total events were analysed per sample. No normalisation was done for Treatments 1-3. Treatment 4 contained no antibodies and Treatments 5-7 contained 1 µg, 2 µg, and 5 µg of antibodies respectively. Treatments 4-7 contained 300 ng of each gWIZ-GFP and pDsRed-Express2-N1.

B: Experiment 2 -- A minimum of 20000 viable events were analysed per sample. No normalisation was done for Treatments 1-3. Treatment 4 contained no antibodies and Treatments 5-7 contained 1 µg, 2 µg, and 5 µg of antibodies respectively. Treatments 4-7 contained 300 ng of each gWIZ-GFP and pDsRed-Express2-N1. Treatment 8 was a no transfection reagent control with 5 µg of antibodies.

C: Experiment 3 -- A minimum of 20000 total events were analysed per sample. See Experiment 2 for treatment descriptions.

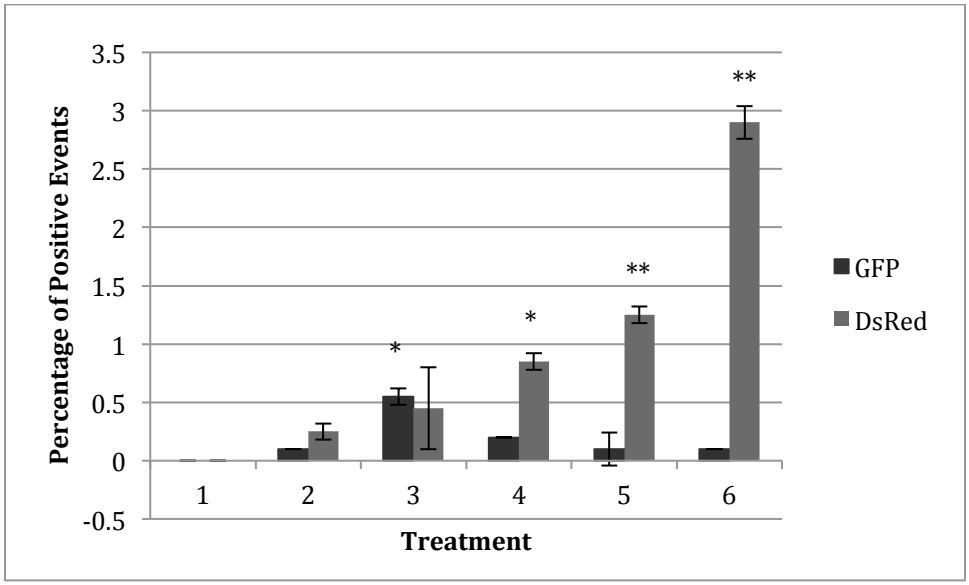

Figure 3.8: The percentage of fluorescing events in HI5c cells transfected with 300 ng of pDsRed-Express2-N1 (Clontech) and 300 ng, 600 ng or 1200 ng of I-*Sce*I expression vector using Lipofectamine 2000 (Life Technologies). Treatment 1 was a cells only control, Treatment 2 was a pDsRed-Express2-N1 (Clontech) control, and Treatment 3 was a gWIZ-GFP (Genlantis) control. Treatments 4-6 contained 300 ng of pDsRed-Express2-N1 (Clontech) and increasing amounts of I-*Sce*I expression vector – 300 ng, 600 ng, and 1200 ng. Fluorescence was measured using a BD FACSCanto II flow cytometer. Cells were harvested 24 hours after transfection. Each treatment contained two replicates and a minimum of 10000 events were analysed per sample. The data are shown as an average percentage of positive events per treatment with s.d. A significant change in the percentage of GFP positive events in Treatments 3 – 6 when compared to Treatment 2 where $P<0.05$ is represented by an asterisk and two asterisks represents $P<0.01$.

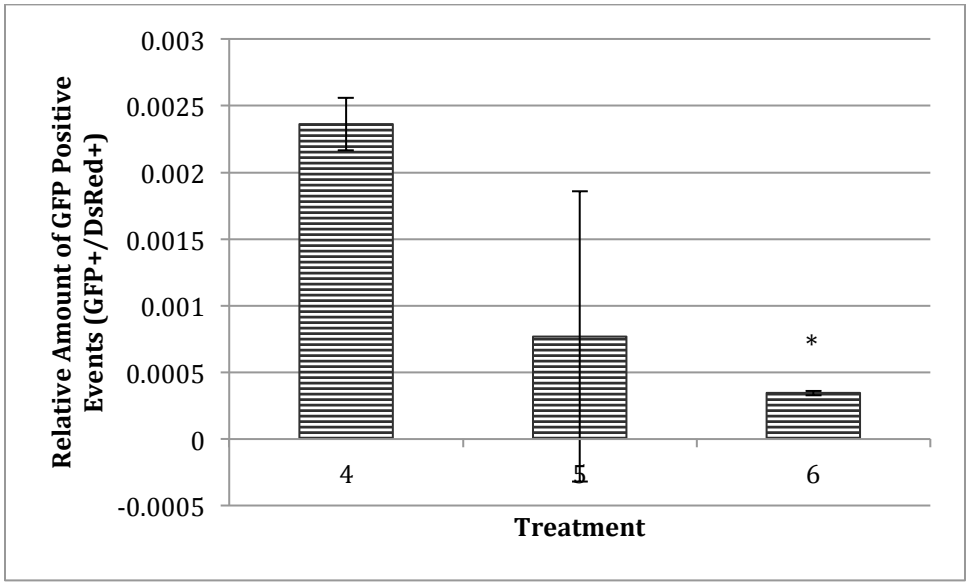

Figure 3.9: The relative amount of GFP positive events after normalisation in HI5c cells transfected with 300 ng of pDsRed-Express2-N1 (Clontech) and 300 ng, 600 ng or 1200 ng of I-*Sce*I expression vector using Lipofectamine 2000 (Life Technologies). Treatments 4-6 contained 300 ng of pDsRed-Express2-N1 (Clontech) and increasing amounts of I-*Sce*I expression vector – 300 ng, 600 ng, and 1200 ng. Fluorescence was measured using a BD FACSCanto II flow cytometer. Cells were harvested 24 hours after transfection. Each treatment contained two replicates and a minimum of 10000 events were analysed per sample. The data are shown as the relative amount of GFP positive events per treatment with s.d. A significant change in the relative amount of GFP positive events in Treatments 5 – 6 when compared to Treatment 4 where $P<0.05$ is represented by an asterisk.

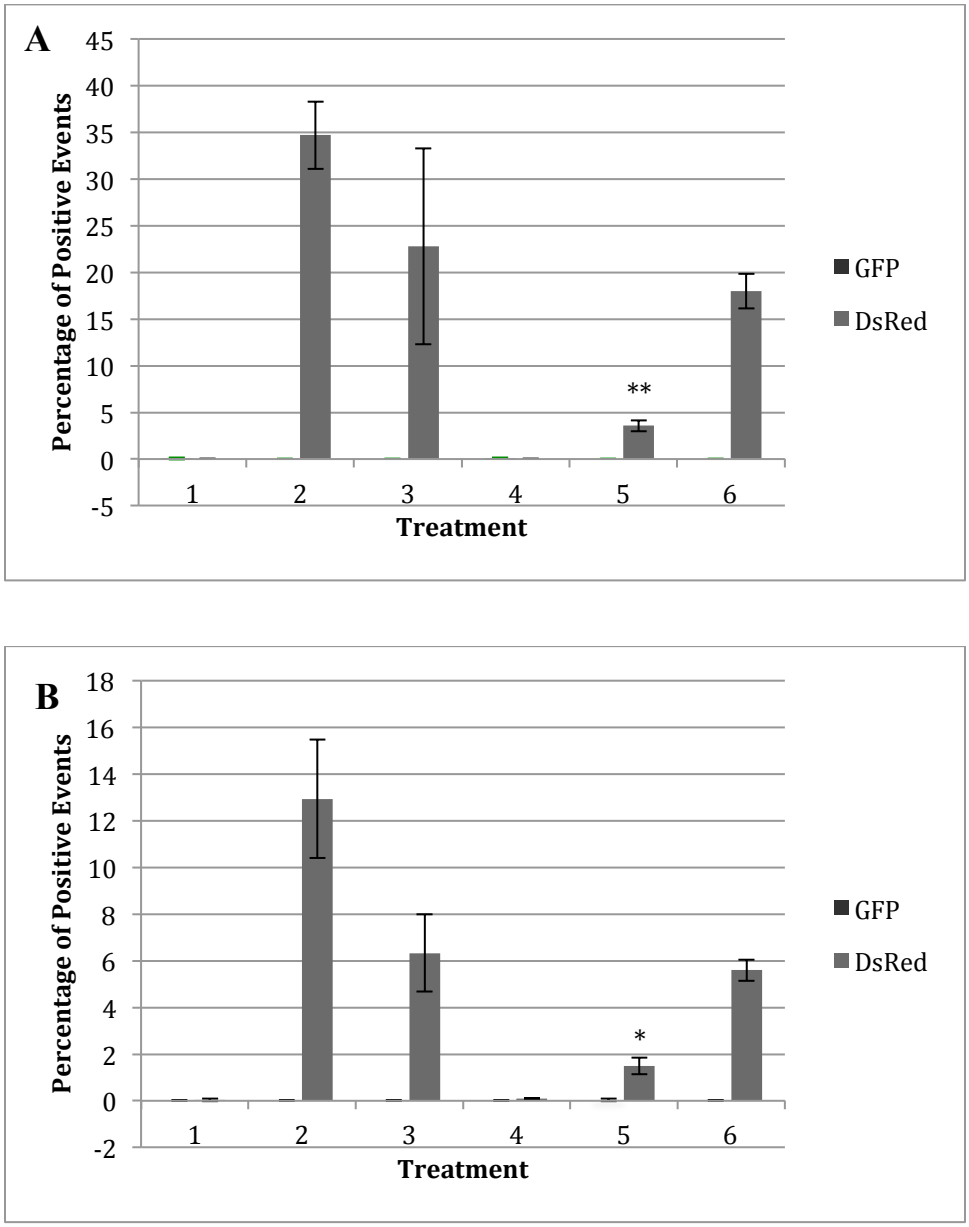

Figure 3.10: The percentage of positive fluorescing events in HI5c and I9a cells transfected with either 500 ng of pDsRed-Express2-N1 (Clontech) (Treatments 2 and 5) or 500 ng of both pDSRed-Express2-N1 (Clontech) and I-*Sce*I expression vector (Treatments 3 and 6) using Lipofectamine LTX with PLUS Reagent (Life Technologies) or TranSIT LT1 (Mirus) (Treatments 1-3 and 4-6 respectively).

Treatments 1 and 4 were cells only controls. Fluorescence was measured using a BD

FACSCanto II flow cytometer. Cells were harvested 24 hours after transfection. Each treatment contained three replicates and a minimum of 10000 events were analysed per sample. The data are shown as an average percentage of positive events per treatment with s.d. A significant change in the percentage of GFP positive events from Treatments 4 – 6 (transfected with Lipofectamine LTX with PLUS Reagent) respectively when compared to Treatment 1-3 (transfected with TranSIT LT1) respectively where $P<0.05$ is represented by an asterisk and two asterisks represents $P<0.01$.

A: HI5c

B: I9a

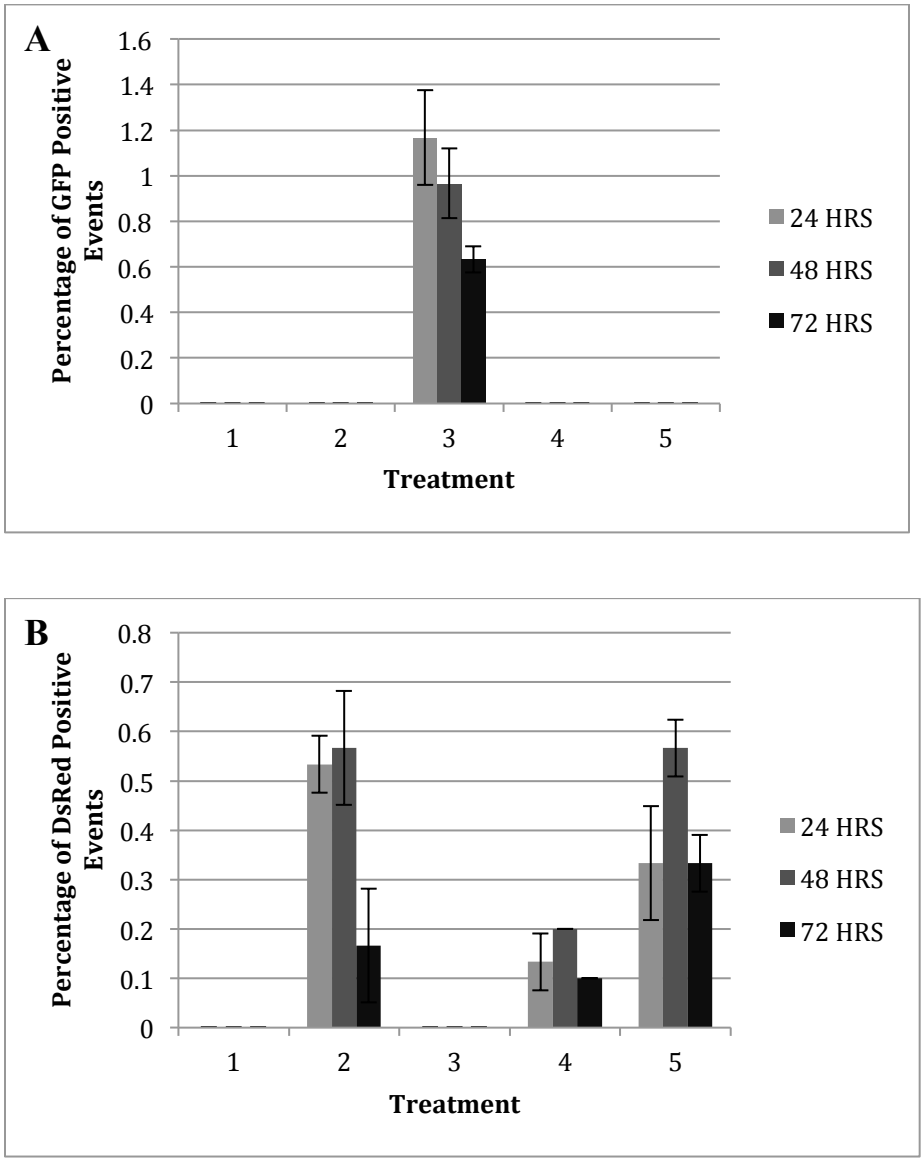

Figure 3.11: Comparing the percentage of positive fluorescing events in HI5c cells at three different post-transfection harvest time points: 24, 48, or 72 hours. Cells were transfected with: 600 ng of pZP500 (Treatment 1); 600 ng of pDsRed-Express2-N1 (Clontech) (Treatment 2); 600 ng of gWIZ-GFP (Genlantis) (Treatment 3); and two different amounts of the I-*Sce*I expression vector and pDsRed-Express2-N1 (Clontech) using TranSIT LT1 (Mirus). Treatment 4 contained 550 ng of I-*Sce*I expression vector and 50 ng of pDsRed-Express2-N1 (Clontech) while Treatment 5 contained 1100 ng and

100 ng respectively. Fluorescence was measured using a BD FACSCanto II flow cytometer. Each treatment contained three replicates and a minimum of 20000 events were analysed per sample. The data are shown as an average percentage of positive events per treatment with s.d. Significant differences between the different time points and treatments are shown in Table 3.7.

A: Comparison of GFP positive events at three post-transfection time points

B: Comparison of DsRed positive events at three post-transfection time points

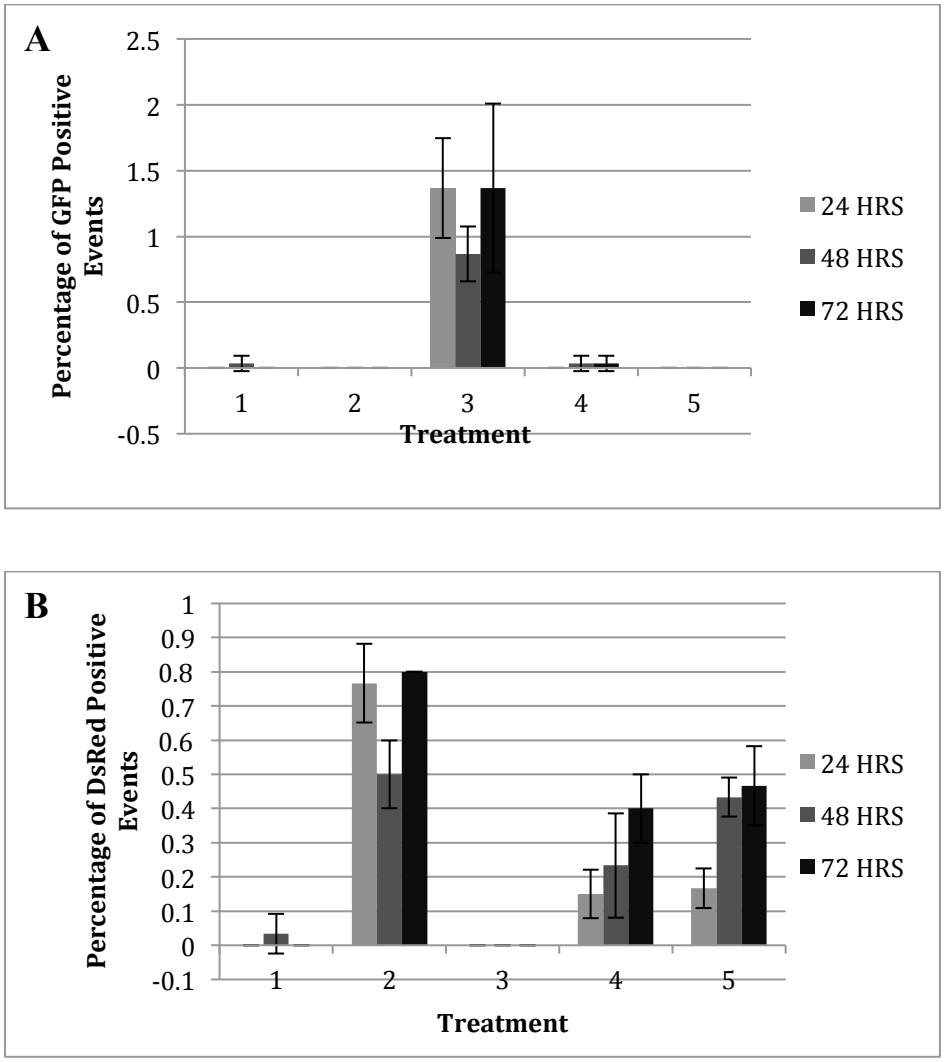

Figure 3.12: Comparing the percentage of positive fluorescing events in I9a cells at three different post-transfection harvest time points: 24, 48, or 72 hours. Cells were transfected with: 600 ng of pZP500 (Treatment 1); 600 ng of pDsRed-Express2-N1 (Clontech) (Treatment 2); 600 ng of gWIZ-GFP (Genlantis) (Treatment 3); and two different amounts of the I-*Sce*I expression vector and pDsRed-Express2-N1 (Clontech) using TranSIT LT1 (Mirus). Treatment 4 contained 550 ng of I-*Sce*I expression vector and 50 ng of pDsRed-Express2-N1 (Clontech) while Treatment 5 contained 1100 ng and 100 ng respectively. Fluorescence was measured using a BD FACSCanto II flow

cytometer. Each treatment contained three replicates and a minimum of 20000 events were analysed per sample. The data are shown as an average percentage of positive events per treatment with s.d. Significant differences between the different time points and treatments are shown in Table 3.8.

A: Comparison of GFP positive events at three post-transfection time points

B: Comparison of DsRed positive events at three post-transfection time points

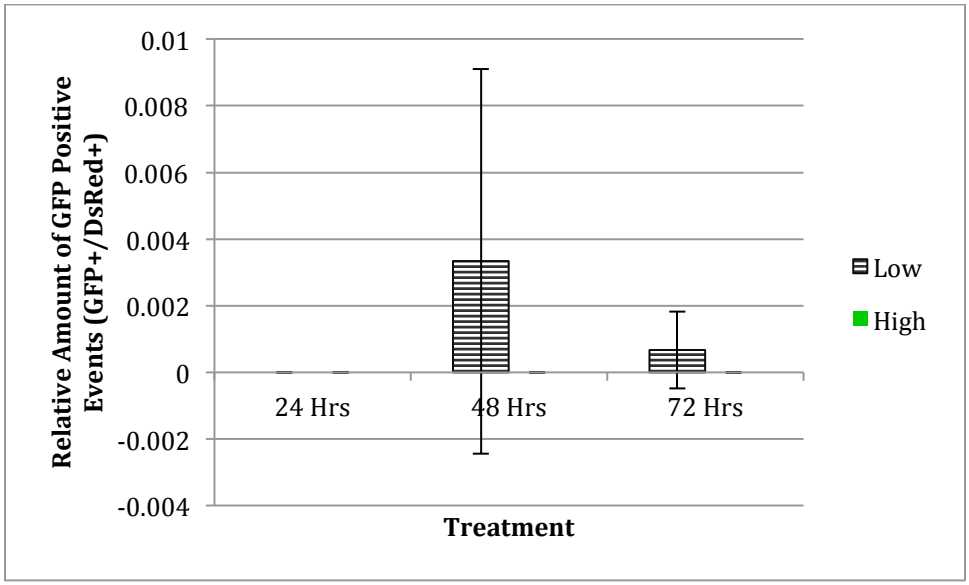

Figure 3.13: Comparing the relative amount of GFP positive events after normalisation in I9a cells at three different post-transfection harvest time points: 24, 48, or 72 hours. In experimental treatments, cells were transfected with two different amounts of the I-*Sce*I expression vector and pDsRed-Express2-N1 (Clontech) using TranSIT LT1 (Mirus). The low treatment contained 550 ng of I-*Sce*I expression vector and 50 ng of pDsRed-Express2-N1 (Clontech) while the high treatment contained 1100 ng and 100 ng respectively. Fluorescence was measured using a BD FACSCanto II flow cytometer. Each treatment contained three replicates and a minimum of 20000 events were analysed per sample. The data are shown as an average relative amount of GFP positive events per treatment with s.d. Significant differences between the different time points and treatments are shown in Table 3.7 and 3.8.

`

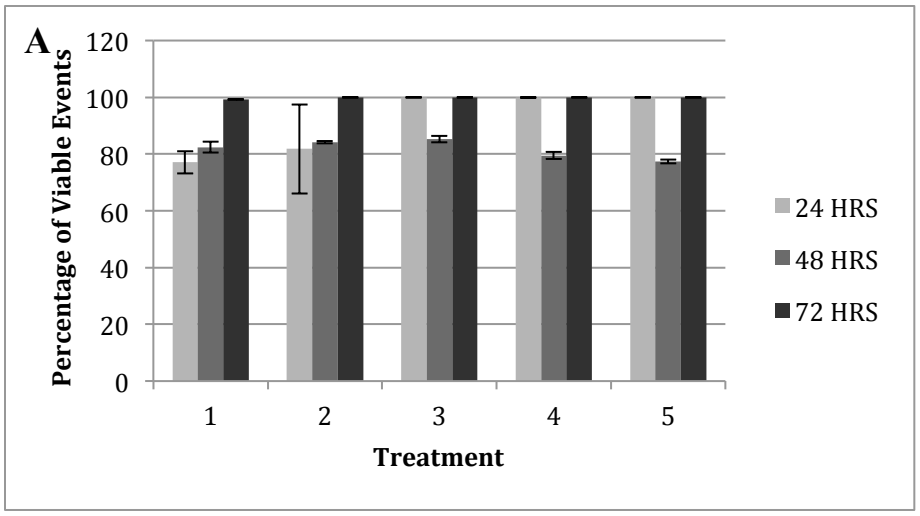

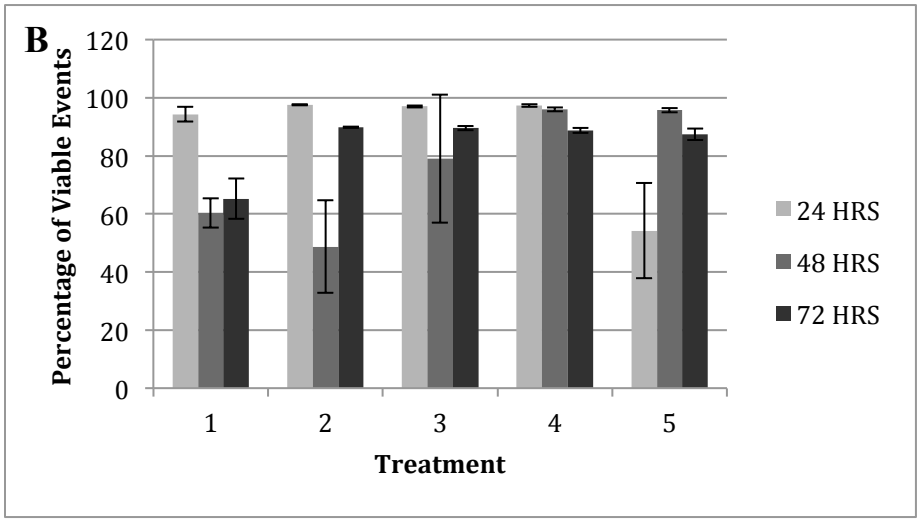

Figure 3.14: Comparing the percentage of viable events in HI5c and I9a cells at three different post-transfection harvest time points: 24, 48, or 72 hours. Cells were transfected with: 600 ng of pZP500 (Treatment 1); 600 ng of pDsRed-Express2-N1 (Clontech) (Treatment 2); 600 ng of gWIZ-GFP (Genlantis) (Treatment 3); and two different amounts of the I-*Sce*I expression vector and pDsRed-Express2-N1 (Clontech) using TranSIT LT1 (Mirus). Treatment 4 contained 550 ng of I-*Sce*I expression vector

and 50 ng of pDsRed-Express2-N1 (Clontech) while Treatment 5 contained 1100 ng and 100 ng respectively. Each treatment contained three replicates. A minimum of 20000 events were analysed per sample on a BD FACSCanto II flow cytometer. The data are shown as an average percentage of viable events per treatment with s.d. Significant differences between the different time points and treatments are shown in Table 3.7 and 3.8.

A: HI5c

B: I9a

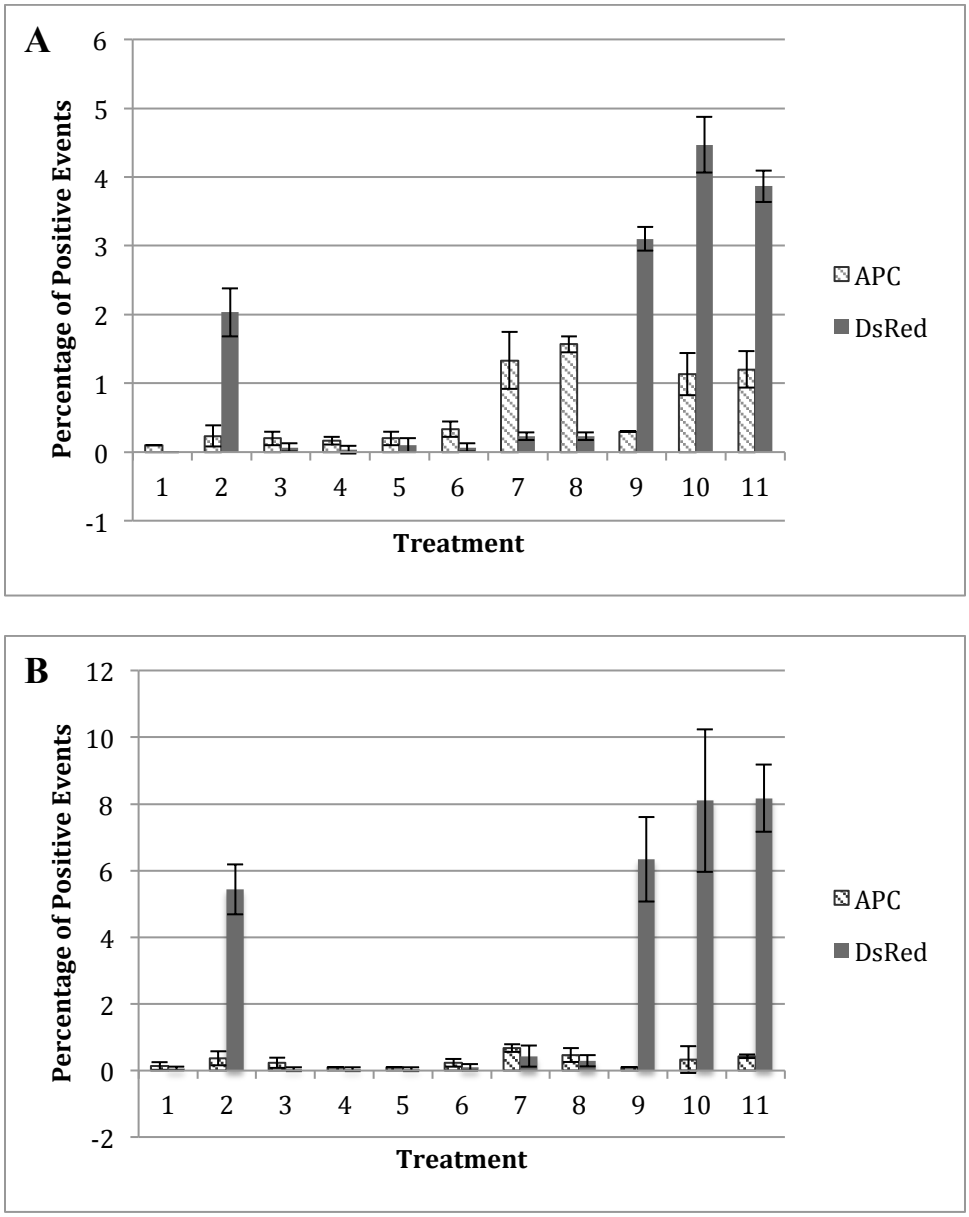

Figure 3.15: Comparison of APC and DsRed positive fluorescing events in experiments comparing pCMV-Neo-Bam APC and pDSRed-Express2-N1 as transfection controls. HI5c and I9a cells were transfected with: pDsRed-Express2-N1 (Clontech); pCMV-Neo-Bam APC (Addgene); I-*Sce*I expression vector; gWIZ-GFP (Genlantis); different ratios of pDsRed-Express2-N1 (Clontech) and I-*Sce*I expression vector; and different ratios of pCMV-Neo-Bam APC (Addgene) and I-*Sce*I expression

vector using Lipofectamine LTX with PLUS Reagent (Life Technologies). Treatment 1 is a cells only control, Treatment 2 is a pDsRed-Express2-N1 only control, Treatment 3 is a pCMV-Neo-Bam APC only control, Treatment 4 is an I-*Sce*I expression vector only control, and Treatment 5 is gWIZ-GFP only control. Treatments 6-8 contain pCMV-Neo-Bam APC and I-*Sce*I expression vector in ratios of 300 ng:300 ng, 500 ng:500 ng, and 400 ng:600 ng respectively. Treatments 9-11 contain pDsRed-Express2-N1 and I-*Sce*I expression vector in ratios of 300 ng:300 ng, 500 ng:500 ng, and 400 ng:600 ng respectively. Fluorescence was measured using a BD FACSCanto II flow cytometer. Cells were harvested 30 hours after transfection. Each treatment contained three replicates and a minimum of 10000 viable events were analysed per sample. The data are shown as an average percentage of positive events per treatment with s.d.

A: HI5c

B: I9a

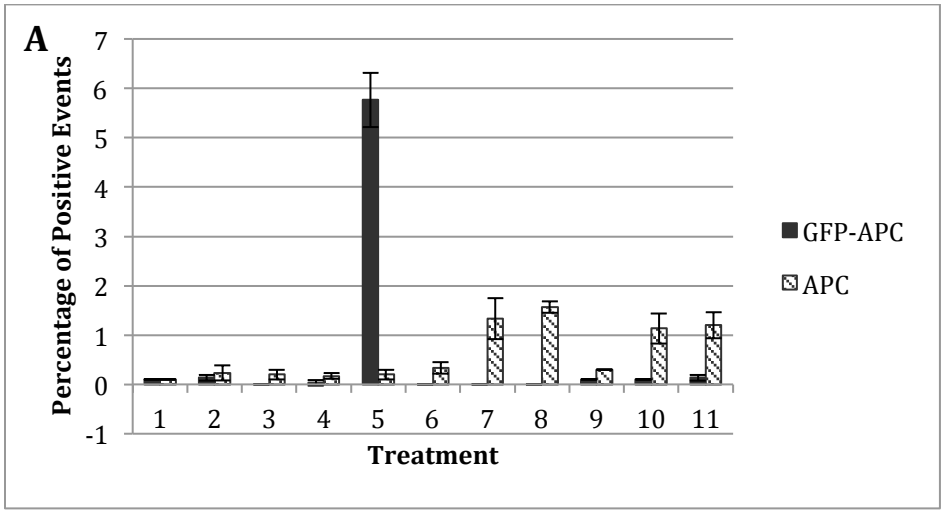
A
Percentage of Positive Events
7
6
5
4
3
2
1
0
-1
1 2 3 4 5 6 7 8 9 10 11
Treatment
GFP-APC
APC

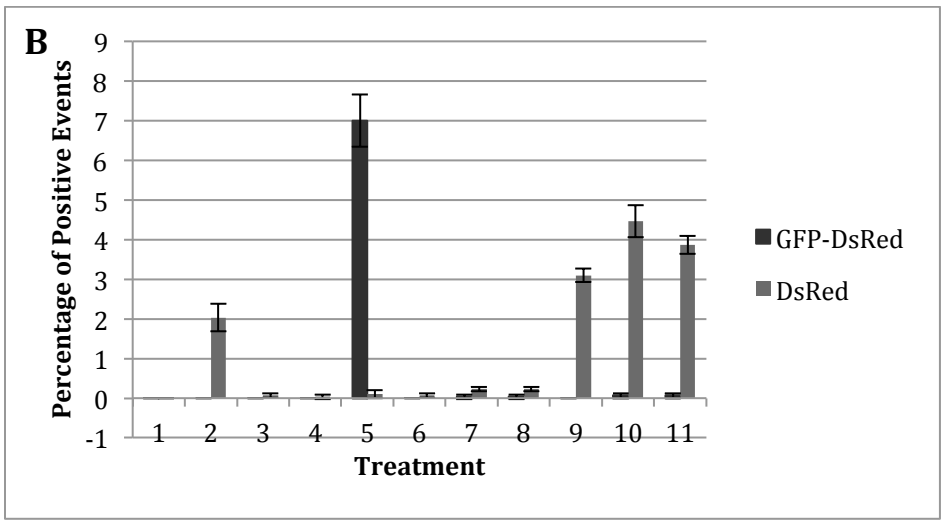
B
Percentage of Positive Events
9
8
7
6
5
4
3
2
1
0
-1
1 2 3 4 5 6 7 8 9 10 11
Treatment
GFP-DsRed
DsRed

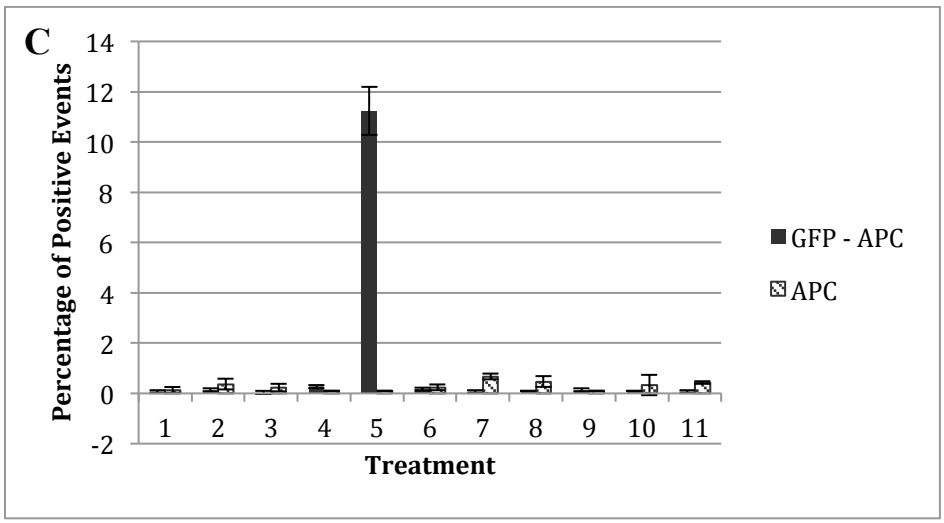
C
Percentage of Positive Events
14
12
10
8
6
4
2
0
-2
1 2 3 4 5 6 7 8 9 10 11
Treatment
GFP - APC
APC

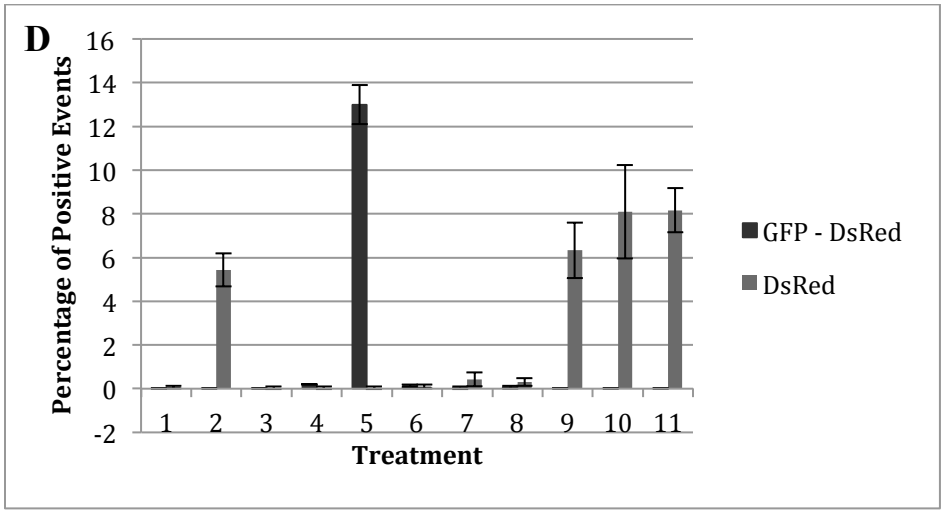

Figure 3.16: The percentage of positive fluorescing events in experiments comparing pCMV-Neo-Bam APC and pDSRed-Express2-N1 as transfection controls. HI5c and I9a cells were transfected with: pDsRed-Express2-N1 (Clontech); pCMV-Neo-Bam APC (Addgene); I-*Sce*I expression vector; gWIZ-GFP (Genlantis); different ratios of pDsRed-Express2-N1 (Clontech) and I-*Sce*I expression vector; and different ratios of pCMV-Neo-Bam APC (Addgene) and I-*Sce*I expression vector using Lipofectamine LTX with PLUS Reagent (Life Technologies). Treatment 1 is a cells only control, Treatment 2 is a pDsRed-Express2-N1 only control, Treatment 3 is a pCMV-Neo-Bam APC only control, Treatment 4 is an I-*Sce*I expression vector only control, and Treatment 5 is gWIZ-GFP only control. Treatments 6-8 contain pCMV-Neo-Bam APC and I-*Sce*I expression vector in ratios of 300 ng:300 ng, 500 ng:500 ng, and 400 ng:600 ng respectively. Treatments 9-11 contain pDsRed-Express2-N1 and I-*Sce*I expression vector in ratios of 300 ng:300 ng, 500 ng:500 ng, and 400 ng:600 ng respectively. Fluorescence was measured using a BD FACSCanto II flow cytometer. Cells were harvested 30 hours after transfection. Each treatment contained three replicates and a minimum of 10000 viable events were

analysed per sample. The data are shown as an average percentage of positive events per treatment with s.d.

A: HI5c – Comparison of GFP and DsRed positive events gated on a FITC vs. PE scatterplot

B: HI5c – Comparison of GFP and APC positive events gated on a FITC vs. APC scatterplot

C: I9a – Comparison of GFP and DsRed positive events gated on a FITC vs. PE scatterplot

D: I9a – Comparison of GFP and APC positive events gated on a FITC vs. APC scatterplot

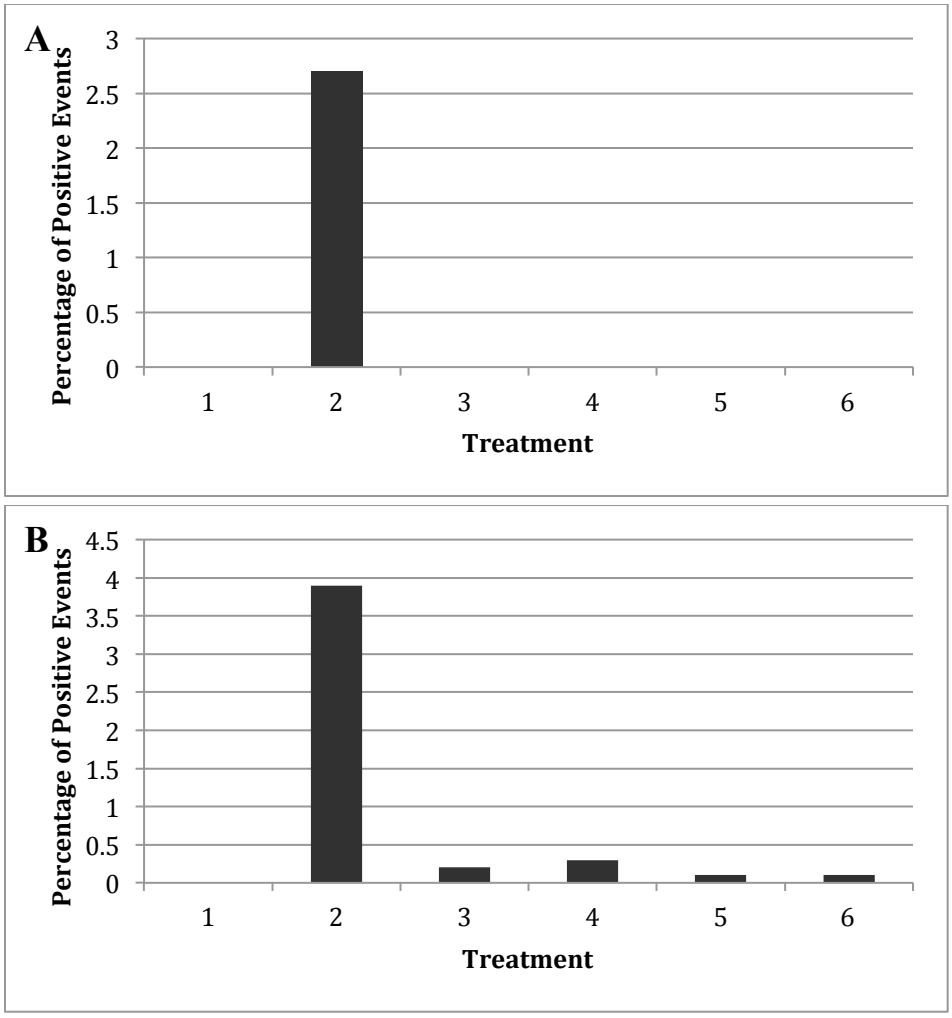

Figure 3.17: The percentage of GFP positive events in HI5c and I9a cells transfected with either 600 ng or 1000 ng of I-*Sce*I expression vector and 3 µl or 5 µl of Lipofectamine LTX with PLUS Reagent (Life Technologies). Treatment 1 is a cells only control and Treatment 2 is a gWIZ-GFP only control. Treatment 3 and 4 were transfected with 600 ng and 1000 ng of I-*Sce*I expression vector respectively and 3 µl of transfection reagent. Treatment 5 and 6 were transfected with 600 ng and 1000 ng of I-*Sce*I expression vector respectively and 5 µl of transfection reagent. Fluorescence was measured using a BD FACSCanto II flow cytometer. Cells were harvested 24 hours after

transfection. A minimum of 10000 events were analysed per sample. There was only one sample per treatment so no averages or standard deviations were calculated.

A: HI5c

B: I9a

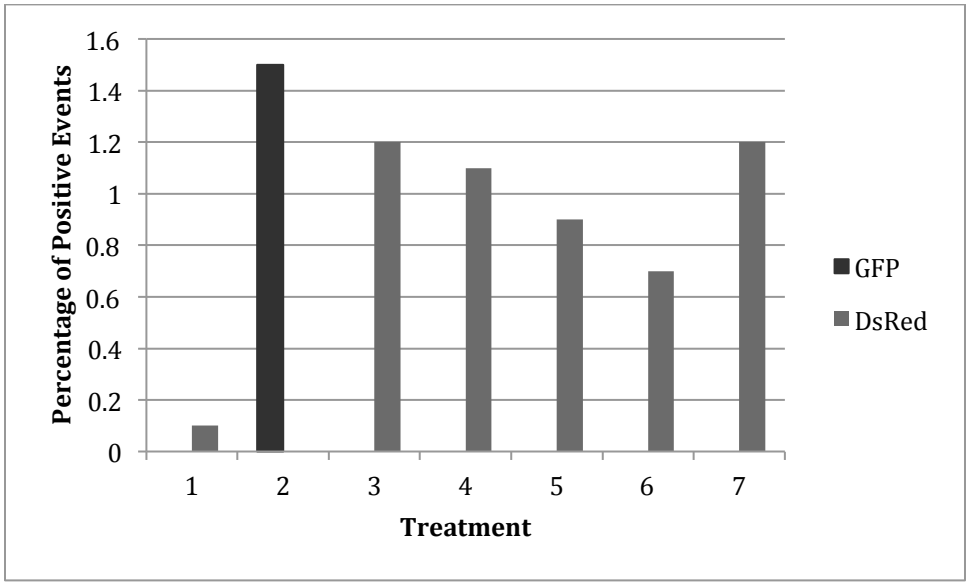

Figure 3.18: The percentage of positive fluorescing events in HI5c cells transfected with 100 ng of pDsRed-Express2-N1 (Clontech) and 500 ng of one of four I-*Sce*I expression vector stocks (Treatments 4-7) using Lipofectamine 2000 (Life Technologies). Treatment 1 was a pZP500 control, Treatment 2 was a gWIZ-GFP (Genlantis) control, and Treatment 3 was a pDsRed-Express2-N1 (Clontech) control. In each control 600 ng of plasmid was used. Fluorescence was measured using a BD FACSCanto II flow cytometer. Cells were harvested 30 hours after transfection and a minimum of 10000 events were analysed per sample. There was only one sample per treatment so no averages or standard deviations were calculated.

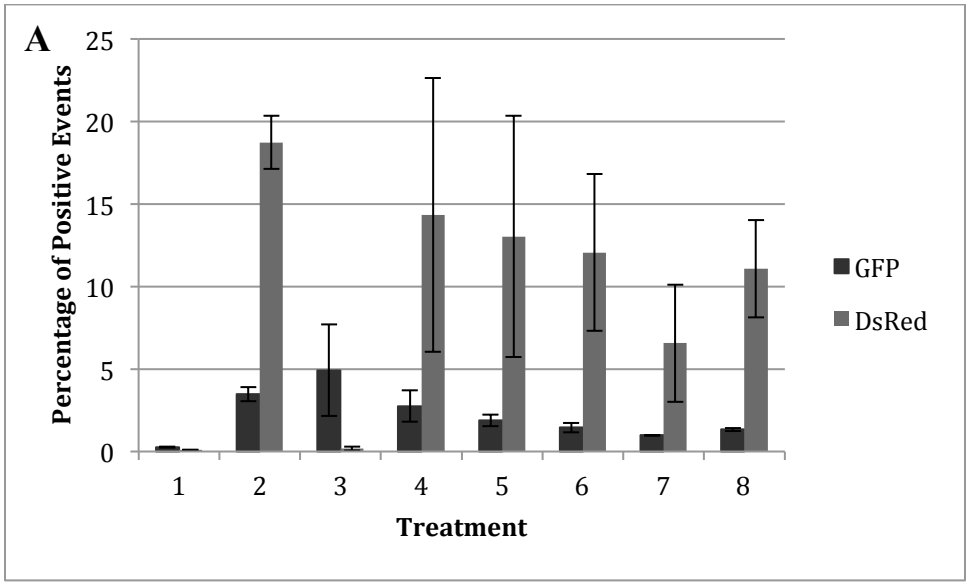

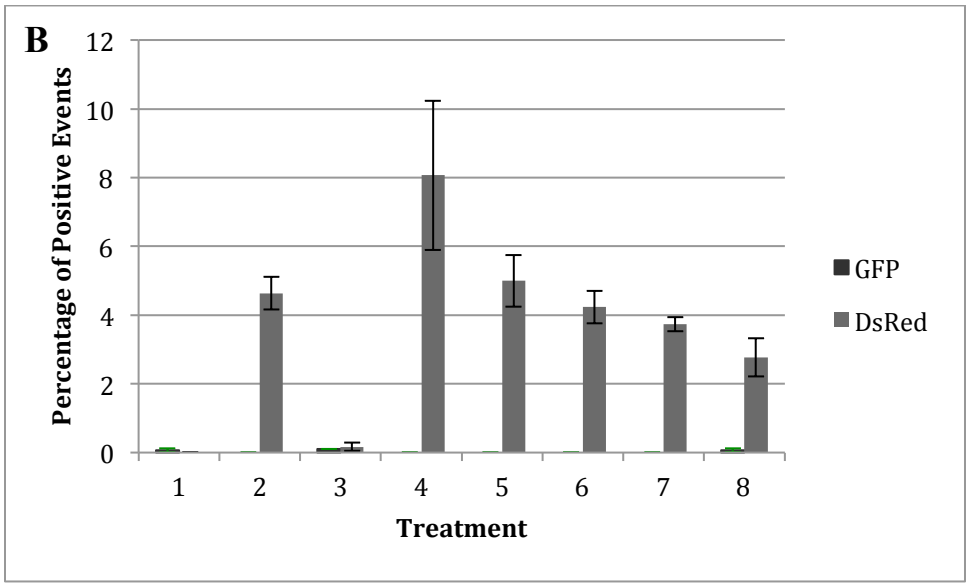

Figure 3.19: The percentage of positive fluorescing events in HI5c and I9a cells transfected with 400 ng of pDsRed-Express2-N, 600 ng of I-*Sce*I expression vector, and either 0.5 µg or 1.0 µg of anti-Ku or anti-DNA-PK$_{cs}$ antibodies using Lipofectamine LTX with PLUS Reagent (Life Technologies). Treatment 1 is a cells only control, Treatment 2 is pDsRed-Express2-N1 only control, Treatment 3 is an I-*Sce*I expression vector, and Treatment 4 is a no antibody control. Treatments 5 and 6 contained 0.5 µg and 1 µg of anti-Ku70 antibodies respectively. Treatments 7 and 8

contained 0.5 µg and 1 µg of anti-DNA-PK_{CS} antibodies respectively. Treatments 4-8 also contained 400 ng of pDsRed-Express2-N1 and 600 ng of I-*Sce*I expression vector. Fluorescence was measured using a BD FACSCanto II flow cytometer. Cells were harvested 24 hours after transfection. Each treatment contained three replicates and a minimum of 10000 events were analysed per sample. The data are shown as an average percentage of positive events per treatment with s.d. No significant changes in the percentages of positive events were found in Treatments 5-8 (antibodies present) when compared to Treatment 4 (no antibody control).

A: HI5c

B: I9a

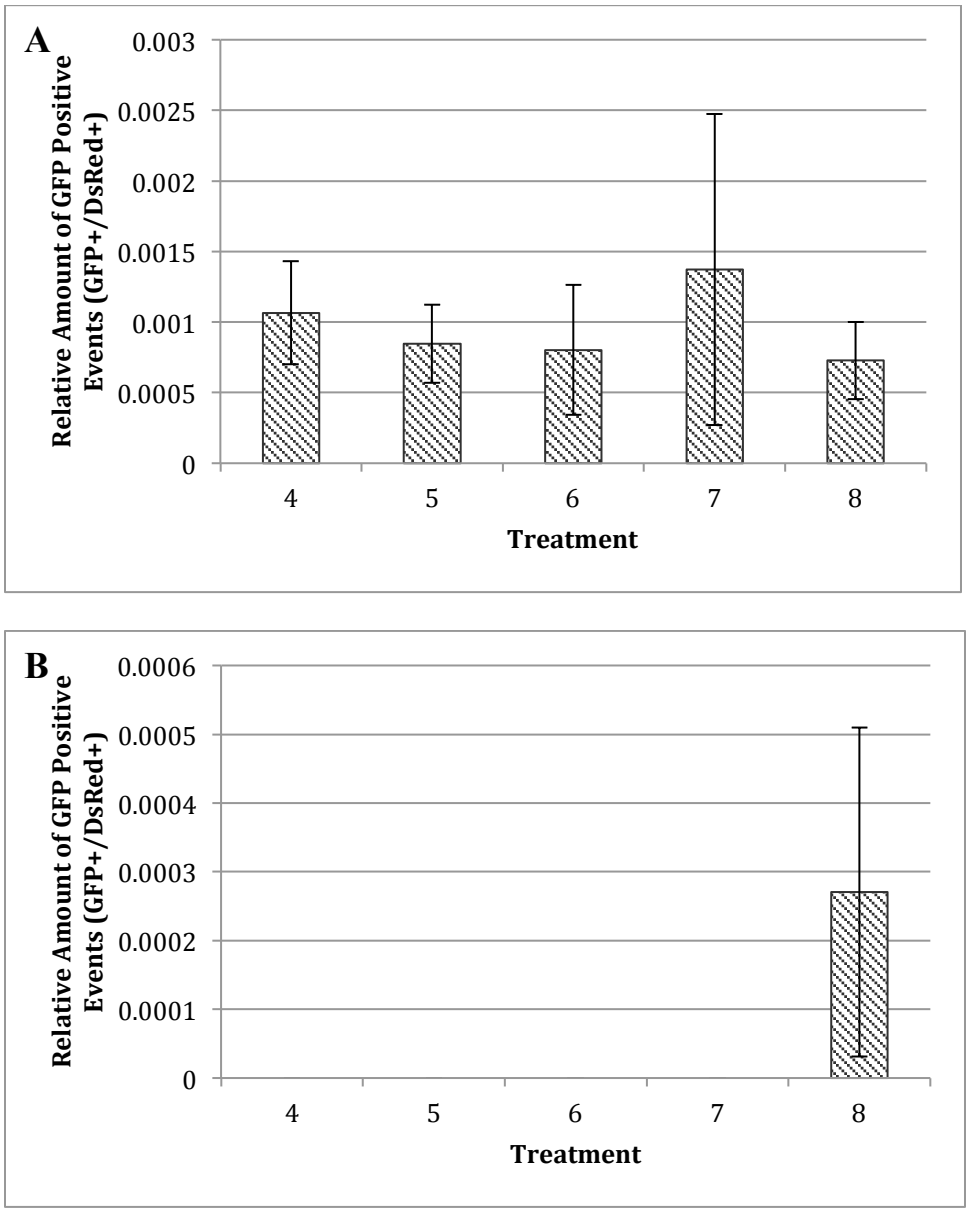

Figure 3.20: The relative amount of GFP positive events in HI5c and I9a cells transfected with 400 ng of pDsRed-Express2-N1 (Clontech), 600 ng of I-*Sce*I expression vector, and either 0.5 µg or 1.0 µg of anti-Ku or anti-DNA-PK$_{cs}$ antibodies using Lipofectamine LTX with PLUS Reagent (Life Technologies). No normalisation was done for Treatments 1-3. Treatment 4 is a no antibody control, Treatments 5 and 6 contained 0.5 µg and 1 µg of anti-Ku70 antibodies respectively, and

Treatments 7 and 8 contained 0.5 µg and 1 µg of anti-DNA-PK_{CS} antibodies respectively. Treatments 4-8 also contained 400 ng of pDsRed-Express2-N1 and 600 ng of I-*Sce*I expression vector. Fluorescence was measured using a BD FACSCanto II flow cytometer. Cells were harvested 24 hours after transfection. The data are shown as an average relative amount of GFP positive events per treatment with s.d. No significant changes in the percentages of positive events in Treatments 5-8 (antibodies present) when compared to Treatment 4 (no antibody control) were present.

A: HI5c

B: I9a

Supplementary Table 3.1: Treatments comparing Lipofectamine 2000 (Life Technologies) and Chariot (Active Motif) as transfection reagents in HEK293. Cells were harvested 24 hours after transfection. Each treatment contained three replicates. A minimum of 10000 events were analysed per sample on a BD FACSCanto II flow cytometer.

No.	Treatment	Delivery Method	gWIZ-GFP (ng)	pDsRed-Express2-N1 (ng)	pZP500 (ng)	Anti-GFP (µg)
1	Cells Only	Lipofectamine 2000	---------	---------	---------	---------
2	Cells Only	Chariot	---------	---------	---------	---------
3	gWIZ-GFP, pDsRed-Express2-N1	Lipofectamine 2000	300	300	---------	---------
4	gWIZ-GFP, pDsRed-Express2-N1	Chariot	300	300	---------	---------
5	pZP500	Lipofectamine 2000	---------	---------	300	---------
6	pZP500	Chariot	---------	---------	300	---------
7	gWIZ-GFP, pDsRed-Express2-N1, Ab 1 µg	Lipofectamine 2000	300	300	---------	1
8	gWIZ-GFP, pDsRed-Express2-N1, Ab 1 µg	Chariot	300	300	---------	1
9	gWIZ-GFP, pDsRed-Express2-N1, Ab 2 µg	Chariot	300	300	---------	2
10	gWIZ-GFP, pDsRed-Express2-N1, Ab 4 µg	Chariot	300	300	---------	4

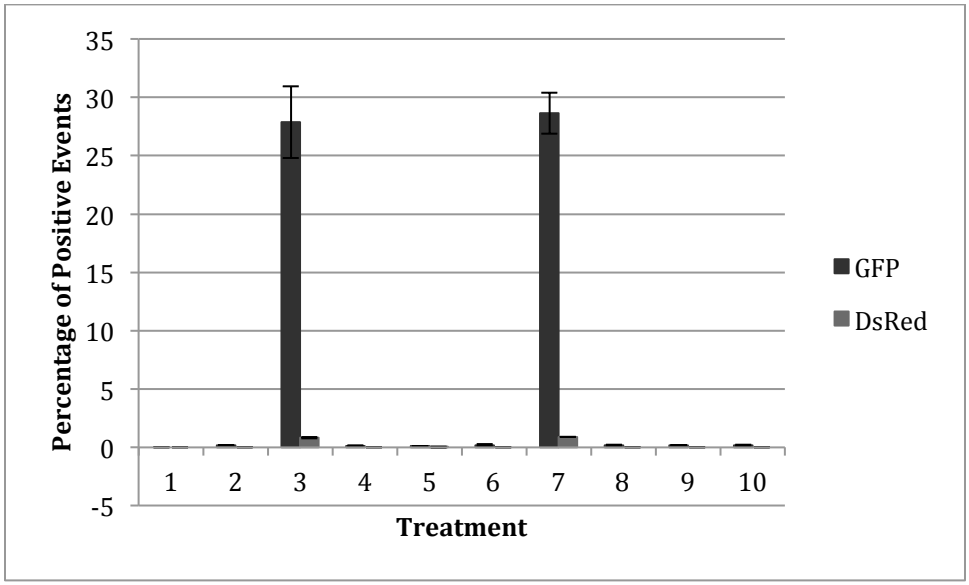

Supplementary Figure 3.1: The percentage of positive fluorescing events in HEK293 cells transfected with 300 ng of both gWIZ-GFP (Genlantis) and pDsRed-Express2-N1 (Clontech) in addition to 1 µg, 2 µg, or 4 µg of anti-GFP antibodies (Santa Cruz Biotechnology). Treatments 1, 3, 5, and 7 were transfected with Lipofectamine 2000 (Life Technologies). Treatments 2, 4, 6, and 8-10 were transfected with Chariot (Active Motif). Treatments 1 and 2 are cells only controls, Treatment 5 and 6 are pZP500 only controls, Treatments 3 and 4 are no antibody controls. Treatments 7 and 8 contain 1 µg of antibodies, Treatment 9 contains 2 µg of antibodies, and Treatment 10 contains 4 µg of antibodies. Treatments 3-4 and 7-10 contain both 300 ng of gWIZ-GFP and 300 ng of pDsRed-Express2-N1. Fluorescence was measured using a BD FACSCanto II flow cytometer. Cells were harvested 24 hours after transfection. Each treatment contained three replicates and a minimum of 10000 events were analysed per sample. The data are shown as an average percentage of positive events per treatment with s.d.

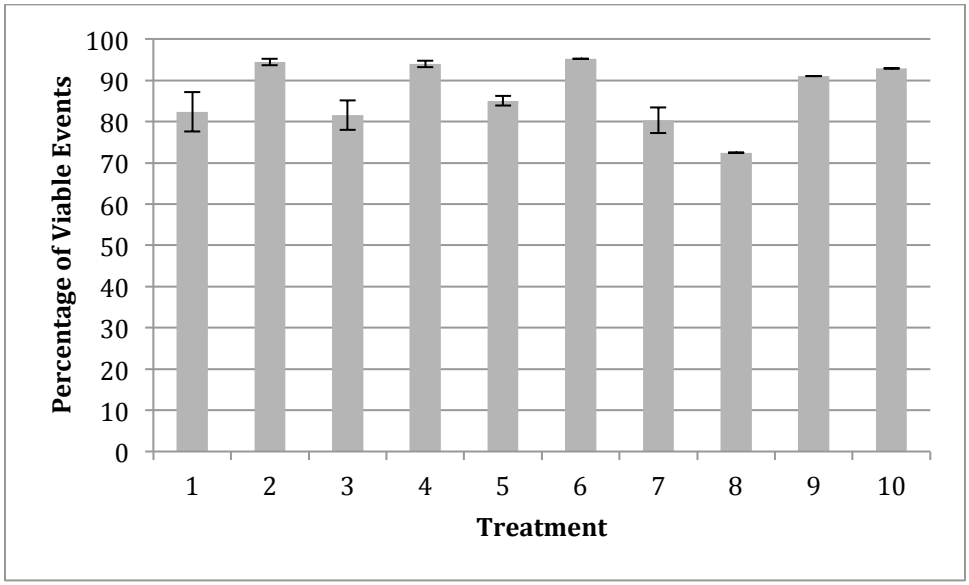

Supplementary Figure 3.2: The percentage of viable events in HEK293 cells transfected with 300ng of both gWIZ-GFP (Genlantis) and pDsRed-Express2-N1 (Clontech) in addition to 1µg, 2µg, or 4µg of anti-GFP antibodies (Santa Cruz Biotechnology) using Lipofectamine 2000 (Life Technologies) or Chariot (Active Motif). Treatments 1, 3, 5, and 7 were transfected with Lipofectamine 2000 (Life Technologies). Treatments 2, 4, 6, and 8-10 were transfected with Chariot (Active Motif). Treatments 1 and 2 are cells only controls, Treatment 5 and 6 are pZP500 only controls, Treatments 3 and 4 are no antibody controls. Treatments 7 and 8 contain 1 µg of antibodies, Treatment 9 contains 2 µg of antibodies, and Treatment 10 contains 4 µg of antibodies. Treatments 3-4 and 7-10 contain both 300 ng of gWIZ-GFP and 300 ng of pDsRed-Express2-N1. Cells were harvested 24 hours after transfection. Each treatment contained three replicates and a minimum of 10000 events were analysed per sample on a BD FACSCanto II flow cytometer. The data are shown as an average percentage of viable events per treatment with s.d.

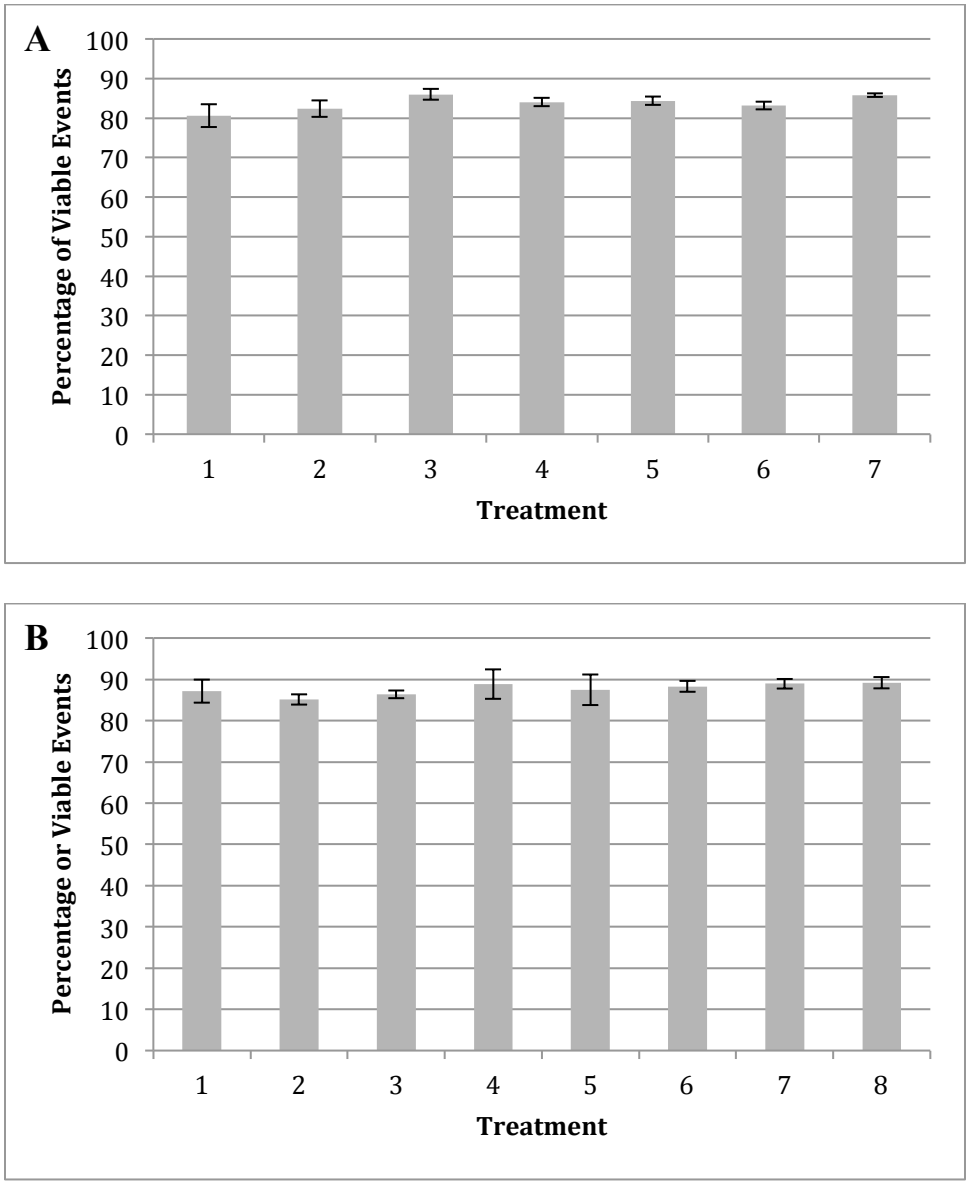

Supplementary Figure 3.3: The percentage of viable events in HEK293 cells transfected with 300 ng of both gWIZ-GFP (Genlantis) and pDsRed-Express2-N1 (Clontech) in addition to either 1 µg, 2 µg, or 5 µg of anti-GFP antibodies (Santa Cruz Biotechnology) using Lipofectamine 2000 (Life Technologies). Cells were harvested 24 hours after transfection. Each treatment contained three replicates and a minimum of 10000 events were analysed per sample on a BD FACSCanto II flow cytometer. The data are shown as an average percentage of viable events per treatment

with s.d. No significant changes in the percentages of viable events were present in Treatments 5-7 (antibodies present) when compared to Treatment 4 (no antibody control).

A: Experiment 1 -- Treatment 1 is a cells only control; Treatment 2 is a pZP500 only control; Treatment 3 is a pDsRed-Express2-N1 only control; Treatment 4 contained no antibodies; Treatments 5-7 contained 1 µg, 2 µg, and 5 µg of antibodies respectively. Treatments 4-7 contained 300 ng of each gWIZ-GFP and pDsRed-Express2-N1.

B: Experiment 2 -- Treatment 1 is a pZP500 only control; Treatment 2 is a pDS-Red-Express2-N1 only control; Treatment 3 is a gWIZ-GFP only control; Treatment 4 contained no antibodies; Treatments 5-7 contained 1 µg, 2 µg, and 5 µg of antibodies respectively. Treatments 4-7 contained 300 ng of each gWIZ-GFP and pDsRed-Express2-N1. Treatment 8 was a no transfection reagent control with 5 µg of antibodies.

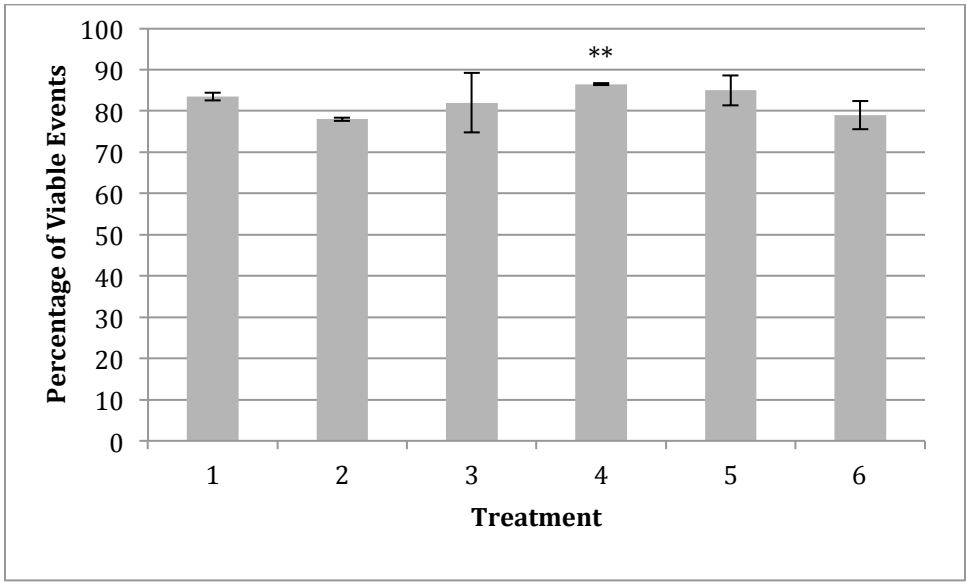

Supplementary Figure 3.4: The percentage of viable events in HI5c cells transfected with 300 ng of pDsRed-Express2-N1 (Clontech) and 300 ng, 600 ng or 1200 ng of I-*Sce*I expression vector using Lipofectamine 2000 (Life Technologies). Treatment 1 was a cells only control, Treatment 2 was a pDsRed-Express2-N1 (Clontech) only control, and Treatment 3 was a gWIZ-GFP (Genlantis) only control. Treatments 4-6 contained 300 ng of pDsRed-Express2-N1 (Clontech) and increasing amounts of I-*Sce*I expression vector – 300 ng, 600 ng, and 1200 ng. Cells were harvested 24 hours after transfection. Each treatment contained two replicates. A minimum of 10000 events were analysed per sample on a BD FACSCanto II flow cytometer. The data are shown as an average percentage of viable events per treatment with s.d. A significant change in the percentage of viable events in Treatments 3 – 6 when compared to Treatment 2 where $P<0.01$ is represented by two asterisks.

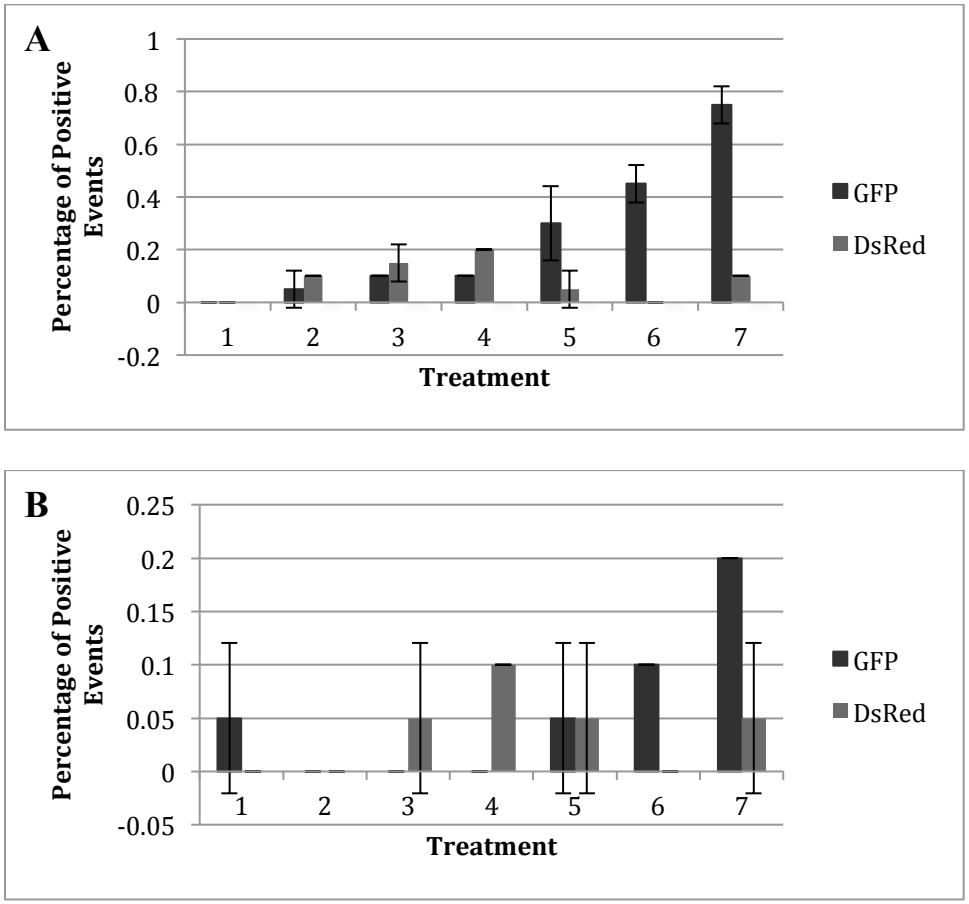

Supplementary Figure 3.5: The percentage of positive fluorescing events in HI5c and I9a cells transfected with 300 ng, 600 ng, or 1200 ng of pDsRed-Express2-N1 (Clontech) (Treatments 2-4 respectively) or gWIZ-GFP (Genlantis) (Treatments 5-7 respectively) using Lipofectamine 2000 (Life Technologies). Treatment 1 was a cells only control. Fluorescence was measured using a BD FACSCanto II flow cytometer. Cells were harvested 24 hours after transfection. Each treatment contained two replicates and a minimum of 10000 events were analysed per sample. The data are shown as an average percentage of fluorescing events per treatment with s.d.

A: HI5c

B: I9a

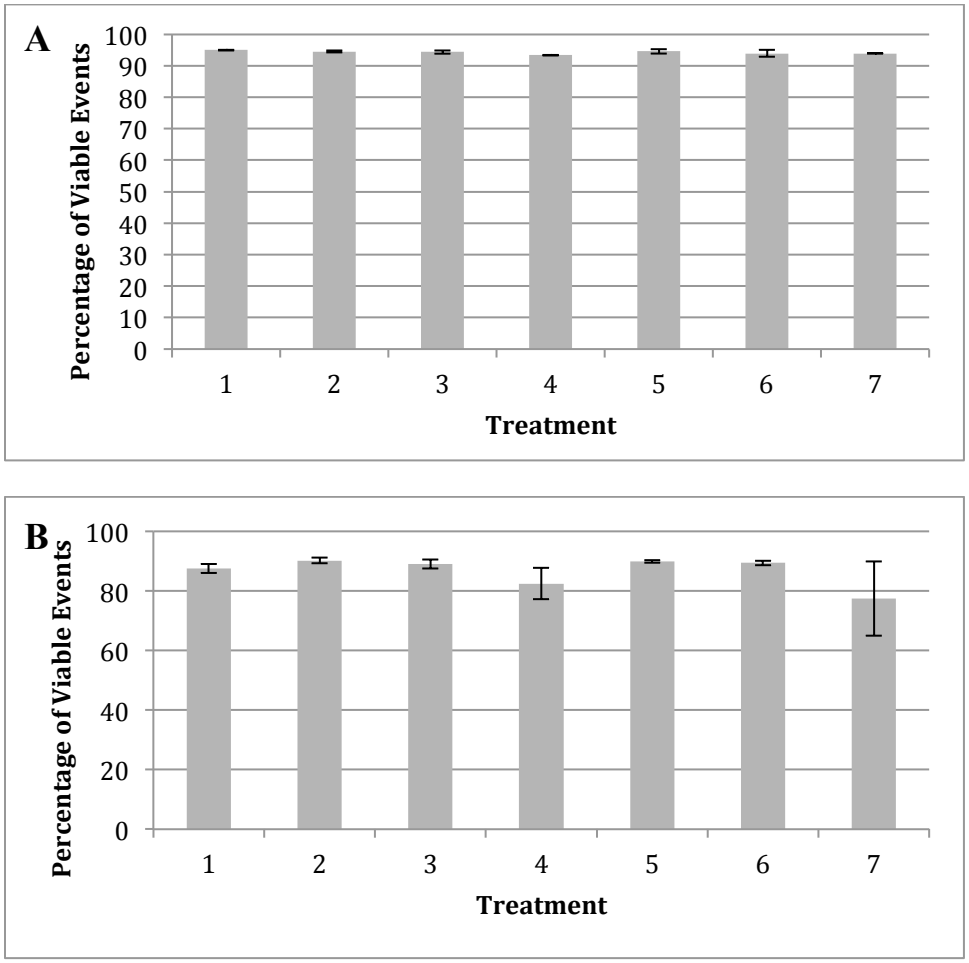

Supplementary Figure 3.6: The percentage of viable events in HI5c and I9a cells transfected with 300 ng, 600 ng, or 1200 ng of pDsRed-Express2-N1 (Clontech) (Treatments 2-4 respectively) or gWIZ-GFP (Genlantis) (Treatments 5-7 respectively) using Lipofectamine 2000 (Life Technologies). Treatment 1 was a cells only control. Cells were harvested 24 hours after transfection. Each treatment contained two replicates. A minimum of 10000 events were analysed per sample on a BD FACSCanto II flow cytometer. The data are shown as an average percentage of viable events per treatment with s.d.

A: HI5c

B: I9a

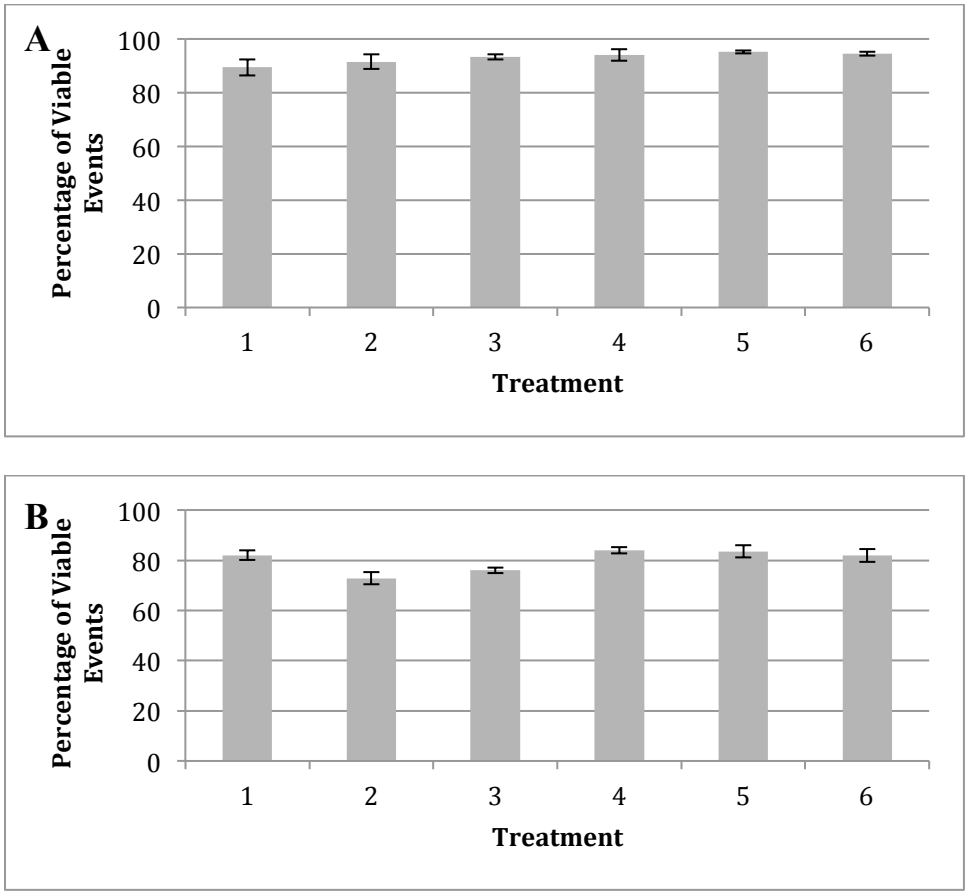

Supplementary Figure 3.7: The percentage of viable events in HI5c and I9a cells transfected with either 500 ng of pDsRed-Express2-N1 (Clontech) (Treatments 2 and 5) or 500 ng of both pDSRed-Express2-N1 (Clontech) and I-*Sce*I expression vector (Treatments 3 and 6) with PLUS reagent using Lipofectamine LTX with PLUS Reagent (Life Technologies) or TranSIT LT1 (Mirus) (Treatments 1-3 and 4-6 respectively). Treatments 1 and 4 were cells only controls. Cells were harvested 24 hours after transfection. Each treatment contained three replicates. A minimum of 10000 events were analysed per sample on a BD FACSCanto II flow cytometer. The data are shown as an average percentage of viable events per treatment with s.d.

A: HI5c

B: I9a

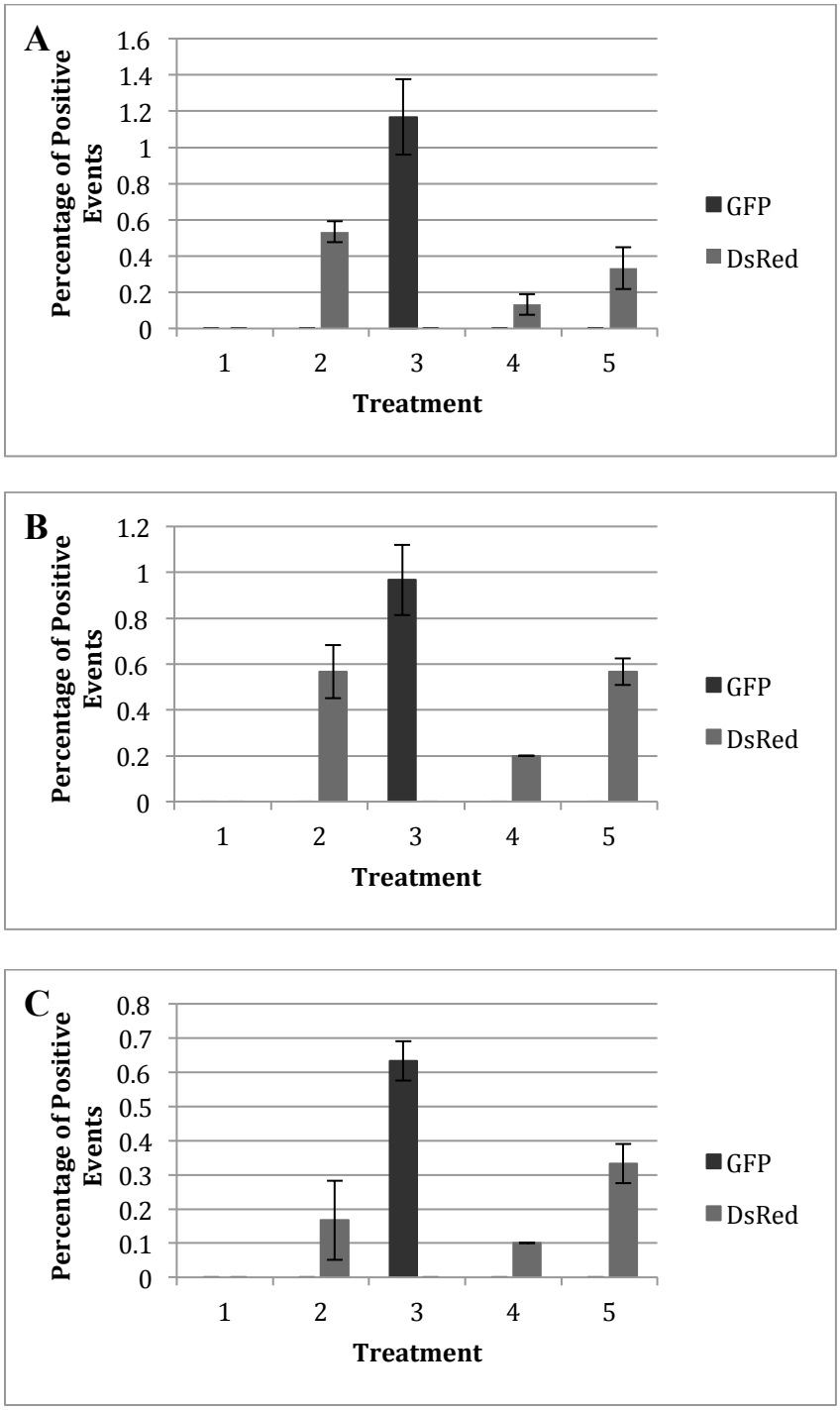

Supplementary Figure 3.8: The percentage of positive fluorescing events in HI5c cells transfected with: pZP500 (Treatment 1); pDsRed-Express2-N1 (Clontech) (Treatment 2); gWIZ-GFP (Genlantis) (Treatment 3); and two different amounts of the I-*Sce*I expression vector and pDsRed-Express2-N1 (Clontech) using TranSIT

LT1 (Mirus). The controls contained 600 ng of plasmid. Treatment 4 contained 550 ng of I-*Sce*I expression vector and 50 ng of pDsRed-Express2-N1 (Clontech) while Treatment 5 contained 1100 ng of I-*Sce*I expression vector and 100 ng of pDsRed-Express2-N1 (Clontech). Cells were harvested 24, 48, or 72 hours after transfection. Fluorescence was measured using a BD FACSCanto II flow cytometer. Each treatment contained three replicates and a minimum of 10000 events were analysed per sample. Each treatment contained three replicates. A minimum of 10000 events were analysed per sample. The data are shown as an average percentage of positive events per treatment with s.d.

A: 24 hour post-transfection harvest time point

B: 48 hour post-transfection harvest time point

C: 72 hour post-transfection harvest time point

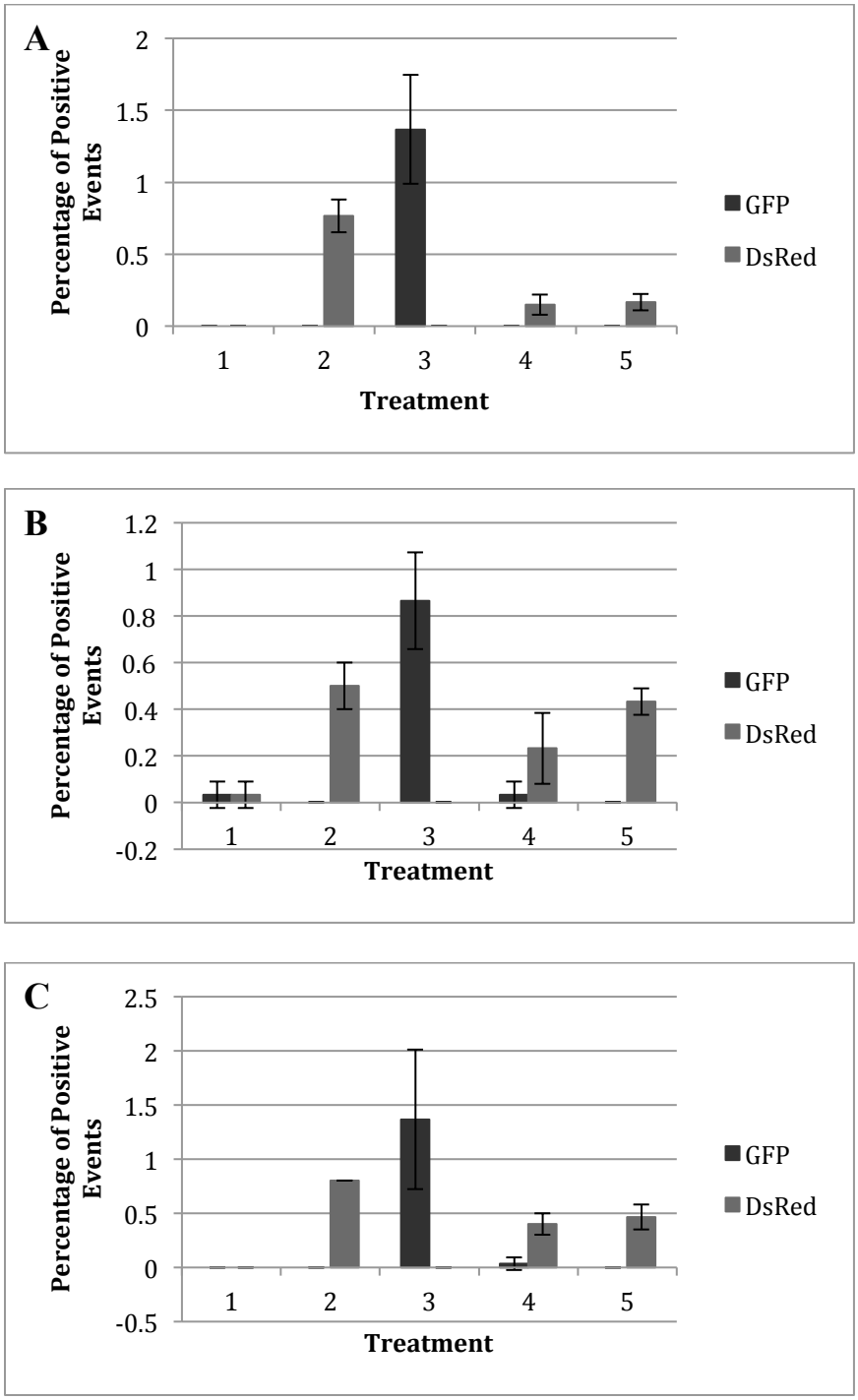

Supplementary Figure 3.9: The percentage of positive fluorescing events in I9a cells transfected with: pZP500 (Treatment 1); pDsRed-Express2-N1 (Clontech) (Treatment 2); gWIZ-GFP (Genlantis) (Treatment 3); and two different amounts of the I-*Sce*I expression vector and pDsRed-Express2-N1 (Clontech) using TranSIT

LT1 (Mirus). The controls contained 600 ng of plasmid. Treatment 4 contained 550 ng of I-*Sce*I expression vector and 50 ng of pDsRed-Express2-N1 (Clontech) while Treatment 5 contained 1100 ng of I-*Sce*I expression vector and 100 ng of pDsRed-Express2-N1 (Clontech). Cells were harvested 24, 48, or 72 hours after transfection. Fluorescence was measured using a BD FACSCanto II flow cytometer. Each treatment contained three replicates and a minimum of 10000 events were analysed per sample. The data are shown as an average percentage of positive events per treatment with s.d.

A: 24 hour post-transfection harvest time point

B: 48 hour post-transfection harvest time point

C: 72 hour post-transfection harvest time point

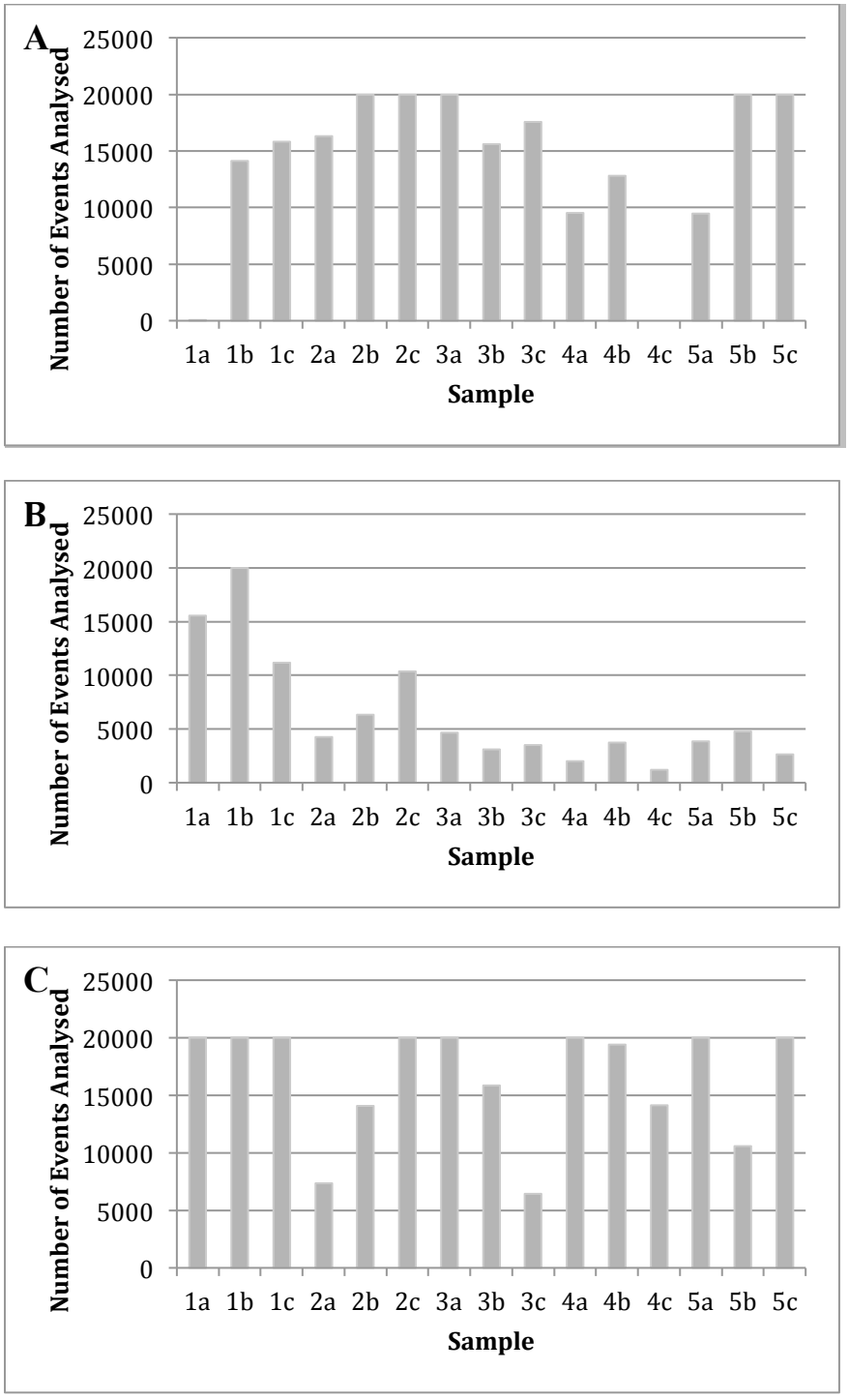

Supplementary Figure 3.10: The number of events analysed by a BD FACSCanto II flow cytometer per I9a sample. Samples were transfected with: pZP500 (Treatment 1); pDsRed-Express2-N1 (Clontech) (Treatment 2); gWIZ-GFP (Genlantis) (Treatment 3);

or two different amounts of the I-*Sce*I expression vector and pDsRed-Express2-N1 (Clontech) using TranSIT LT1 (Mirus). The controls contained 600 ng of plasmid. Treatment 4 contained 550 ng of I-*Sce*I expression vector and 50 ng of pDsRed-Express2-N1 (Clontech) while Treatment 5 contained 1100 ng of I-*Sce*I expression vector and 100 ng of pDsRed-Express2-N1 (Clontech). Each treatment contained three samples. Cells were harvested 24, 48, or 72 hours after transfection. Samples with 20000 events analysed were those that met the minimum 20000 events requirement.

A: 24 hour post-transfection harvest time point

B: 48 hour post-transfection harvest time point

C: 72 hour post-transfection harvest time point

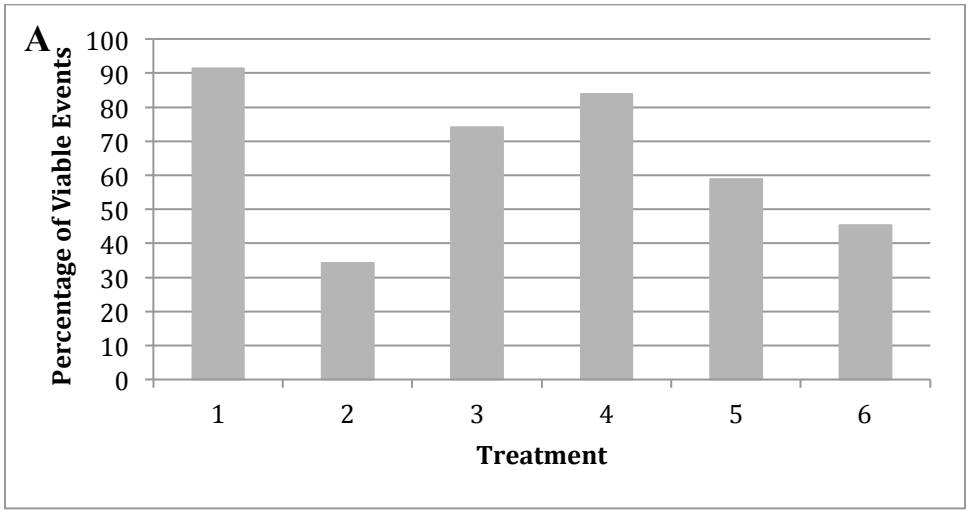

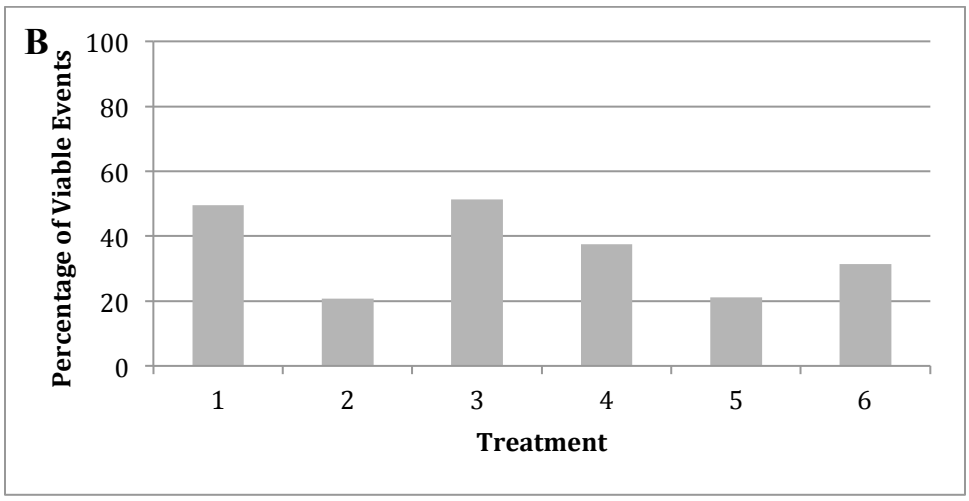

Supplementary Figure 3.11: The percentage of viable events in HI5c and I9a cells transfected with 600 ng or 1000 ng of I-*Sce*I expression vector and 3 µl or 5 µl of Lipofectamine LTX with PLUS Reagent (Life Technologies). Treatment 1 is a cells only control and Treatment 2 is a gWIZ-GFP only control. Treatment 3 and 4 were transfected with 600 ng and 1000 ng of I-*Sce*I expression vector respectively and 3 µl of transfection reagent. Treatment 5 and 6 were transfected with 600 ng and 1000 ng of I-*Sce*I expression vector respectively and 5 µl of transfection reagent. Cells were harvested 24 hours after transfection. A minimum of 10000 events were analysed per sample on a BD FACSCanto II flow cytometer. There was only one sample per treatment.

A: HI5c

B: I9a

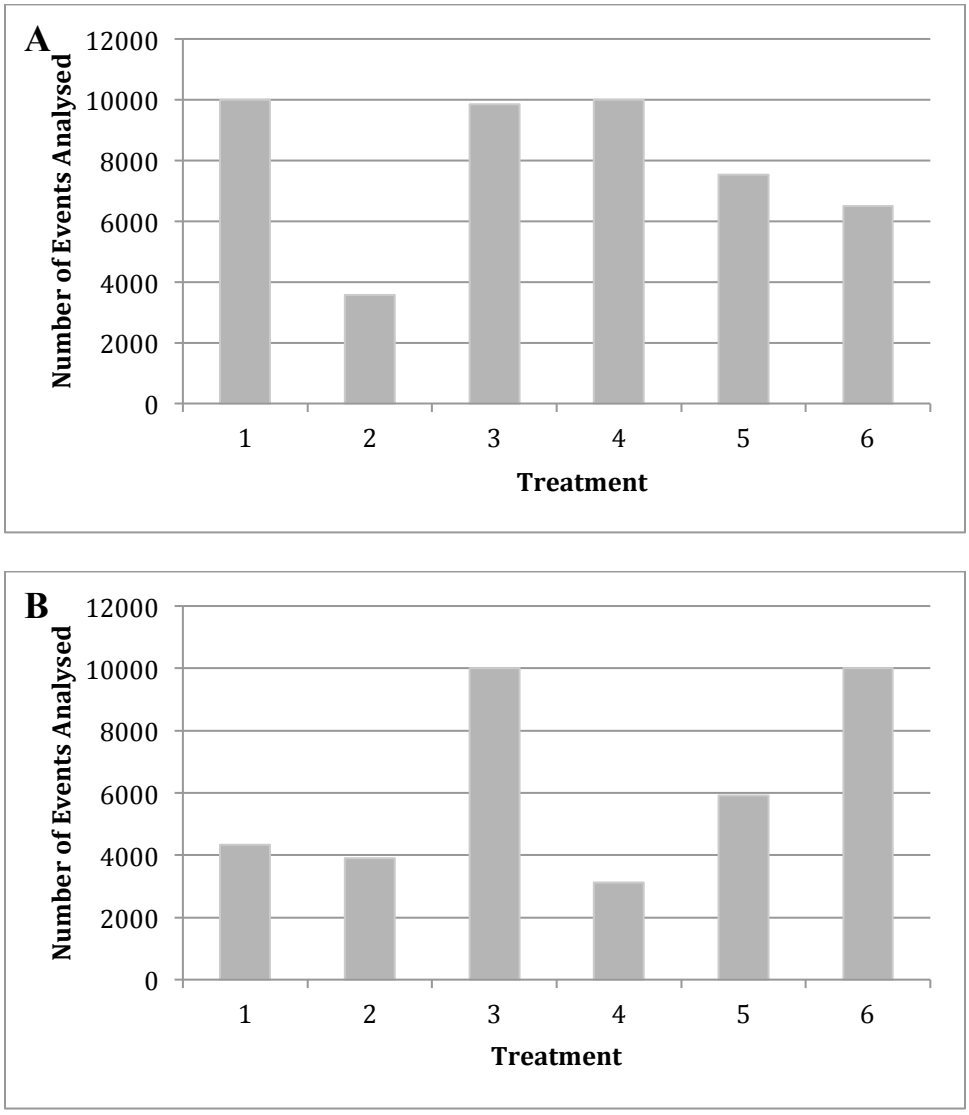

Supplementary Figure 3.12: The number of events analysed by a BD FACSCanto II flow cytometer per HI5c and I9a sample. Samples were transfected with 600 ng or 1000 ng of I-*Sce*I expression vector and 3 µl or 5 µl of Lipofectamine LTX with PLUS Reagent (Life Technologies). Treatment 1 is a cells only control and Treatment 2 is a gWIZ-GFP only control. Treatment 3 and 4 were transfected with 600 ng and 1000 ng of I-*Sce*I expression vector respectively and 3 µl of transfection reagent. Treatment 5 and 6 were transfected with 600 ng and 1000 ng of I-*Sce*I expression vector respectively and 5

µl of transfection reagent. Cells were harvested 24 hours after transfection. There was only one sample per treatment.

A: HI5c

B: I9a

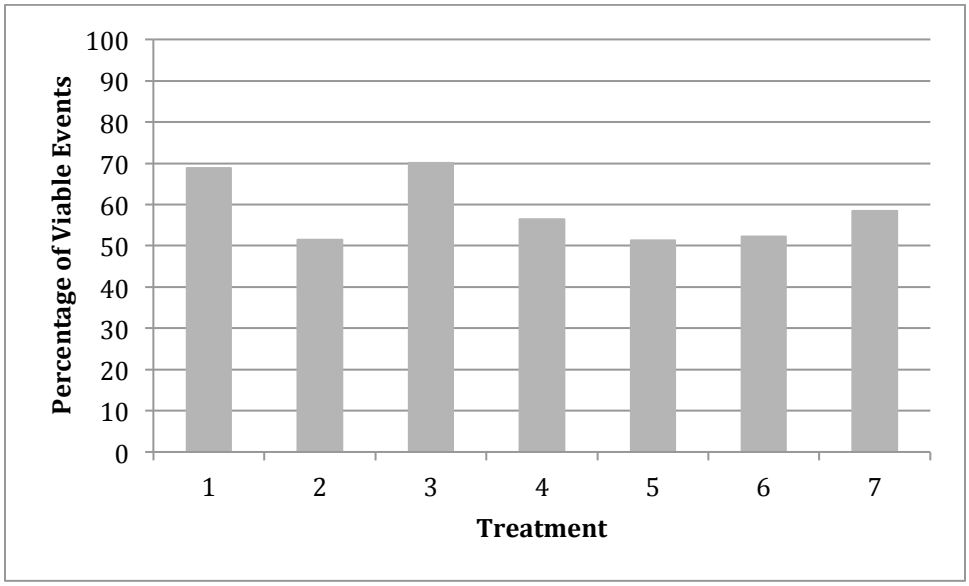

Supplementary Figure 3.13: The percentage of viable events in HI5c cells transfected with 100 ng of pDsRed-Express2-N1 (Clontech) and 500 ng of one of four I-*Sce*I expression vector stocks (Treatments 4-7) using Lipofectamine 2000 (Life Technologies). Treatment 1 was a pZP500 control, Treatment 2 was a gWIZ-GFP (Genlantis) control, and Treatment 3 was a pDsRed-Express2-N1 (Clontech) control. In each control 600 ng of plasmid was used. Cells were harvested 30 hours after transfection. A minimum of 10000 events were analysed per sample on a BD FACSCanto II flow cytometer. There was only one sample per treatment.

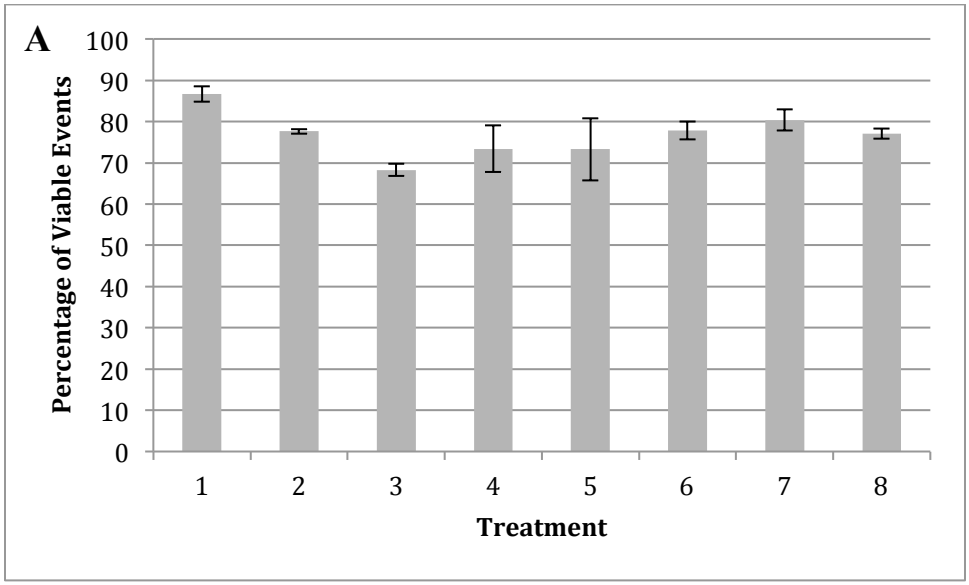

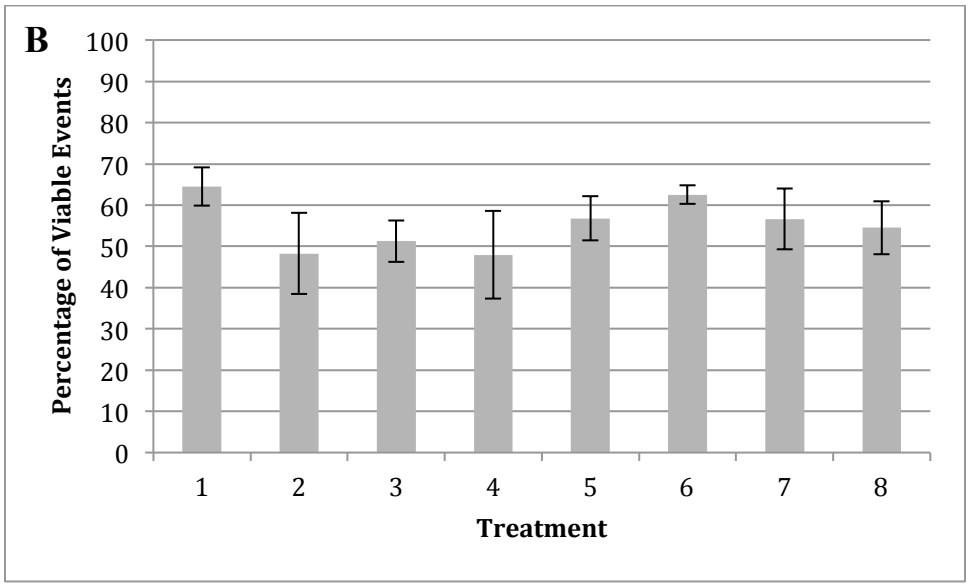

Supplementary Figure 3.14: The percentage of viable events in HI5c and I9a cells transfected with 400 ng of pDsRed-Express2-N1 (Clontech), 600 ng of I-*Sce*I expression vector, and either 0.5 µg or 1.0 µg of anti-Ku or anti-DNA-PK$_{cs}$ antibodies using Lipofectamine LTX with PLUS Reagent (Life Technologies).

Treatment 1 is a cells only control, Treatment 2 is pDsRed-Express2-N1 only control, Treatment 3 is an I-*Sce*I expression vector, and Treatment 4 is a no antibody control. Treatments 5 and 6 contained 0.5 µg and 1 µg of anti-Ku70 antibodies respectively.

Treatments 7 and 8 contained 0.5 µg and 1 µg of anti-DNA-PK_{CS} antibodies respectively. Treatments 4-8 also contained 400 ng of pDsRed-Express2-N1 and 600 ng of I-*Sce*I expression vector. Fluorescence was measured using a BD FACSCanto II flow cytometer. Cells were harvested 24 hours after transfection. Each treatment contained three replicates. A minimum of 10000 events were analysed per sample. The data are shown as an average percentage of viable events per treatment with s.d. A significant change in the percentage of viable events in Treatments 5-8 (antibodies present) when compared to Treatment 4 (no antibody control) is represented by an asterisk; two asterisks represents $P<0.01$ and three asterisks represent $P<0.001$.

A: HI5c

B: I9a

3.3 References

Mao, Z., Bozzella, M., Seluanov, A., & Gorbunova, V. (2008). Comparison of nonhomologous end joining and homologous recombination in human cells. *DNA Repair, 7*(10), 1765-1771. doi: 10.1016/j.dnarep.2008.06.018

Palm, M., Baumstark-Khan, C., & Horneck, G. (1999). Green fluorescent protein (GFP) expression in mammalian cells after UV-irradiation. In C. Baumstark, C. Khan, S. Kozubek, & G. Horneck (Eds.), *Fundamentals for the assessment of risks from environmental radiation* (Vol. 55), 311-316. Dordrecht, Netherlands: Springer. doi: 10.1007/978-94-011-4585-5_40.

Chapter 4: Discussion

4.1 Delivery of gWIZ-GFP and Antibodies Against GFP into HEK293 Cells

DSBs are primarily repaired in eukaryotic cells by two different mechanisms – NHEJ or HR. In mammalian somatic cells NHEJ is the preferred mechanism for repairing these breaks. Because gene targeting utilizes HR repair to alter a defined gene locus, this has proven to be a challenge to the advancement of the field and its applications. To address this problem, the present study attempted to use antibodies to target key DSB repair proteins to shift the balance from NHEJ to HR. The successful introduction of antibodies was pertinent to this investigation. In an attempt to demonstrate this, flow cytometry was used to assess the simultaneous introduction of gWIZ-GFP (Genlantis) and antibodies against GFP into human cells.

The anti-GFP antibody utilized was a mouse monoclonal antibody that binds to amino acids 1-238 of GFP, a range representative of the entire protein. It was predicted that the binding of the antibody to expressed GFP would interfere with the proteins ability to fluoresce. Thus successful introduction and binding could be quantified by a decrease in GFP positive events. In reality the opposite effect was seen. In experimental treatments where antibodies were present the percentage of GFP positive events was elevated and in many cases significantly increased when compared to the no antibody control. Before normalisation, the increase seen did not correspond to increasing amounts of plasmid (Figure 3.6). However, after normalisation as the amount of antibodies increased from 1

µg to 5 µg there was a trend of increasing relative amounts of GFP positive events (Figure 3.7). This cannot be attributed to antibodies binding to GFP and enhancing fluorescence because a positive event is considered a positive event when it falls within the gated region regardless of fluorescence intensity. Interestingly, in conjunction with the increase in GFP positive events, there was also a decrease in DsRed positive events (Figure 3.6).

Two possible explanations might explain the unexpected observations -- the presence of antibodies affects the transfection efficiencies of the plasmids or the presence of antibodies affects plasmid expression once entry into the cell has occurred. Given the target and source of the antibodies it is unlikely plasmid expression is affected. In addition, if expression machinery was being targeted, the effect on the production of the fluorescent products from gWIZ-GFP (Genlantis) and pDsRed-Express2-N1 (Clontech) would likely be similar. There is a possibility, however, the antibodies may interact with the plasmids once they have entered the cell and can alter their expression but again this explanation would need to be investigated.

Based on the changes seen in both GFP and DsRed positive events, it is also probable that the presence of antibodies may have an effect on the efficiency of transfection -- simultaneously encouraging uptake of gWIZ-GFP (Genlantis) and discouraging the uptake of pDsRed-Express2-N1 (Clontech). Consequently after taking into consideration the decreasing effect the presence of gWIZ-GFP (Genlantis) has on DsRed positive events (Figure 3.6), it is also possible that the antibodies may only affect the transfection

efficiency of gWIZ-GFP (Genlantis) and that the effect on DsRed positive events is directly the result of increased numbers of GFP positive events. The two plasmids employ a CMV promoter, however, the promoter in gWIZ-GFP (Genlantis) has been modified to increase transcriptional activity. In cells where both plasmids have successfully been transfected it is reasonable to assume gWIZ-GFP (Genlantis) would be preferentially transcribed resulting in a decrease in DsRed events. Because all antibody treatments were done with both plasmids present, it is difficult to know what affect the presence antibodies have on the transfection of the plasmids and what affect the plasmids have on each other. One way to test this would be to have treatments with consistent amounts of either gWIZ-GFP (Genlantis) or pDsRed-Express2-N1 (Clontech) and increasing amounts of antibodies. To determine if any outcomes seen are specific to the anti-GFP antibodies, a control antibody could be utilized. Regardless of whether the antibodies affect the expression or transfection efficiency, if they affect the plasmids differently, the reliability of the normalisation method used may need to be considered.

Because transfection efficiencies are not always consistent from reaction to reaction despite using similar conditions, normalisation was done to counteract any effect it could have on the results collected. This was done using pDsRed-Express2-N1 (Clontech) as a transfection control. In experimental treatments where both gWIZ-GFP (Genlantis) and pDsRed-Express2-N1 (Clontech) were used in consistent amounts, the number of GFP positive events was divided by the number of DsRed positive events. In theory it is expected that as the transfection efficiency of a reaction changes, the change would subsequently be mirrored similarly in both the number of GFP and DsRed positive

events. However, if the plasmids are affected differently by the antibodies or in the case that they affect one another, the present normalisation method may not provide a complete picture of what is actually happening. This point can be illustrated by considering the reciprocal trends of the normalised results from the gWIZ-GFP (Genlantis)/anti-GFP antibody experiments with the DsRed positive events (Figure 3.6 and 3.7). If there is a separate and distinct effect on the number of DsRed positive events, using the present method of normalisation the distinct effect on DsRed positive events will be reflected in the normalised GFP positive events, potentially masking or altering what is actually happening to the number of GFP positive events. Coupled with experiments designed to see how increasing amounts of the antibodies impact the number of GFP and DsRed positive events, it would also be beneficial to investigate how the amount of each plasmid impacts the transfection efficiency or expression of the other.

While the unexpected results did signify detectable changes in fluorescence, they were unable to confirm whether antibodies had been successfully introduced into cells. If the deviation in the number of positive events is in actuality the result of the antibodies interfering with transfection, it is reasonable to assume this is possible regardless of successful antibody delivery into cells. It would have been beneficial to harvest cells and run western blots on the cell extracts in an attempt to determine if antibodies were in fact being successfully delivered. In the event it is found antibodies are not entering the cell, it may be necessary to explore other antibody delivery reagents or possibly even introduce antibody-encoding plasmids instead of the antibodies directly.

4.2 Delivery of I-*Sce*I Expression Vector and Antibodies Against DSB DNA Repair Factors into HI5c and I9a Cells

Somatic human cell lines containing reporter cassettes for either NHEJ or HR were exploited to examine the consequences antibodies against DSB repair proteins have on natural NHEJ and HR repair levels. The cassettes were designed to detect repair events of one of the two DSB repair mechanisms following artificially induced DSBs by the endonuclease I-*Sce*I. An expression vector that was transfected into the cells along with the antibodies encoded the endonuclease responsible. Without the successful transfection and expression of the I-*Sce*I expression vector, there can be no detection of NHEJ or HR repair events.

In all experiments conducted, despite the successful transfection and expression of the control plasmids, gWIZ-GFP (Genlantis) and pDsRed-Express2-N1 (Clontech), there was no indication the I-*Sce*I expression vector was effectively transfected and expressed in HI5c or I9a (Figure 3.8-13, 3.16-20, Supplementary Figure 3.8 & 3.9). Even in experiments where there were low levels of GFP positive events present in treatments containing I-*Sce*I expression vector, the levels were similar to background GFP amounts seen in the cells only or pDsRed-Express2-N1 (Clontech) controls making it impossible to differentiate any GFP positive events produced as a result of HR or NHEJ repair (Figure 3.8, 3.16, 3.17, 3.19). There are a few different reasons that may explain why no definitive results were observed. One of the major differences between what was used in this study and what was done by the authors of the paper originally describing the cell

lines, was the different transfection methods employed. The original method of transfection utilised the Amaxa Nucleofector System (Mao et al., 2008a). Because our lab was not equipped with a Nucleofector device, transfection reagents from Life Technologies and Mirus were used. It is difficult to know whether or not this may have contributed to our lack of success without having access to the Amaxa Nucleofector System for comparison purposes. If future work is to proceed with the cells lines and endonuclease expression vector this will be an area that will need to be further explored. In addition, to rule out any possibility that the negligible amounts of GFP positive events are not the result of defective reporter cassettes or the I-*Sce*I expression vector, further sequencing should be done to ensure no mutations exist.

Another factor that may have an impact on the results of the experiments is the link between viability and GFP positive events. The possible connection surfaced following the experiment in HEK293 where large standard deviations for viability and GFP positive events in treatments 3 and 5 were the result of single outliers (Figure 3.3a and 3.5a). For most HEK293 experiments the level of viability was fairly consistent, unfortunately, this was not always the case for HI5c and I9a. With both cell lines there was a higher degree of variability that may have had some influence on the results observed. To help alleviate this problem, 2% FBS in DPBS was used to harvest cells instead of just using DPBS. Improvements were seen, but not enough to completely eliminate deviations. Accordingly, for future work it may be beneficial to only look at the percentage of positive fluorescence events in viable cells to eliminate any influence viability may have on the percentage of GFP positive events.

Although the work done in this study was unable to successfully demonstrate whether or not antibodies against DSB repair proteins can cause a shift in the repair balance, other studies have. An early study done *in vitro*, looked at the repair of linearlized plasmid DNA in whole cell extract from human cell lines. It found that NHEJ could be inhibited by anti-Ku antibodies but in order for the inhibition to effective, DNA-PK_{CS} needed to be present (Wang et al., 2003). In the presence of antibodies, Ku still had the capacity to bind to DNA ends, indicating the anti-Ku antibodies inhibited the actions of Ku later on in the NHEJ repair process. The effect does not appear to be solely restricted to mammalian cells. In *Xenopus* egg extract it was shown that four different anti-Ku autoimmune sera had inhibitory effects on NHEJ reactions (Labhart, 1999). The inhibitory effect was abolished when the sera was pre-incubated with human Ku. Antibodies against DNA-PK_{CS} were also utilised but no observable differences in NHEJ were established. A final study was conducted in one-celled mouse embryos. RNA/DNA, morpholino, or ssDNA constructs along with other factors were introduced using microinjection (Morozov & Wawrousek, 2008). The constructs were designed to insert a point mutation in an αβ-crystallin gene within the embryos. When no additional factors were present there was no evidence to indicate successful incorporation of the point mutation. However, when antibodies against Ku were used in conjunction with the ssDNA constructs there were mutational insertions detected. The use of mammalian nuclear extract, DNA-PK, or antibodies against rad51 had no effect on the efficiency of mutational insertion.

Each of the monoclonal antibodies used in this study bind to active domains within the targeted proteins. The anti-Ku70 antibody binds to amino acids 506-541 near the C-terminal arm, a region has been implicated in interactions with both Ku80 and DNA-PK_{CS} (Gell & Jackson, 1999). The antibody against DNA-PK_{CS} binds to the 1-2713 amino acid region at the N-terminal. Reviewed entries in the UniProtKB database recognize within this range of amino acids a region that binds to kinase interacting protein (KIP), a protein believed to be involved in DNA DSB repair (Wu & Lieber, 1997). The region also contains a leucine-zipper domain that is suspected be involved in interactions with C1D, a protein with a strong affinity for DNA (Yavuzer et al., 1998), as well as a possible caspase-3 cleavage site (Teraoka et al., 1996). Finally the antibodies against PARP-1 target amino acids 764-1014, a region that contains the PARP catalytic domain (Rolli et al., 1997; Simonin et al., 1990). All the targets of the antibodies chosen are involved to some degree in DNA repair. If antibodies are able to enter the cell and bind to the target protein then, in theory and based on previous research, there should be some repercussions to DSB DNA repair.

Over the past few decades there have been many studies investigating the relationship between HR and NHEJ and how this knowledge can be used to improve current gene targeting methods (Kass & Jasin, 2010; Mills et al., 2004). The relationship is intricate and involves various levels of cooperation and competition (Kass & Jasin, 2010). The choice between HR and NHEJ is determined by many factors including the nature of the break and the stage within the cell cycle, indicating the two mechanisms work collaboratively towards DSB repair. However, despite the co-operative efforts of HR and

NHEJ, there is evidence competition exists between the two pathways (Kass & Jasin, 2010). It has been shown that mutants with a defective NHEJ repair pathways display increased levels of resectioned DNA ends (Lee et al., 1998). Conversely mutants with reduced levels of resectioned ends exhibit more NHEJ activity (Yun & Hiom, 2009). It is this competitive aspect of the relationship between HR and NHEJ that has driven using downregulation of NHEJ proteins to enhance HR and subsequently improve gene targeting efficiencies. Past research has been done that both supports and opposes this approach. A study done in mouse embryonic stem cells found that despite increases in HR frequencies when cells were Ku70, XRCC4, or DNA-PK_{CS} null, no changes in gene targeting levels were observed (Pierce et al., 2001). Similar results were established with the gene targeting frequencies in *Arabidopsis thaliana* Ku mutants (Jia et al., 2012). However, in studies investigating single-celled eukaryotic Ku70 mutants, increases in gene targeting frequencies were seen (Ushimaru et al., 2010; Yamana et al., 2005). These findings were also supported with research done using human cells. A 5- to 10-fold increase in gene targeting was uncovered in Ku70+/- cells during an attempt to generate Ku70 null human somatic cells using the rAAV (Fattah et al., 2008). Further investigation revealed this was not specific to the Ku70 loci. Additionally, the effect could be mimicked using RNAi and shRNA targeting Ku70. The use of RNAi against Ku70 and XRCC4 in human HCT116 cells also revealed higher gene targeting frequencies that were associated with a reduction in random integrations (Bertolini et al., 2009). Together these lend some credence to the results seen when using anti-Ku antibodies.

One explanation that has been proposed as an explanation for the inconsistencies seen is B-NHEJ. The theory that a backup NHEJ pathway exists gained momentum as DSB repair activity emerged that could not be attributed to HR or NHEJ (Iliakis, 2009; Wu et al., 2008). When Ku or DNA-PK_{CS} is incapacitated but still able to bind to DNA, end-joining activity decreases (Morozov & Wawrousek, 2008; Perrault et al., 2004; Wang et al., 2003). However, this is only the case when the other DNA-PK complex components are present. Moreover, complete removal of Ku or DNA-PK_{CS} from the system results in seemingly normal levels of end joining that upon closer investigation show discernable differences from the wild type (Morozov & Wawrousek, 2008; Perrault et al., 2004; Wang et al., 2003). This evidence suggests that in the presence of Ku and DNA-PK_{CS} B-NHEJ activity is inhibited while in the absence of Ku or DNA-PK_{CS} B-NHEJ factors can readily gain access to the breaks and proceed with DSB repair (Wang et al., 2003). The B-NHEJ mechanism has been found to proceed at a slower rate than C-NHEJ and is purportedly mediated by Ligase III, Parp-1, and Histone H1 (Iliakis, 2009; Perrault et al., 2004; Terzoudi et al., 2008; Wu et al., 2008). Evidence suggests end resectioning is involved and that the mechanism routinely makes use of microhomologies (Rass et al., 2012). Consequently microhomology-mediation has also been implicated in the random integration of gene targeting vectors, a contributing factor to the problematic low frequency of gene targeting (Iiizumi et al., 2008). As a result the present study also proposed to investigate how the down-regulation of B-NHEJ proteins impact the repair balance between HR and NHEJ.

Parp-1 promotes DNA repair by binding to damaged sites and then recruiting repair factors (Bryant et al., 2005). Parp-1 has been associated with base excision repair (BER), single-strand break (SSB), and more recently B-NHEJ repair (Bryant et al., 2005; Iliakis, 2009; Paddock et al., 2011; Perrault et al., 2004; Terzoudi et al., 2008; Wu et al., 2008). Research in mice has shown that the manipulation of Parp-1 levels in the cell can affect gene targeting efficiencies (Dominguez-Bendala et al., 2006). In mouse embryonic stem cells lacking Parp-1 increases in gene targeting were observed (Dominguez-Bendala et al., 2006). The effect was also seen with inhibitors of Parp-1 albeit to a lesser extent (Dominguez-Bendala et al., 2006). The use of 3-methoxybenzamide (3-MB), a Parp inhibitor, in mouse Ltk- cells contributes to a reduction in random integrations indirectly resulting in a gene targeting increase (Waldman & Waldman, 1990). But despite the reported successes, a separate study in mice embryonic stem and embryonic fibroblast cells using Parp-1 deficient cells found no differences in DSB repair and gene targeting efficiencies (Yang et al., 2004).

Many of the studies focus on the downregulation of each candidate DSB repair factor individually. But with new evidence bringing to light an increasingly complex picture of DSB repair, the co-inhibition of different combinations of factors may be a more appropriate approach. A recent study noticed that double NHEJ factor mutants repaired DSB less efficiently and were more sensitive to ionizing radiation than either single mutant suggesting that the role of each factor may be compensated for by other DSB repair factors (Zhuang et al., 2011). Thus the transient downregulation of one factor may not be as effective as the downregulation of multiple factor when attempting to shift the

repair balance. Furthermore as evidence of a B-NHEJ pathway emerges simultaneously targeting both end joining pathways might prove to be necessary for increasing the frequency of HR.

Besides targeting multiple proteins, there is also some promise in shifting the focus to other less explored repair proteins. The p53 binding protein (53BP1) is a protein that has been linked to the NHEJ repair pathway (Nakamura et al., 2006; Stavnezer et al., 2008). It is recruited quickly to DNA DSBs and mutants show increased radiosensitivity in the G1 cell cycle phase (Nakamura et al., 2006; Stavnezer et al., 2008; Xie et al., 2007). Targeting the protein 53BP1 with siRNA in mice embryonic stem (ES) cells increases HR while chicken DT40 cells lacking 53BP1 display increased levels of gene targeting (Nakamura et al., 2006; Xie et al., 2007). Other proteins worth investigating include XRCC4 and LIGIV. In CHO cells XRCC4 mutations show signs of increased HR activity (Delacote et al., 2002; Johnson et al., 1999), and in *Arabidopsis thaliana*, LIGIV mutants showed increased gene targeting efficiencies (Tanaka et al., 2010). Additionally, mouse ES cells (Arbones et al., 1994; Capecchi, 1989; Hall et al., 2009), chicken DT40 cells (Buerstedde & Takeda, 1991; Yamazoe et al., 2004), and the human pre-B cell line Nalm-6 (Adachi et al., 2008; Adachi et al., 2006) all have naturally increased gene targeting levels relative to comparative cell lines. What distinguishes these from other vertebrate cells? And which of these differences contribute to the increased levels of gene targeting? Identifying what separates the cell lines with naturally enhanced gene targeting efficiencies may also help uncover promising proteins to target for downregulation.

4.3 Conclusions

Two dominant DSB repair mechanisms exist – HR and NHEJ. Another mechanism, known as B-NHEJ, has been uncovered in recent year and its contributions to DSB repair continues to be investigated. Over the last half century the HR DSB repair mechanism has been exploited by researchers to genetically alter specific loci in a wide range of different organisms. This process termed gene targeting is part of an emerging field that has useful applications for both the laboratory and clinical setting (de Semir & Aran, 2006; Fattah et al., 2008). In the past it has been used to generate knockouts and in the recent decade it has been researched as a promising treatment option for many diseases through the pretext of gene therapy (Edelstein et al., 2007; Fattah et al., 2008; Tani et al., 2011). Thus overcoming the challenges impeding the progression and advancement of this field continues to be important. Because the low frequency of HR in higher eukaryotic organisms has been linked to low gene targeting efficiencies, manipulation of DSB repair proteins has been utilised to shepherd the repair balance towards HR. However, an overview of studies targeting NHEJ and B-NHEJ repair proteins for downregulation does not reveal a unified picture. As more information about the different repair pathways and how they co-exist emerges, the list of potential targets and approaches to manipulate those targets expands. The approach of the present study attempted to utilize antibodies to transiently downregulate various DNA repair proteins. The objectives of this experiment were primarily to manipulate the balance of DNA repair within human cells so that it shifts away from NHEJ and towards HR. Successful

manipulation of the DSB repair has the potential to advance gene targeting in somatic mammalian cells and while the attempts of this particular study were unable to successfully achieve this, it should continue to be pursued.

4.4 References

Adachi, N., Nishijima, H., & Shibahara, K. (2008). Gene targeting using the human Nalm-6 pre-B cell line. *Bioscience Trends, 2*(5), 169-180.

Adachi, N., *et al.* (2006). The human pre-B cell line Nalm-6 is highly proficient in gene targeting by homologous recombination. [Article]. *DNA and Cell Biology, 25*(1), 19-24. doi: 10.1089/dna.2006.25.19

Arbones, M. L., Austin, H. A., Capon, D. J., & Greenburg, G. (1994). Gene targeting in normal somatic-cells - Inactivation of the interferon-gamma receptor in myoblasts. *Nature Genetics, 6*(1), 90-97. doi: 10.1038/ng0194-90

Bertolini, L. R., Bertolini, M., Maga, E. A., Madden, K. R., & Murray, J. D. (2009). Increased gene targeting in Ku70 and Xrcc4 transiently deficient human somatic cells. *Molecular Biotechnology, 41*(2), 106-114. doi: 10.1007/s12033-008-9098-8

Bryant, H. E., *et al*. (2005). Specific killing of BRCA2-deficient tumours with inhibitors of poly(ADP-ribose) polymerase. *Nature, 434*(7035), 913-917. doi: 10.1038/nature03443

Buerstedde, J. M., & Takeda, S. (1991). Increased ratio of targeted to random integration after transfection of chicken B-cell lines. *Cell, 67*(1), 179-188. doi: 10.1016/0092-8674(91)90581-i

Capecchi, M. R. (1989). The new mouse genetics - Altering the genome by gene targeting. *Trends in Genetics, 5*(3), 70-76. doi: 10.1016/0168-9525(89)90029-2

de Semir, D., & Aran, J. M. (2006). Targeted gene repair: The ups and downs of a promising gene therapy approach. *Current Gene Therapy, 6*(4), 481-504. doi: 10.2174/156652306777934847

Delacote, F., Han, M. G., Stamato, T. D., Jasin, M., & Lopez, B. S. (2002). An xrcc4 defect or Wortmannin stimulates homologous recombination specifically induced by double-strand breaks in mammalian cells. *Nucleic Acids Research, 30*(15), 3454-3463. doi: 10.1093/nar/gkf452

Dominguez-Bendala, J., Masutani, M., & McWhir, J. (2006). Down-regulation of PARP-1, but not of Ku80 or DNA-PKcs, results in higher gene targeting efficiency. *Cell Biology International, 30*(4), 389-393. doi: 10.1016/j.cellbi.2005.12.005

Edelstein, M. L., Abedi, M. R., & Wixon, J. (2007). Gene therapy clinical trials worldwide to 2007 - An update. *Journal of Gene Medicine, 9*(10), 833-842. doi: 10.1002/jgm.1100

Fattah, F. J., Lichter, N. F., Fattah, K. R., Oh, S., & Hendrickson, E. A. (2008). Ku70, an essential gene, modulates the frequency of rAAV-mediated gene targeting in human somatic cells. *Proceedings of the National Academy of Sciences of the United States of America, 105*(25), 8703-8708. doi: 10.1073/pnas.0712060105

Gell, D., & Jackson, S. P. (1999). Mapping of protein-protein interactions within the DNA-dependent protein kinase complex. *Nucleic Acids Research, 27*(17), 3494-3502. doi: 10.1093/nar/27.17.3494

Hall, B., Limaye, A., & Kulkarni, A. B. (2009). Overview: Generation of gene knockout mice. *Current protocols in cell biology / editorial board, Juan S. Bonifacino ... [et al.], Chapter 19*, Unit 19.12 19.12.11-17.

Iiizumi, S., *et al*. (2008). Impact of non-homologous end-joining deficiency on random and targeted DNA integration: Implications for gene targeting. *Nucleic Acids Research, 36*(19), 6333-6342. doi: 10.1093/nar/gkn649

Iliakis, G. (2009). Backup pathways of NHEJ in cells of higher eukaryotes: Cell cycle dependence. *Radiotherapy and Oncology, 92*(3), 310-315. doi: 10.1016/j.radonc.2009.06.024

Jia, Q., Bundock, P., Hooykaas, P. J. J., & de Pater, S. (2012). *Agrobacterium tumefaciens* T-DNA integration and gene targeting in *Arabidopsis thaliana* non-homologous end-joining mutants. *Journal of Botany, 2012*, 1-13. doi: doi:10.1155/2012/989272

Johnson, R. D., Liu, N., & Jasin, M. (1999). Mammalian XRCC2 promotes the repair of DNA double-strand breaks by homologous recombination. *Nature, 401*(6751), 397-399. doi: 10.1038/43935

Kass, E. M., & Jasin, M. (2010). Collaboration and competition between DNA double-strand break repair pathways. *Febs Letters, 584*(17), 3703-3708. doi: 10.1016/j.febslet.2010.07.057

Labhart, P. (1999). Ku-dependent nonhomologous DNA end joining in *Xenopus* egg extracts. *Molecular and Cellular Biology, 19*(4), 2585-2593.

Lee, S. E., Moore, J. K., Holmes, A., Umezu, K., Kolodner, R. D., & Haber, J. E. (1998). *Saccharomyces* Ku70, Mre11/Rad50, and RPA proteins regulate adaptation to G2/M arrest after DNA damage. *Cell, 94*(3), 399-409. doi: 10.1016/s0092-8674(00)81482-8

Mao, Z., Bozzella, M., Seluanov, A., & Gorbunova, V. (2008a). Comparison of nonhomologous end joining and homologous recombination in human cells. *DNA Repair, 7*(10), 1765-1771. doi: 10.1016/j.dnarep.2008.06.018

Mills, K. D., Ferguson, D. O., Essers, J., Eckersdorff, M., Kanaar, R., & Alt, F. W. (2004). Rad54 and DNA Ligase IV cooperate to maintain mammalian chromatid stability. *Genes & Development, 18*(11), 1283-1292. doi: 10.1101/gad.1204304

Morozov, V., & Wawrousek, E. F. (2008). Single-strand DNA-mediated targeted mutagenesis of genomic DNA in early mouse embryos is stimulated by Rad51/54 and by Ku70/86 inhibition. *Gene Therapy, 15*(6), 468-472. doi: 10.1038/sj.gt.3303088

Nakamura, K., Sakai, W., Kawamoto, T., Bree, R. T., Lowndes, N. F., Takeda, S., & Taniguchi, Y. (2006). Genetic dissection of vertebrate 53BP1: A major role in non-homologous end joining of DNA double strand breaks. *DNA Repair, 5*(6), 741-749. doi: 10.1016/j.dnarep.2006.03.008

Paddock, M. N., Bauman, A. T., Higdon, R., Kolker, E., Takeda, S., & Scharenberg, A. M. (2011). Competition between PARP-1 and Ku70 control the decision between high-fidelity and mutagenic DNA repair. *DNA Repair, 10*(3), 338-343. doi: 10.1016/j.dnarep.2010.12.005

Perrault, R., Wang, H. C., Wang, M. L., Rosidi, B., & Iliakis, G. (2004). Backup pathways of NHEJ are suppressed by DNA-PK. *Journal of Cellular Biochemistry, 92*(4), 781-794. doi: 10.1002/jcb.20104

Pierce, A. J., Hu, P., Han, M. G., Ellis, N., & Jasin, M. (2001). Ku DNA end-binding protein modulates homologous repair of double-strand breaks in mammalian cells. *Genes & Development, 15*(24), 3237-3242. doi: 10.1101/gad.946401

Rass, E., Grabarz, A., Bertrand, P., & Lopez, B. S. (2012). Double Strand Break Repair, one mechanism can hide another: Alternative non-homologous end joining. *Cancer Radiotherapie, 16*(1), 1-10. doi: 10.1016/j.canrad.2011.05.004

Rolli, V., Ofarrell, M., MenissierdeMurcia, J., & deMurcia, G. (1997). Random mutagenesis of the poly(ADP-ribose) polymerase catalytic domain reveals amino acids involved in polymer branching. *Biochemistry, 36*(40), 12147-12154. doi: 10.1021/bi971055p

Simonin, F., *et al*. (1990). Expression and site-directed mutagenesis of the catalytic domain of human poly(ADP-ribose)polymerase in *Escherichia coli* - Lysine-893 is critical for activity. *Journal of Biological Chemistry, 265*(31), 19249-19256.

Stavnezer, J., Guikema, J. E. J., & Schrader, C. E. (2008). Mechanism and regulation of class switch recombination. *Annual Review of Immunology* 26, 261-292.

Tanaka, S., Ishii, C., Hatakeyama, S., & Inoue, H. (2010). High efficient gene targeting on the AGAMOUS gene in an Arabidopsis AtLIG4 mutant. *Biochemical and Biophysical Research Communications, 396*(2), 289-293. doi: 10.1016/j.bbrc.2010.04.082

Tani, J., Faustine, & Sufian, J. T. (2011). Updates on current advances in gene therapy. *West Indian Medical Journal, 60*(2), 188-194.

Teraoka, H., Yumoto, Y., Watanabe, F., Tsukada, K., Suwa, A., Enari, M., & Nagata, S. (1996). CPP32/Yama/apopain cleaves the catalytic component of DNA-dependent protein kinase in the holoenzyme. [Article]. *Febs Letters, 393*(1), 1-6. doi: 10.1016/0014-5793(96)00842-3

Terzoudi, G. I., Singh, S. K., Pantelias, G. E., & Iliakis, G. (2008). Premature chromosome condensation reveals DNA-PK independent pathways of chromosome break repair. *International Journal of Oncology, 33*(4), 871-879. doi: 10.3892/ijo_00000075

Ushimaru, T., Terada, H., Tsuboi, K., Kogou, Y., Sakaguchi, A., Tsuji, G., & Kubo, Y. (2010). Development of an efficient gene targeting system in *Colletotrichum higginsianum* using a non-homologous end-joining mutant and *Agrobacterium tumefaciens*-mediated gene transfer. *Molecular Genetics and Genomics, 284*(5), 357-371. doi: 10.1007/s00438-010-0572-1

Waldman, B. C., & Waldman, A. S. (1990). Illegitimate and homologous recombination in mammalian cells differential sensitivity to an inhibitor of poly-ADP-ribosylation. *Nucleic Acids Research, 18*(20), 5981-5988. doi: 10.1093/nar/18.20.5981

Wang, H. C., Perrault, A. R., Takeda, Y., Qin, W., Wang, H. Y., & Iliakis, G. (2003). Biochemical evidence for Ku-independent backup pathways of NHEJ. *Nucleic Acids Research, 31*(18), 5377-5388. doi: 10.1093/nar/gkg728

Wu, W., Wang, M., Wu, W., Singh, S. K., Mussfeldt, T., & Iliakis, G. (2008). Repair of radiation induced DNA double strand breaks by backup NHEJ is enhanced in G2. *DNA Repair, 7*(2), 329-338. doi: 10.1016/j.dnarep.2007.11.008

Wu, X. T., & Lieber, M. R. (1997). Interaction between DNA-dependent protein kinase and a novel protein, KIP. *Mutation Research-DNA Repair, 385*(1), 13-20. doi: 10.1016/s0921-8777(97)00035-9

Xie, A., *et al*. (2007). Distinct roles of chromatin-associated proteins MDC1 and 53BP1 in mammalian double-strand break repair. *Molecular Cell, 28*(6), 1045-1057. doi: 10.1016/j.molcel.2007.12.005

Yamana, Y., Maeda, T., Ohba, H., Usui, T., Ogawa, H. I., & Kusano, K. (2005). Regulation of homologous integration in yeast by the DNA repair proteins Ku70 and RecQ. *Molecular Genetics and Genomics, 273*(2), 167-176. doi: 10.1007/s00438-005-1108-y

Yamazoe, M., Sonoda, E., Hochegger, H., & Takeda, S. (2004). Reverse genetic studies of the DNA damage response in the chicken B lymphocyte line DT40. *DNA Repair, 3*(8-9), 1175-1185. doi: 10.1016/j.dnarep.2004.03.039

Yang, Y. G., Cortes, U., Patnaik, S., Jasin, M., & Wang, Z. Q. (2004). Ablation of PARP-1 does not interfere with the repair of DNA double-strand breaks, but compromises the reactivation of stalled replication forks. *Oncogene, 23*(21), 3872-3882. doi: 10.1038/sj.onc.1207491

Yavuzer, U., Smith, G. C. M., Bliss, T., Werner, D., & Jackson, S. P. (1998). DNA end-independent activation of DNA-PK mediated via association with the DNA-binding protein C1D. *Genes & Development, 12*(14), 2188-2199. doi: 10.1101/gad.12.14.2188

Yun, M. H., & Hiom, K. (2009). CtIP-BRCA1 modulates the choice of DNA double-strand-break repair pathway throughout the cell cycle. *Nature, 459*(7245), 460-U184. doi: 10.1038/nature07955

Zhuang, L., *et al*. (2011). Suppression of DNA-PKcs and Ku80 individually and in combination: Different effects of radiobiology in HeLa cells. *International Journal of Oncology, 39*(2), 443-451. doi: 10.3892/ijo.2011.1041